



**Study of Natural Background Radionuclides Content in Mosses and  
Other Environmental Samples in the Southern Thailand**

**Komrit Wattanavatee**

**A Thesis Submitted in Fulfillment of the Requirements for the  
Degree of Doctor of Philosophy in Physics  
Prince of Songkla University  
2018  
Copyright of Prince of Songkla University**



**Study of Natural Background Radionuclides Content in Mosses and  
Other Environmental Samples in the Southern Thailand**

**Komrit Wattanavatee**

**A Thesis Submitted in Fulfillment of the Requirements for the  
Degree of Doctor of Philosophy in Physics  
Prince of Songkla University  
2018  
Copyright of Prince of Songkla University**

**Thesis Title** Study of Natural Background Radionuclides Content in Mosses and Other Environmental Samples in the Southern Thailand

**Author** Mr. Komrit Wattanavatee

**Major Program** Physics

---

**Major Advisor**

.....  
 (Assoc. Prof. Dr. Tripob Bhongsuwan)

**Examining Committee :**

.....Chairperson  
 (Assoc. Prof. Nares Chankow)

**Co-advisor**

.....  
 (Full Prof. Dr. Miodrag Krmar)

.....Committee  
 (Assoc. Prof. Dr. Thawat Chittrakarn)

.....Committee  
 (Assoc. Prof. Dr. Tripob Bhongsuwan)

The Graduate School, Prince of Songkla University, has approved this thesis as fulfillment of the requirements for the Doctor of Philosophy Degree in Physics

.....  
 (Prof. Dr. Damrongsak Faroongsarng)  
 Dean of Graduate School

**This is to certify that the work here submitted is the result of the candidate's own investigations. Due acknowledgement has been made of any assistance received.**

.....Signature  
(Assoc. Prof. Dr. Tripob Bhongsuwan)  
Major Advisor

.....Signature  
(.....)  
Candidate

I hereby certify that this work has not been accepted in substance for any degree, and is not being currently submitted in candidature for any degree.

.....Signature  
(.....)  
Candidate

ชื่อวิทยานิพนธ์	การศึกษาปริมาณนิวไคลด์กัมมันตรังสีภูมิหลังในธรรมชาติในมอสและตัวอย่างอื่นๆ ในสิ่งแวดล้อมในภาคใต้ของประเทศไทย
ผู้เขียน	นายคมฤทธิ วัฒนวาที
สาขาวิชา	ฟิสิกส์
ปีการศึกษา	2560

### บทคัดย่อ

วัตถุประสงค์ของการศึกษานี้คือเพื่อหาความเข้มข้นกัมมันตภาพรังสีของนิวไคลด์กัมมันตรังสีในธรรมชาติในมอสที่ขึ้นอยู่ตามธรรมชาติ นิวไคลด์ที่ตรวจสอบประกอบด้วย นิวไคลด์กัมมันตรังสีที่มาจากพื้นโลก ( $^{238}\text{U}$ ,  $^{226}\text{Ra}$ ,  $^{232}\text{Th}$  and  $^{40}\text{K}$ ), จากอากาศ ( $^{210}\text{Pb}$ ,  $^{210}\text{Pb}_{\text{ex}}$  and  $^7\text{Be}$ ) และนิวไคลด์กัมมันตรังสีที่มนุษย์สร้างขึ้น ( $^{137}\text{Cs}$ ) ตัวอย่างมอสที่ตรวจสอบ 2 สายพันธุ์ จำนวน 9 ตัวอย่าง เก็บจาก 3 บริเวณรอบอำเภอหาดใหญ่ จังหวัดสงขลา และ ตัวอย่างมอสอีก 17 สายพันธุ์ รวม 46 ตัวอย่าง เก็บมาจาก 17 บริเวณในเขตอุทยานแห่งชาติและเขตรักษาพันธุ์สัตว์ป่าซึ่งตั้งอยู่ในพื้นที่ภูเขาาระหว่างตอนบนถึงตอนล่างของคาบสมุทรไทย ( $7 - 12^\circ\text{N}$ ,  $99 - 102^\circ\text{E}$ ) เตรียมตัวอย่างมอสด้วยการอบแห้ง ตรวจวัดตัวอย่างด้วยเครื่องวิเคราะห์รังสีแกมมาแบบระดับรังสีภูมิหลังต่ำมาก ผลการศึกษาพบว่า ความเข้มข้นกัมมันตภาพรังสีของทุกนิวไคลด์กัมมันตรังสีในธรรมชาติมีการกระจายเชิงพื้นที่ไม่สม่ำเสมอ ในขณะที่กัมมันตภาพรังสีของ  $^{137}\text{Cs}$  มีค่าน้อยกว่าค่าต่ำสุดที่สามารถตรวจวัดได้ของเครื่องมือวัด จากการวิเคราะห์ผลด้วยเทคนิคการวิเคราะห์องค์ประกอบหลัก (Principle component analysis) และเทคนิคการจัดกลุ่ม (Cluster analysis) พบว่า สามารถแยกแหล่งกำเนิดของนิวไคลด์ที่ศึกษาออกเป็น 2 กลุ่ม กลุ่มแรกประกอบด้วย  $^{226}\text{Ra}$ ,  $^{232}\text{Th}$ ,  $^{238}\text{U}$  และ  $^{40}\text{K}$  อีกกลุ่มหนึ่งประกอบด้วย  $^{210}\text{Pb}$  and  $^{210}\text{Pb}_{\text{ex}}$  โดยนิวไคลด์ที่อยู่ในกลุ่มเดียวกันจะมีความสัมพันธ์กันสูงมากโดยดูจากค่าสัมประสิทธิ์เพียร์สัน อย่างไรก็ตามไม่พบความสัมพันธ์กันระหว่างนิวไคลด์ทั้งสองกลุ่ม อีกทั้งไม่พบความสัมพันธ์กับ  $^7\text{Be}$  ตามที่คาดการณ์ไว้ เนื่องมาจากความต่างกันของแหล่งกำเนิดของนิวไคลด์แต่ละกลุ่ม นอกจากนี้ค่าความเข้มข้นกัมมันตภาพของนิวไคลด์ในมอสยังมีการแปรปรวนในช่วงกว้างมาก อาจเนื่องมาจากความหลากหลายของสายพันธุ์มอส รวมถึงสภาพภูมิประเทศ สภาพธรณีวิทยา และสภาพอุตุนิยมวิทยาของจุดเก็บตัวอย่างอีกด้วย ค่ากัมมันตภาพรังสีที่สูงผิดปกติของนิวไคลด์บางตัวในมอส แสดงถึงความเป็นไปได้ที่มีความเกี่ยวข้องของระหว่างกัมมันตรังสีในธรรมชาติจากพื้นโลกกับลักษณะทาง

ธรณีวิทยาท้องถิ่นของจุดเก็บตัวอย่าง นอกจากนี้กัมมันตภาพรังสีของ  $^7\text{Be}$  ยังมีความเชื่อมโยงกับทั้งสภาพภูมิประเทศรวมถึงลมมรสุมตะวันออกเฉียงเหนือที่เคลื่อนที่จากจีนแผ่นดินใหญ่มายังคาบสมุทรไทย

<b>Thesis title</b>	Study of Natural Background Radionuclides Content in Mosses and Other Environmental Samples in the Southern Thailand
<b>Author</b>	Mr. Komrit Wattanavatee
<b>Department</b>	Physics
<b>Academic year</b>	2017

### Abstract

The purpose of this study is to determine the activity concentration of natural terrestrial radionuclides ( $^{238}\text{U}$ ,  $^{226}\text{Ra}$ ,  $^{232}\text{Th}$  and  $^{40}\text{K}$ ), airborne radionuclides ( $^{210}\text{Pb}$ ,  $^{210}\text{Pb}_{\text{ex}}$  and  $^7\text{Be}$ ) and anthropogenic radionuclide ( $^{137}\text{Cs}$ ) in naturally growing mosses. Totally 9 moss samples from 2 different species were collected from 3 sampling sites around Hatyai city (Songkhla province), and 46 moss samples from 17 different species were collected from the 17 particular sampling localities in the National Parks and Wildlife Sanctuaries of Thailand, where are situated in the mountainous areas between the northern to the southern ends of Peninsular Thailand ( $7 - 12^\circ\text{N}$ ,  $99 - 102^\circ\text{E}$ ). Their activity concentrations were measured using an ultra – low background gamma spectrometer. The results revealed non – uniform spatial distributions of all natural radionuclides in the study areas, while  $^{137}\text{Cs}$  activity concentrations are below minimum detectable activity. Principal component analysis and cluster analysis revealed the two distinguish origins of those radionuclides; furthermore, the Pearson coefficients showed the strong correlations between radionuclides in the same group ( $^{226}\text{Ra}$ ,  $^{232}\text{Th}$ ,  $^{238}\text{U}$  and  $^{40}\text{K}$ ) as well as  $^{210}\text{Pb}$  and  $^{210}\text{Pb}_{\text{ex}}$ . However, not only there is no any correlation between the two distinguish groups but also with  $^7\text{Be}$  as expected, this is due to difference in their origins. The measured activity concentrations in moss samples varied largely due to the differences of moss species, topography, geology and meteorology of sampling areas. The abnormally high concentrations of some radionuclides indicated probably that a high concentration of terrestrial radionuclide in moss samples directly related to local geological features in the sampling site, or that a high level of  $^7\text{Be}$  most probably linked with topography and regional North - East monsoonal wind coming from mainland China to the Peninsular Thailand.



## Acknowledgment

I wish to express my sincere thanks to my supervisor Assoc. Prof. Dr. Tripob Bhongsuwan for his encouragement, and Assoc. Prof. Dr. Miodrag Krmar for his helpful in the measuring of moss samples, all discussions and suggestions in the thesis.

I am grateful to Dr. Nawee Noon-Anant for his advice and helpful in fieldworks, and I am also grateful to Assist. Prof. Dr. Sahut Chantanaorrrpint for help in classification of moss samples.

I am grateful to Prince of Songkla University for funding of registration fees of my Ph. D. program.

This work was financial supported in part by the Graduate School, Prince of Songkla University.

The most special thank is to the Department of Physics, Faculty of Science, Prince of Songkla University, for the occasions, and times to me for finishing my thesis.

Finally, to my family, my wife, my aunt, my sisters and my brothers, who take care and give the willpower throughout my study.

Komrit Wattanavatee

April, 2018

## Contents

	<b>Page</b>
Title	i
Approval	ii
Certification	iii
Abstract (Thai)	v
Abstract (English)	vii
Acknowledgment	viii
Contents	ix
List of Tables	xi
List of Figures	xii
Chapter	
1. Introduction	1
1.1 Preface	1
1.2 Literature reviews	5
1.3 The present work	13
2. Research methodology	15
2.1 Fieldwork/Laboratory works, equipment and measuring instrument	16
2.1.1 Field work equipment setting	16
2.1.2 Laboratory work equipment setting	16
2.1.3 Measuring instrument	17
2.2 Methodology	
2.2.1 Brief of geography, meteorology, and geology of the sampling sites	17
2.2.2 Moss sample collection	18
2.2.3 Moss sample preparation	24
2.3 Instrumentation and moss sample measurement	30
3. Results and discussions	36
3.1 Activity concentration of $^7\text{Be}$ , $^{210}\text{Pb}_{\text{ex}}$ , $^{226}\text{Ra}$ , $^{232}\text{Th}$ and $^{40}\text{K}$ in moss samples collected around Hatyai City, Songkhla Province.	37

## Contents (Continue)

	<b>Page</b>
3.2 Activity concentration of $^7\text{Be}$ , $^{210}\text{Pb}_{\text{ex}}$ , $^{226}\text{Ra}$ , $^{232}\text{Th}$ and $^{40}\text{K}$ in moss samples collected around Peninsular Thailand.	41
3.2.1 General statistic of activity concentration of studied radionuclides	41
3.2.2 Spatial distribution, correlation and probable factors affecting to the activity concentration of terrestrial radionuclides; $^{40}\text{K}$ , $^{226}\text{Ra}$ , $^{232}\text{Th}$ and $^{238}\text{U}$ .	48
3.2.3 Spatial distributions, correlation and probable factors affecting to the Activity concentration of airborne radionuclides; $^7\text{Be}$ and $^{210}\text{Pb}$ .	54
- 3.2.3.1 Beryllium – 7	54
- 3.2.3.2 Lead – 210	58
4. Conclusion and Future works	62
4.1 Conclusion	62
4.2 Suggestion and future works	64
5. References	65
6. Appendices	
A1 Radioactive decay and radioactivity	74
A2 Short brief of general statistic, principle component analysis (PCA) and cluster analysis (CA)	78
A3 First publication “Airborne radionuclide in different latitude”	86
A4 Second publication “A Preliminary Survey of Natural Terrestrial and Airborne Radionuclides in Moss Samples from the Peninsular Thailand”	91
7. Vitae	107

## List of Tables

<b>Table</b>	<b>Page</b>
2.1 Sites, altitude (above mean sea level), latitude and longitude of sampling sites, sampling code and type of moss samples.	21
2.2 Species and photographs of moss samples.	26
2.3 NIST – 4350B Standard Reference Materials.	32
3.1 Activity concentrations of studied radionuclides in moss samples collected around Hatyai City.	37
3.2 Activity concentrations ( $\pm 1\sigma$ interval) of radionuclides presented in moss samples.	42
3.3 Pearson's correlation analysis of studied radionuclides.	47
3.4 Total variance explained for the analyzing of moss samples.	47
3.5 Factor loadings for the analyzing of moss samples.	47
3.6 Average activity concentrations of $^{40}\text{K}$ , $^{210}\text{Pb}_{\text{ex}}$ , $^{232}\text{Th}$ and $^{238}\text{U}$ and types of bedrock where sampling sites located on.	51
3.7 Range and mean values of activity concentrations of $^7\text{Be}$ , $^{40}\text{K}$ , $^{226}\text{Ra}$ , $^{210}\text{Pb}$ , $^{232}\text{Th}$ and $^{238}\text{U}$ from those reported literatures comparing to this study.	55

## List of Figures

Figure	Page
2.1 Map of the Peninsular of Thailand, (a) simplified geologic map of the study areas and (b) SRTM digital elevation model of southern Thailand and sampling sites.	19
2.2 (a) Sampling sites locations, (b) Tone – Nga – Chang waterfall and (c) moss sample collected from Tone – Nga – Chang waterfall ( <i>Leucobrym aduncum</i> Dozy & Molk).	20
2.3 Mosses sampling, mosses sample preparation and analyzing of radionuclides content in moss samples.	24
2.4 (a) Decay scheme of $^7\text{Be}$ , (b) Decay chain of $^{238}\text{U}$ – series, (c) Decay of $^{234}\text{Th}$ nucleus; a direct daughter of $^{238}\text{U}$ , (d) Decay chain of $^{226}\text{Ra}$ ; a progeny of $^{238}\text{U}$ , (e) Decay scheme of $^{210}\text{Pb}$ , (f) Decay chain of $^{232}\text{Th}$ – series, and (g) branching decay of $^{40}\text{K}$ .	31
3.1 Scatter graphs of activity concentrations between (a) $^7\text{Be}$ - $^{210}\text{Pb}_{\text{EX}}$ , (b) $^7\text{Be}$ – $^{226}\text{Ra}$ , (c) $^7\text{Be}$ – $^{232}\text{Th}$ , (d) $^7\text{Be}$ – $^{40}\text{K}$ , (e) $^{210}\text{Pb}_{\text{EX}}$ – $^{226}\text{Ra}$ , (f) $^{210}\text{Pb}_{\text{EX}}$ – $^{232}\text{Th}$ , (g) $^{210}\text{Pb}_{\text{EX}}$ – $^{40}\text{K}$ , (h) $^{226}\text{Ra}$ – $^{232}\text{Th}$ , (i) $^{226}\text{Ra}$ – $^{40}\text{K}$ and (j) $^{232}\text{Th}$ – $^{40}\text{K}$ .	39
3.2 Frequency distribution of measured radionuclides (a) $^7\text{Be}$ , (b) $^{40}\text{K}$ , (c) $^{210}\text{Pb}$ , (d) $^{226}\text{Ra}$ , (e) $^{232}\text{Th}$ and (f) $^{238}\text{U}$ .	45
3.3 (a) Component plot in a rotated space for 7 radionuclides and (b) A dendrogram is obtained by cluster analysis for activity concentrations in moss samples; the degrees of correlation between variables are related to the distances.	49
3.4 the scatter graph of activity concentrations measured in moss samples (a) $^{238}\text{U}$ – $^{232}\text{Th}$ , (b) $^{226}\text{Ra}$ – $^{238}\text{U}$ , (c) $^{40}\text{K}$ – $^{232}\text{Th}$ , (d) $^{226}\text{Ra}$ – $^{210}\text{Pb}$ , (e) $^7\text{Be}$ – $^{210}\text{Pb}_{\text{EX}}$ , and (f) $^{40}\text{K}$ – $^{226}\text{Ra}$ .	52
3.5 Activity concentrations of radionuclides at various geographic of studied areas; (a) $^{238}\text{U}$ , (b) $^{232}\text{Th}$ , (c) $^{40}\text{K}$ , (d) $^{226}\text{Ra}$ , (e) $^7\text{Be}$ and (f) $^{210}\text{Pb}$ .	53

### List of Figures (continue)

Figure	Page
A2.1 (a) Euclidean distance between two variables, (b) calculated values of $d(i,j)$ between all variables, (c) calculated values of $d(i,j)$ between $X_3X_n - X_1$ , $X_3X_n - X_2$ , $X_3X_n - X_4$ , $X_1 - X_4$ and $X_2 - X_4$ , (d) calculated values of $d(i,j)$ between $X_3X_n - X_1X_2$ , $X_3X_n - X_4$ , and $X_1X_2 - X_4$ , and (e) calculated values of $d(i,j)$ between $X_3X_nX_4 - X_1X_2$	84
A2.2 The dendrogram of $X_1, X_2, X_3, X_4$ and $X_n$	85

## Chapter One

### 1. Introduction

#### 1.1 Preface

There are three general categories of natural occurring radionuclides in environments: (1) primordial radionuclides, (2) cosmogenic radionuclides and (3) anthropogenic radionuclides. The first one is the nuclides (i.e.,  $^{238}\text{U}$ ,  $^{232}\text{Th}$  and  $^{40}\text{K}$ ) which have found on the Earth and existed in their form since the time before the Earth was formed.  $^{40}\text{K}$ ,  $^{232}\text{Th}$  and  $^{238}\text{U}$  originated from crustal materials in soil with world average values of activity concentration (The activity per unit mass of that nuclide) are around 400, 35 and 30 Bq/kg, respectively (UNSCEAR, 2000). An important factor affects the contents of these radionuclides found in the environment is the geological setting of sampling areas (McCartney et al., 2000). In addition, they can be transported and removed from the atmosphere by dry or wet depositions of the dust particles (Karunakara et al., 2003; Dragović and Mandić, 2010; Krmar et al., 2007). The presence of them in atmosphere (as well as in biota) are affected by a number of factors that mainly related to emission of dust particles from coal – fired ash, fossil fuel combustions, phosphates fertilizer usages, and phosphate plants (Belivermiş and Çotuk, 2010). On the other hand, anthropogenic radionuclides (3<sup>rd</sup> category) such as  $^{137}\text{Cs}$  and  $^{90}\text{Sr}$  associated with the nuclear fission events; for example by nuclear weapon testing and accident in fission nuclear power plants. They were released into the environment due to atmospheric deposition varying with geographical locations and precipitation such as rainfall (Ritchie et al., 1990).

Airborne radionuclides  $^7\text{Be}$  and  $^{210}\text{Pb}$  (2<sup>nd</sup> category), released to the atmosphere originate from different origins. Beryllium – 7 is produced by spallation reactions between high energy proton in galactic cosmic rays with  $^{14}\text{N}$ ,  $^{16}\text{O}$  and  $^{12}\text{C}$  in lower stratosphere and upper

troposphere. Its variation in the atmosphere depended on the galactic cosmic ray flux, proton flux from sun during solar events, stratosphere – troposphere exchange and meteorological parameters of transportation of aerosols in ground level air (Petrova et al., 2009). Lead-210 is a progeny in decaying of  $^{222}\text{Rn}$  in  $^{238}\text{U}$  decay chains. Its concentration in surface air depends mainly onto the rate of emanation of  $^{222}\text{Rn}$  and local meteorological parameters. After release to atmosphere as aerosol particles,  $^{210}\text{Pb}$  falls to the earth surface by washout and sedimentation (Uğur et al., 2003).

The variation of activity concentration of terrestrial radionuclides in environment is generally homogeneous compared with anthropogenic and cosmogenic radionuclides. Furthermore, it may not only depend onto meteorology such as temperature, pressure, local rainfall and local windblown etc., but human activities (fossil fuel combustion, exhaust gases released from coal – fired power plant, phosphate fertilizer usage) also affect to their variations (Mccartney et al., 2000).

High volume air sampler is a good method to monitor the variation of these radionuclides in earth surface air, a certain volume of air contains atmospheric aerosol passed through the glass filter paper consequently, and they are trapped onto the paper. After moisture released from the paper by heating (as well as burning to be ash) the activity concentrations of these radionuclides (Bq/kg) are determined by mean of gamma ray spectroscopy (Momoshima et al., 2006; Bourcier et al., 2011). Another method is to measure their deposition flux in  $\text{Bq/m}^2$  named ‘precipitation method’; a certain area of metal tray is installed on the roof in a period of time, the atmospheric aerosols deposited onto the tray by wet and dry deposition. By some chemical procedures, the aerosols were removed, collected, heated and kept into the container. Consequently, after leave for radioactive equilibrium, the gamma spectrometer was used to determine the activity concentration of those radionuclides. However, those two methods are appropriate for a long – term study at a fixed sampling site which is limited by number of sampling stations and



electrical power supplies in order to study their spatial distribution over large areas. Thus the dense sampling site with inexpensive is required; a good solution is the moss technique which used to be a promising media in order to purpose those studies (Krmr et al, 2007).

It is well known that terrestrial mosses are growing in the forests of different climate zones and it is used as bio – monitoring due to its advantages;

1) Lack of well – developed root – system and has no cuticle; direct take up radionuclide from the atmosphere.

2) It can be found in broad regions in several climatic zones.

3) Morphology does not vary with season (grow very slowly); it retains or accumulates the deposited radionuclides throughout the year which is good for long-term study.

4) High surface-to-volume ratio and growing like a carpet; increase efficient in trap the aerosol particles and water (Anicic et al., 2007).

5) High CEC (cation exchange capacity)

6) Sample collection and preparation are simple and inexpensive; the chemical usage is not required.

The using of mosses as bio – monitoring has rapidly increased since the works of Jenkins and coworkers which have been reported in 1972. The study of some radionuclides content in mosses was done from Olympic National Park, Washington, U.S.A. (Jenkins et al., 1972), as well as in European Countries, after the use of mosses as a media for determination of the heavy metal elements (Rühling and Taylor, 1973). However, those studied were limited around the small area and a few number of sampling site, thus the spatial distribution of studied radionuclides (as well as heavy metals) over a large sampling area performed by a number of sampling station cannot be obtained. The use of terrestrial mosses in detection of radionuclides

over a large area has been reported from an area around 100 km along the coast in Syrian mountain (Al-Masri et al., 2005), or over 400 km along an international freeway in Serbia (Krmr et al., 2007) and over 67,000 km<sup>2</sup> from Marmara region in Turkey (Belivermiş and Çotuk, 2010). It can be indicated that, the moss technique has high potential in usage as a bio – monitor of radionuclide deposition over large areas if adequate number and density of sampling locations can be provided.

In addition, due to the accumulation capacity of mosses for airborne elements is higher than the other vascular plants which are grown in the same habitat (Aleksiayenak et al., 2013) and their morphologies do not vary with the season, thus they can retain and accumulate both pollutants throughout the whole year (Szczepaniak and Biziuk, 2003). Consequently, mosses have been widely used in the field of radiology as monitors of radionuclides in the environments, for examples: (1) Uranium mine (Pettersson et al., 1988), (2) Lignite center (Tsikritzis, 2005), (3) Areas near nuclear and coal – fired power plants (Sumerling, 1984; Delfanti et al., 1999; Karunakara et al., 2003; Uğur et al., 2003; Sert et al., 2011), and (4) Monitoring of <sup>137</sup>Cs in many areas in European countries after nuclear accident at Chernobyl (Kirchner and Dalilliant, 2002; Dragović and Mihailović, 2009; Krmr et al., 2007).

Although moss technique is widely used worldwide, in fact there was no report of systematic studies using mosses for the natural radioactivity measurements in Thailand. This study is the first attempt at utilizing Thai's mosses as bio – monitors of natural radionuclides (<sup>7</sup>Be, <sup>40</sup>K, <sup>210</sup>Pb, <sup>226</sup>Ra, <sup>232</sup>Th and <sup>238</sup>U) collected in the Peninsular Thailand; covered the sampling areas located in Changwat Songkhla, Changwat Trang, Changwat Krabi, Changwat Phang Nga, Changwat Ranong, Changwat Chumporn, Changwat Surathani, Changwat Nakhonsithammarat and Changwat Phthalung.

## 1.2 Literature reviews

After Chernobyl accident in 1986, there were a number of reported in using of moss as a bio – monitoring for  $^{137}\text{Cs}$ ,  $^{90}\text{Sr}$  in European countries. For example, the activity concentration of  $^{137}\text{Cs}$  in mosses collected in Greece were ranged from 270 – 4,750 Bq/kg (Papastefanou, 1989), or  $^{137}\text{Cs}$  flux was below 60 Bq/m<sup>2</sup> in France (Barci – Funel et al., 1989). The decreasing of  $^{137}\text{Cs}$  during 15 years after the accident from 1,400 – 3,200 to 60 – 140 Bq/kg in mosses collected in Russia on 1995 – 2004 (Nifontova et al, 2006), which is more rapidly than its physical half – life, this is may be associated with biological properties of bryophytes such as leaching process. Aleksiyenak (2012) found that the  $^{137}\text{Cs}$  content in mosses collected from Belarus and Slovakia (*Hylocomium splendens* and *Pleurozium schreberi*) ranged from 5 – 6,827 Bq/kg, which were originated from Chernobyl fall-out deposition. They also suggested that the activity concentration of  $^{137}\text{Cs}$  in mosses relate to its migration from the older part to younger part of the bryophytes (Aleksiayenak et al., 2012). In addition,  $^{137}\text{Cs}$  content in mosses collected from sampling sites located in high land or tip mountain area; such as in Turkey (Al – Masri et al., 2005) and Zlatibor mountain (Rep. of Serbia; Dragović et al., 2010) were generally high compared to the sampling sites located in low land. The author suggested that moss samples were direct contact through Chernobyl radioactive cloud in the high land sampling sites, these means the altitude of sampling sites (geographic of sampling sites) affects the  $^{137}\text{Cs}$  content in moss samples.

Mosses are also used as the bio – monitor in study of the pollutant sources of natural radionuclide and their distribution in environment. For example, Uğur (2003) reported the anomaly of  $^{210}\text{Pb}$  content in moss samples collected around a coalmine of Yatakan (Turkey), which has no any correlation with  $^{226}\text{Ra}$  in soil samples collected at the same sampling sites. He suggested that not only emanation of  $^{222}\text{Rn}$  in the sampling site but the fine ashes from the power plant is also a main source of lead-210. In agreement to a report by Sert (2011), there were no

any correlation between measured activity concentration of  $^{222}\text{Rn}$  in air and  $^{210}\text{Pb}$  ( $^{226}\text{Ra}$ ) in soil as similar as  $^{210}\text{Pb}$  in moss samples and  $^{226}\text{Ra}$  in soil samples collected around a coal – fired power station in the western of Turkey. It was indicated that a significant source of  $^{210}\text{Pb}$  in moss sample is  $^{222}\text{Rn}$  in chimney gases exhausted by the plant. In addition, the variation in their concentration in mosses depends on moss species, moss – covered plants, ecology, morphology and physiology of the bryophytes (Sert et al., 2011; Dragović et al., 2010).

By using method of PCA (Principle component analysis), Tsikritzis (2005) grouped 5 studied radionuclides ( $^{40}\text{K}$ ,  $^{137}\text{Cs}$ ,  $^{134}\text{Cs}$ ,  $^{226}\text{Ra}$  and  $^{228}\text{Ra}$ ) in moss samples collected around the Lignite Center (Central Greece) into 2 separated origins;  $^{40}\text{K}$  –  $^{134}\text{Cs}$  –  $^{137}\text{Cs}$  are belonged in the first group called “*Chernobyl and re – suspension*” which originated from surrounding soil, while the second group ( $^{226}\text{Ra}$  –  $^{228}\text{Ra}$ ) called “*Fly – ashes*” which originated from the fly – ashes and presented in mosses by deposition of atmospheric aerosols (Tsikritzis et al., 2005).

Karunakara (2003) reported the activity concentration of  $^{226}\text{Ra}$ ,  $^{210}\text{Pb}$ ,  $^{40}\text{K}$ , and  $^7\text{Be}$  in plants collected over 8 km radius around nuclear power plant installed in Kaiga, India. The high values of  $^7\text{Be}$  contents in mosses were observed in agreement with high value of other airborne radionuclides ( $^{210}\text{Pb}$ ,  $^{210}\text{Po}$  and  $^{137}\text{Cs}$ ); it ranged from 72 – 106 Bq/kg and may be associated with high wet deposition rate during sampling period. Furthermore, there was a significant correlation between  $^{40}\text{K}$  and  $^{226}\text{Ra}$  due to their chemical properties are homologue and  $^{40}\text{K}$  is a necessary element for growing of the plants (Karunakara et al., 2003; Belivermiş and Çotuk, 2010; Mietelski et al., 2000).

Previous literatures report examples of using mosses as bio – monitor for natural and artificial radionuclides worldwide, which were performed in one fix place with small sampling area. An interesting of study of deposition of radionuclides over large area was reported by Al – Masri (2005); moss samples were collected from an area around 100 km along the coast in Syrian mountain (Ceria). The high value of  $^{210}\text{Pb}$  can be observed from the sampling area

located near the active fault such as Al-Gaab fault locates in Abu Kbee city, which correlated to the high emanation rate of  $^{222}\text{Ra}$  near the fault zone (Al-Masri et al., 2005).

Krmar (2007) reported activity concentration of  $^7\text{Be}$ ,  $^{40}\text{K}$  and  $^{137}\text{Cs}$  in 19 moss samples (*Hypnum cupressiforme*) which were collected along the 400 km international freeway from northern – southern part of Rep. of Serbia ( $42^\circ 26' 19''\text{N} - 45^\circ 23' 12''\text{N}$  and  $19^\circ 35' 9''\text{E} - 22^\circ 8' 20''\text{E}$ ). The author suggested spatial distribution of activity concentration of  $^7\text{Be}$  in moss samples was not uniform; this may be associated with local meteorology parameters of sampling site such as local rainfall.  $^7\text{Be}$  and  $^{40}\text{K}$  (and  $^{137}\text{Cs}$ ) deposited onto moss by different origins; atmospheric aerosol deposition for  $^7\text{Be}$  and in contrary, re – suspension of surrounding soil dust by wind for  $^{40}\text{K}$  and  $^{137}\text{Cs}$ , which is supported by no correlation between  $^7\text{Be} - ^{137}\text{Cs}$  and  $^7\text{Be} - ^{40}\text{K}$ . In addition, due to uncertainty in measured activity concentration of  $^{210}\text{Pb}$  is too high thus the correlation with  $^7\text{Be}$  is not evident. However, the measured value of  $^{214}\text{Bi}$  is too low compared to  $^{210}\text{Pb}$ ; this is implied that  $^{210}\text{Pb}$  was not originated from emanation of  $^{222}\text{Rn}$  but from the atmospheric deposition similar as  $^7\text{Be}$  (Krmar et al., 2007).

Belivermiş and Çotuk (2010) collected 37 mosses (*Hypnum cupressiforme*) 38 lichens (*Cladonia rangiformis*) over sampling area  $\sim 67,000 \text{ km}^2$  from 47 sampling sites located in Marmara region (Turkey). The measured values of  $^{40}\text{K}$  were high and higher than  $^{238}\text{U}$  and  $^{232}\text{Th}$ . This is because potassium is a macro – element and needed for growing of plants, while uranium and thorium are not required. In addition, authors also suggested that they were presented in mosses/lichens by the suspended soil particles by wind and spattering of raindrops contains soil particles. In contrary,  $^{137}\text{Cs}$  content in mosses/lichens were low (0.36 – 8.13 Bq/kg and BDL – 4.32 Bq/kg, respectively) which are lower than those found in their previous studies in the northern hemisphere. They suggested that  $^{137}\text{Cs}$  content in mosses is higher than lichens due to mosses having relative higher surface-to-volume ratio than lichens. However they presented in those plants through re – suspension of soil by spattering of raindrops. Furthermore,

there is significant correlation between  $^{137}\text{Cs}$  content in mosses and lichens ( $R^2 = 0.6117$ ), it is implied that in sampling location which mosses are not available the calculated radionuclide content in mosses can be estimated using multiplication of its content in lichen with ratio of those radionuclide in mosses and lichens (Belivermiş and Çotuk, 2010).

Sugihara (2008) reported seasonal variations in measured values of  $^7\text{Be}$ ,  $^{40}\text{K}$  and  $^{210}\text{Pb}$  content in vascular plants and mosses (*Quercus acuta*, *Petasitos japonicus*, *Sasa veitchii*, *Miscanthus sinensis*, *Entodon challengerii*, *Ilex crenata*, *Pinus thunbergii* and *Lycopodium clavatum*) collected from the sampling areas located in Sefuti mountain (1,055 m above mean sea level), Fukuoka (Japan). Be-7 and  $^{210}\text{Pb}$  were presented in leaf – samples by atmospheric deposition. Their higher values can be observed in during spring and lower values observed in summer; the first one associated with vertical mixing of air mass from lower stratosphere to upper troposphere and air mass (contains high value of  $^7\text{Be}$  and  $^{210}\text{Pb}$ ) transportation from the northern part of Japan to study areas, the second one related to the wash – out of atmospheric aerosol by rain. The highest and lowest values of  $^{40}\text{K}$  can be observed in spring and winter respectively; because of  $^{40}\text{K}$  is a necessary element which is required for growing of plants and it was presented in plants via root system. In contrary to vascular plants, the high value of  $^7\text{Be}$  and  $^{210}\text{Pb}$  can be observed in mosses samples while  $^{40}\text{K}$  were generally low, the author suggested that the higher values due to airborne radionuclides were deposited onto mosses by atmospheric processes and  $^{40}\text{K}$  was presented by re – suspension of surrounded soil or dust particles. In addition, the higher values of those radionuclides in bryophytes may be due to epicuticular wax or resin on its leaf which is high efficient in order to trap and retention of the atmospheric aerosol from the wash – out by rain (Sugihara et al., 2008).

Although there was a number of using of mosses technique as bio – monitoring worldwide, there was no any report in systematic study in Thailand. In order to purpose of this study, the suggestions and conclusions of the previous studies from neighboring countries

around Thailand;- such as Japan, Korea, China etc. as well as from countries locate other region were summarized as the following;

Paateo (2001) observed seasonal variation in activity concentration in air of  $^7\text{Be}$  (1,880  $\text{mBq/m}^3$  (falls/winter) – 4,680  $\text{mBq/m}^3$  (spring/summer)) and  $^{210}\text{Pb}$  (122  $\text{Bq/m}^3$  (summer) – 347  $\text{mBq/m}^3$  (winter)) in southern part of Finland (60°30'N 24°39'E, 105 m above mean sea level) during January 1997 to December 1999. Variation in their value mainly associated with marine time air mass and transportation of air mass. In summer, although solar heating during daytime increases emanation rate of  $^{222}\text{Rn}$  in ground and surface air, however, by vertical mixing between surface and higher air mass  $^{222}\text{Rn}$  (as well as  $^{210}\text{Pb}$ ) was decreased in surface air, and in addition marine air mass containing lower level of  $^{210}\text{Pb}$  was transported to the continental consequently, the lower value of  $^{210}\text{Pb}$  can be observed in this period. In contrary, the higher level of  $^{210}\text{Pb}$  related to the cool air mass transportation from North America continent through Greenland (70 – 80 °N) to Finland. Higher level of  $^7\text{Be}$  associated with transportation of air mass (contains high level of beryllium) from Arctic and Russian continent low relative moisture in air prevents  $^7\text{Be}$  contained aerosol from washout by rain. Finally, lower measured value of  $^7\text{Be}$  and higher value of  $^{210}\text{Pb}$  observed in falls (winter) may be related to the decrease of air mass transportations thus  $^7\text{Be}$  was decreased while it increases the accumulation of  $^{210}\text{Pb}$  in surface air (Paateo et al., 2001).

Petrova (2009) measured the activity concentration of  $^7\text{Be}$  in surface air collected over 5 years at State Center of Sanitary Epidemiological Super Vision (Moscow, Russia) by using air sampler technique. Its maximum content in surface air was 11.3 – 11.8  $\text{mBq/m}^3$  ( 2000's year) depended onto: 1) The high production rate of  $^7\text{Be}$  in Stratosphere – Troposphere which associated to the proton flux from galactic cosmic ray (GCR); GCR is related to 11 years solar cycle, and 2) The seasonal variation of troposphere air mass intrusion to troposphere during occur often in spring – summer; supported by the higher value of  $^7\text{Be}$  content was observed in

this period of the year and the lower one was observed in falls – winter. In addition, a significant correlation between  $^{212}\text{Pb}$  ( $^{232}\text{Th}$  – series) and  $^7\text{Be}$  can be observed during falls – winter. Authors suggested that this may be related to the washing of atmospheric aerosol from the surface air by snow; lower values of  $^7\text{Be}$  and  $^{212}\text{Pb}$  were measured during this period (Petrova et al., 2001).

Sato (2003) reported seasonal variation in activity concentration in surface air of  $^7\text{Be}$  (BDL –  $4.2 \text{ mBq/m}^3$ ) and  $^{212}\text{Pb}$  ( $0.2 - 2.5 \text{ mBq/m}^3$ ) by using air sampler technique at Sarufutsu, Hokkaido (Japan); lowest and highest values can be observed during summer and winter, respectively. Author suggested that the higher values of their activity concentration are associated with meteorological event such as transportation of the contains high concentration of  $^7\text{Be}$  and  $^{232}\text{Th}$  air mass from Chinese continent, in contrary lower values are related with marine – time air mass contains low concentration of  $^7\text{Be}$  and  $^{232}\text{Th}$  (Sato et al., 2003).

Ueno (2003), who suggested that activity concentrations of  $^7\text{Be}$ ,  $^{40}\text{K}$ ,  $^{137}\text{Cs}$  and  $^{210}\text{Pb}$  in surface collected from Japan Atomic Energy Research Institute, Tokai – Mura (Japan) exhibited seasonal variations and depended on deposition weight (course and fine deposition particles).  $^{40}\text{K}$  and  $^{137}\text{Cs}$  have a significant correlation with course particles size, and their highest measured values are observed in spring. It is due to their similar chemical behavior and  $^{40}\text{K}$  is an essential element for growing of plants. The higher measured values of  $^7\text{Be}$  and  $^{210}\text{Pb}$  can be observed in winter and spring due to transportation of air mass (associated with fine deposition particles) from Siberian continent to study area (Ueno et al., 2003).

Azahra (2004) reported seasonal variation of  $^7\text{Be}$  and  $^{210}\text{Pb}$  in surface air at University of Granada ( $37^{\circ}10'50''\text{N}$   $3^{\circ}35' 44''\text{E}$ , Spain) from October 1993 to September 1997. Their highest and lowest values were observed on summer ( $7.6, 1.1 \text{ mBq/m}^3$ ) and falls ( $3.4, 0.2 \text{ mBq/m}^3$ ) respectively. It is due to the transportation of air mass from stratosphere to troposphere and accumulation of air mass over continental during summer period. In addition, there was linear



correlation between measured values of  $^7\text{Be}$  (as well as  $^{210}\text{Pb}$ ) and temperatures for dry deposition sampling, while precipitation rate (rain fall) is also correlated with their activity concentrations in surface air for wet deposition sampling. Author implied that local meteorology parameters (temperature and wash – out of atmospheric aerosol by rain fall) affect the activity concentration of  $^7\text{Be}$  and  $^{210}\text{Pb}$  (Azahra et al., 2004). Cho (2007) reported the seasonal variation of  $^7\text{Be}$  in surface air at Korea Atomic Energy Research Institute ( $35^{\circ}25'\text{N}$   $127^{\circ}22'\text{E}$ , 153 m above mean sea level). It ranges from 0.5 – 4.80  $\text{mBq}/\text{m}^3$  and highest value can be observed in summer. It is associated with the transportation of air mass (contains high  $^7\text{Be}$ ) over North of Asian continent/ Siberian and Arctic by cold – dry westerly winds (Cho et al., 2007).

Hirose (2004) reported in disagreement with 4 previous studies in Asia countries, by using air sampling technique atmospheric aerosol collected on the roof (10 m above ground) at Nagasaki ( $32^{\circ}45'\text{N}$   $129^{\circ}51'\text{E}$ ) and Tsukuba ( $36^{\circ}03'\text{N}$   $140^{\circ}08'\text{E}$ ) during 2000 – 2001. There was no seasonal variation in activity concentrations of  $^7\text{Be}$  and  $^{210}\text{Pb}$ , however their highest values were observed in spring and fall, respectively, due to vertical mixing of air mass between stratosphere and troposphere of the mid-latitude of northern hemisphere. In contrary, there was seasonal variation in activity concentration of  $^{232}\text{Th}$ , its highest values observed in March – May is associated to “*Kosa events*”; the transportation of Asian dust from Asian continent to Japan (Hirose et al., 2004).

Du (2008) suggested high values of flux of  $^{210}\text{Pb}$  ( $1.68 \pm 0.07 \text{ Bq}/\text{m}^2/\text{day}$ ) in air collected at University of Shanghai ( $31^{\circ}13'39''\text{N}$  –  $121^{\circ}23' 56''\text{E}$ ) observed in winter. It was not only from local precipitations and north – west monsoon which contains high concentrations 600 – 900  $\text{mBq}/\text{m}^2/\text{day}$  from Chinese continent to sampling area but also associated with the raising of Chinese’s economic growth; the increasing of building constructions, using coal in electricity generations etc.). While its lower values observed in summer may be associated with transportations of marine air mass containing low level of  $^{210}\text{Pb}$  (about 8  $\text{mBq}/\text{m}^2/\text{day}$ ). The

highest value of  $^7\text{Be}$  can be observed in spring and a factor controls its flux is stratosphere – troposphere air mass exchange in northern hemisphere which is occurred during the period of year. In addition, there was weak correlation between precipitation and their concentrations ( $r = 0.54$  for  $^7\text{Be}$ ;  $r = 0.23$  for  $^{210}\text{Pb}$ ), however the strong correlations between them were observed in summer ( $r = 0.87$ ), falls and spring ( $r = 0.92$ ) which are implied that they were presented into sampling site by the similar atmospheric deposition processes (Du et al., 2008).

Pharm (2011) reported the highest values of activity concentration of  $^{137}\text{Cs}$  and  $^{210}\text{Pb}$  observed in summer due to high emanation rate of  $^{222}\text{Rn}$  by solar heating and atmospheric inversion which increased and accumulated  $^{210}\text{Pb}$  in surface air. There were significant correlation between temperature and activity concentration in air of  $^7\text{Be}$  ( $r = 0.5$ ) and  $^{210}\text{Pb}$  ( $r = 0.43$ ), moisture and  $^{210}\text{Pb}$  ( $r = 0.41$ ) and precipitation and  $^{137}\text{Cs}$  ( $r = 0.51$ ). Not only stratosphere – troposphere air mass exchange or production rate of  $^7\text{Be}$ , but precipitation is also an important parameter reducing its concentration in surface air (and  $^{137}\text{Cs}$ ). The activity concentration of  $^{137}\text{Cs}$  in air is not only from the steal – smelter accident in Spain; presented in study area by transportation of air mass, but also from the re – suspension of soil dust (Pham et al., 2011).

An advantage of mosses is that it has no developed root system, the pollutant is uptake and accumulated into mosses leaf via atmospheric deposition of aerosol, thus mosses technique is also widely used as bio – monitoring for baseline concentrations and anomalies of heavy metal around industrial communities such as iron or nickel smelter in European countries (Culicov et al., 2002; Frontasyeva et al., 2004; Anicic et al., 2007; Barandovski et al., 2008) or around Capital city of Vietnam (Viet et al., 2010) or Petro – chemical industries located in Malaysia (Abdullah et al., 2012). Neutron activation analysis (NAA) is also performed for determination of the concentration of heavy metal (multi – elements) accumulated in mosses samples, however this method was not appropriate in order to determine some elements (for example Pb or Hg)

due to its detection limit, the alternative method such as Atomic absorption is also used for those elements (Culicov et al., 2002; Grodzinska et al., 2003; Ermakova et al., 2004)

The measured concentration of heavy metals were assessed for significant correlations between them, correlation with geographic or geology and their origins by using multivariate statistical method (Berg and Steinnes, 1997; Faus-Kessler, 2001; Smirnov, 2004); Principle component analysis (PCA) and cluster analysis (CA) (Grodzinska et al., 2003; Frontasyeva et al., 2004; Pesch et al., 2006; Gramatica, 2006; Dragović, 2009). For example, Na, Al, Ti, Fe, Sc, V, Cr, Cs, Ba, REE and Th are the crustal elements, Cu, As, Zn, Ni, Pb are originated from metal smelters, K, Mn, Sr from leaching of higher plants, while I, Ca and Na were associated with sea water. Those studied were reported from mines and metal industries from Romania (Culicov et al., 2002), heavy metal industrial zone in Poland and Rep. of Serbia (Frontasyeva et al., 2004). Heavy metal originated from bedrocks such as Ca and I, or higher plants (K and Sr). (Barandovski et al., 2008); Pb from lead in gasoline or phosphate fertilizer (Dragović et al., 2009). In addition, the enrichment factor (EF) is also used for determination of origin of Mn, Fe, V, Ni, Ca, V, Cr, Co, Zn and Br in moss collected around Belgrade (Rep. of Serbia). Their origins are coal – fired power plant and traffic, in addition, their concentrations associate with local windblown which those metals are transported from neighbor cities and accumulate in mosses (Anicic et al., 2007).

### 1.3 The present work

The purpose of this study are (1) To measure the activity concentrations of natural airborne radionuclides ( $^7\text{Be}$ ,  $^{210}\text{Pb}$  and  $^{210}\text{Pb}_{\text{ex}}$ ), terrestrial radionuclides ( $^{40}\text{K}$ ,  $^{226}\text{Ra}$ ,  $^{232}\text{Th}$  and  $^{238}\text{U}$ ) and anthropogenic radionuclide ( $^{137}\text{Cs}$ ) in Thai's moss samples collected around Hatyai City, Changwat Songkhla and Thai's moss samples collected from the Peninsular Thailand, and

(2) To explain the spatial distribution and correlations in their activity concentrations, furthermore, analyze for the probable factors affecting such distributions.

As previously describing, Chapter 1 introduces the necessities of environmental background radiations study and the conventional sampling methodology as well as the use of moss technique was promoted. The relevant literatures reviews were described; finally, the purpose of the thesis was focused and explained.

Chapter 2 is consideration of research methodology, which is consisted of field work/laboratory works, equipment and measuring instrument, brief of geography, meteorology and geology of sampling site setting. Consideration of moss sample collection & preparation, and instrumental and moss sample measurement.

Chapter 3 describes the activity concentration of studied radionuclides of moss samples into 2 categories; the first is from 3 sampling sites around Hatyai City, Changwat Songkhla and the second one is from 17 sampling sites located in Peninsular Thailand. The measured values are presented, explained and compared, their spatial distribution and correlation are described, furthermore, the probable factors affecting in such distributions are discussed.

Chapter 4 describes the conclusions and suggestions of this thesis; finally the future work is expected.

## Chapter Two

### Research Methodology

This study is a preliminary survey of natural terrestrial ( $^{40}\text{K}$ ,  $^{226}\text{Ra}$ ,  $^{232}\text{Th}$  and  $^{238}\text{U}$ ) and natural airborne radionuclides ( $^7\text{Be}$  and  $^{210}\text{Pb}_{\text{ex}}$ ) in moss samples collected from Peninsular Thailand. However, there was no any prior studying about the use of mosses as a promising media to determination of natural radionuclides in Thailand, thus the research methodology is separated into two categories.

The first category is performed for

- (1) Preliminary surveying in order to find the characteristic of sampling sites over the small areas where are the mosses growing on, and
- (2) Determine the activity concentration of studied radionuclides in collected moss samples.

The second category is performed for

- (1) Preliminary surveying in order to find the characteristic of sampling sites over the large areas from sampling sites located in the Peninsular Thailand.
- (2) Determine the activity concentrations of studied radionuclides in moss samples collected.
- (3) Explain the spatial distribution and correlations in activity concentrations of some radionuclides and analyze for the probable factors affecting such distributions.

Furthermore, the moss samples collection, moss samples preparation, the measurement of activity concentration of studied radionuclides, geography, meteorology, and geology of the sampling sites setting were described in this chapter.

## **2.1 Fieldwork/Laboratory works, equipment and measuring instrument**

### **2.1.1 Field work equipment setting**

In field work, the following equipment is used for moss samples collection at the selected sampling sites;

- 7" x 11" Plastic bags
- Elastic bands
- Labelers
- Gloves
- Shovels
- Magic pens
- GPS (Garmin Etrex, USA)

### **2.1.2 Laboratory work equipment setting**

Equipment for moss samples preparation at the Laboratory, Department of Physics (PSU) is

- Mesh grinder
- Salvers
- Scissors
- 2 – digits digital weighting apparatus ([OHAUS ARB 120, USA](#))
- Electronic oven
- 105 mm x 57 mm cylindrical plastic containers
- Plastic tape
- Labelers

### 2.1.3 Measuring instrument

- NIST standard reference material 4350B ([Columbia River sediment](#))
- HPGe gamma spectrometer with 100% relative efficiency (Canberra model GX10021, n-type, coaxial closed end).
- The bulk of lead shielding – total mass is 1,633 kg and 15 cm. in thickness. (Canberra model 777B).
- Genie 2000 acquisition system ([Canberra, USA](#)).

## 2.2 Methodology

Research methodology consists of 1) Brief of the geography, meteorology and geology of the sampling sites setting, 2) Moss sample collection, 3) Moss sample preparation, and 4) Instrumentation and moss sample measurement.

### 2.2.1 Brief of geography, meteorology, and geology of the sampling sites

The Peninsular Thailand located between the geographic latitude 7 – 12 °N and longitude 99 – 102 °E covers an area around 70,715 km<sup>2</sup>. The longest distance from the northern end to the southern end (Malaysia border) is about 750 km. The Peninsula geographically separated into two parts by a number of high mountains ridges laid in the center along the north to the south and affected the climate of each part. The eastern side of the peninsula is almost wet with high precipitation during November to February which is affected by the North – East monsoon associated with the transportation of cold air from the Chinese mainland and marine air masses from the Gulf of Thailand. This part is warm and dry in summer season (March to June), however there is often raining even in this period which is affected by some depression or typhoons. In contrast, the western side of the peninsula is affected by the South – West monsoon from the Indian Ocean to the Andaman Sea carrying mainly marine air masses. High precipitation during June to October makes the climate different of both sides ([Wangwongchai et al., 2005](#); [Tipayamongkholgul et al., 2009](#)).

The geologic setting of the Peninsula is divided into two parts which called middle and southern peninsular as shown in [Figure 2.1\(a\)](#) ([Bunopas, 1981](#); [Bhongsuwan, 1993](#)). The geology of the western side of middle peninsular is dominated by Permo – Carboniferous rock (Paleozoic sedimentary rock) which consists of mudstones and sandstones. Along the mountain areas from the north to the south, Mesozoic granite intrudes into Paleozoic sedimentary rock and is surrounded by narrow metamorphic aureoles. On the eastern side, Quaternary sediments deposit in valley floor and coastal areas, these areas were also surrounded by cultivation communities. There are two major active faults called Khlong Marui Fault (KMF) and Ranong Fault (RF). The first one lies in North - East direction from Changwat Phung Nga to Suratthani, and second one (RF) lies from Changwat Phung Nga to Ranong.

The southern peninsula extends south – eastward from Krabi and Suratthani Provinces to south of Songkhla and Narathiwat Provinces. A number of Granite Mountain lies from the north to the south in the middle part of the peninsula and continues into the Gulf of Thailand, where the Mesozoic granites are exposed and there are several basin of Cenozoic coal-bearing beds. There are some sampling sites located in forest mountains areas ([Suratthani, Nakorn Sithammarat and Pathalung Provinces](#)) near the Mesozoic granite exposures. In mountain ranges laying from the north to the south between Nakorn Sithammarat and Satun Provinces, Mesozoic granite intruded into the Paleozoic sedimentary rocks (Ordovician limestone) at many places where sampling sites are located. The sampling site in cultivated area in Trang Province located in the Mesozoic sedimentary terrain. At Songkhla Province, a Paleozoic sedimentary rock (Carboniferous shale) exposed at the northern part of Ko Yo, and extends southward into the north-western part of the Malay Peninsula.

## **2.2.2 Moss sample collection**

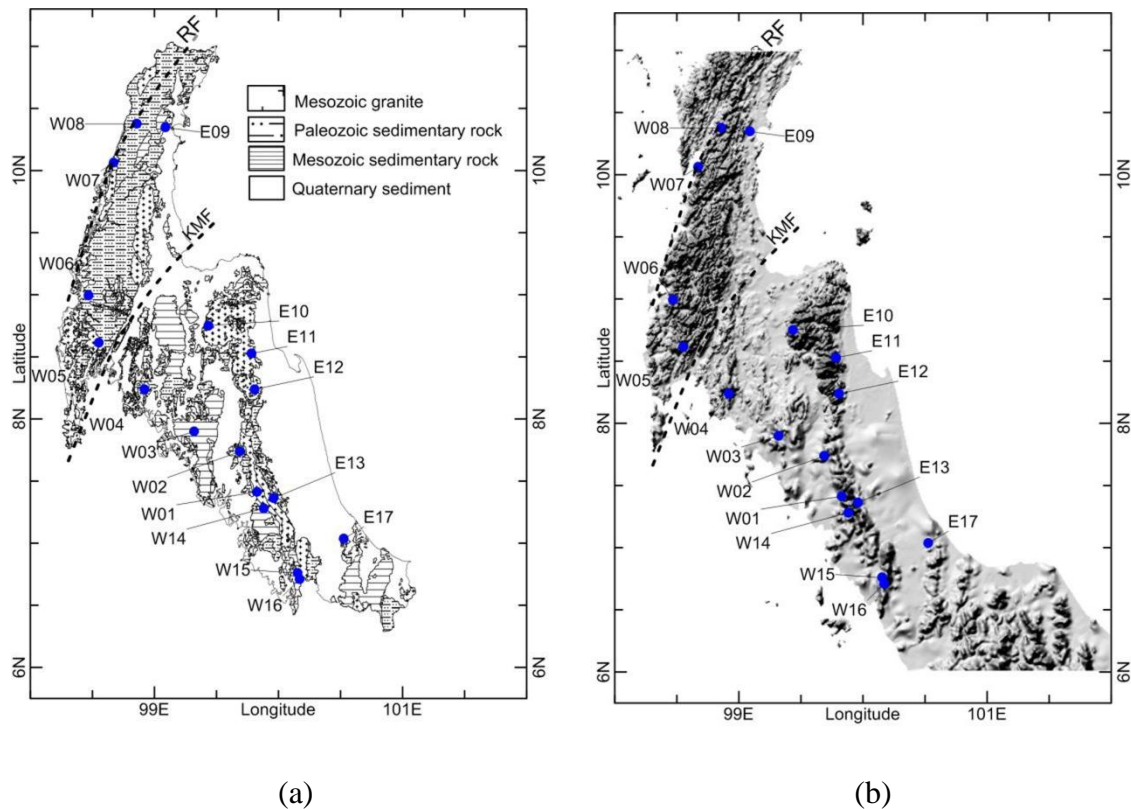
Moss sample collection is separated into 2 categories;

### **2.2.2.1 The first category: Sample collection around Hatyai City.**

The 9 moss samples of *Leucobrym aduncum* Dozy & Molk (Moss code, C) and *Leucobrym arfakianum* C. Muell (Moss code, R) were collected on January 2009 from 3 sampling sites around Hatyai City, Songkhla Province, during period of 2 days. Three moss



samples (M1 – KNN, M2 – KNN and M3 – KNN) are collected from Kho – Numkhang Nation Park located at 6.56°N 100.59°E. Tone – Ya – Plong waterfall locates at 7.00°N 100.46°E and two moss samples (M4 – TYP and M5 – TYP) are collected from this location. Four moss samples (M6 – TNC, M7 – TNC, M8 – TNC and M9 – TNC) are collected from Tone – Nga – Chang waterfall located at 7.23°N 100.46°E. Sampling sites locations, examples of sampling site (Tone – Nga – Chang waterfall) and moss sample (*Leucobrym aduncum* Dozy & Molk) are presented in **Figure 2.2**.



**Figure 2.1** Map of Peninsular Thailand, (a) simplified geologic map of the study areas and (b) SRTM digital elevation model of southern Thailand and sampling sites.

It was noted that;

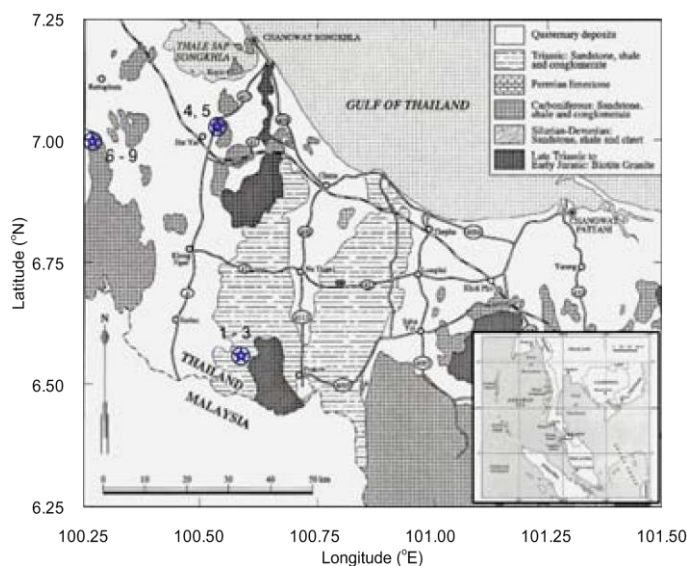
1) Samples number M1 – KNN, M3 – KNN, M5 – TYP, M7 – TNC and M8 – TNC were collected on the rock or roof under treetops, which are exposed to sunshine in some periods of the daytime.

2) Samples number M1 – KNN to M5 – TYP and M6 – KNN to M9 – TNC were collected in the mountainous area between the elevations of 800 – 850 m above mean sea level.

### 2.2.2.2 The second category: Sample collection around Peninsular Thailand.

The 46 moss samples from 17 sampling sites in the Peninsular Thailand were collected on March 2012. Sampling sites are presented in **Figure 2.1 (b)**, sampling sites W01 – W02, W04 – W06, W08, E12 – E13, W14 – W18 located in mountainous areas of National Parks and Wildlife Sanctuaries. These sites are far from the human activities and industrial zones. Sampling sites W03, W08, E10 and E17 located near the cultivated areas and human communities. Sites W01 – W08 and W14 – W16 are geographically on the west side of the Peninsula while E09 – E13 and E17 are on the east side. During the time of mosses sampling the peninsula faced the North - East monsoon coming from the Chinese continent and South China Sea.

The list of sampling sites, moss types, geographically latitude and longitude are presented in Table 2.1. An example of sampling site (Tone – Nga – Chang waterfall) is shown in Figure 2.2; moss sample collected and packed in the field as shown in Figure 2.3. At most sites, moss samples were collected in areas near water (small stream) with exception for sampling sites E11 – 2, E11 – 3, E11 – 4, E12 and W16. Four samples (E12 – 1 to E12 – 4) are collected from topsoil at the top of the mountain called Khao Ram Rome; at ~ 1,000 m above mean sea level.



(a)



(b)



(c)

**Figure 2.2** (a) Sampling sites locations, (b) Tone – Nga – Chang waterfall (<https://travel.thaiza.com/guide/262500/>) and (c) moss sample collected from Tone – Nga – Chang waterfall (*Leucobrym aduncum* Dozy & Molk)

**Table 2.1** Sites, altitude (above mean sea level), latitude and longitude of sampling sites, sampling code and type of moss samples.

Sample sites	Moss code	Moss type	Latitude (°N)	Longitude (°E)	Altitude a.s.l. (m)
W01 PSW	A	<i>Octoblepharum albidum Hedw.</i>	7.41285	99.8275	140
W02 PJ	B	<i>Himantocladium sp.</i>	7.73701	99.6865	200
W03 RCPW	C	<i>Leucobryum aduncum Dozy &amp; Molk</i>	7.89779	99.3180	175
W04-1 HT	D	<i>Thuidium sp.1</i>	8.23773	98.9178	130
W04-2 HT	D	<i>Thuidium sp.1</i>	8.23773	98.9178	130
W05-1 TPRV	C	<i>Leucobryum aduncum Dozy &amp; Molk.</i>	8.61369	98.5495	300
W05-2 TPRV	C	<i>Leucobryum aduncum Dozy &amp; Molk</i>	8.61369	98.5495	300
W05-3 TPRV	B	<i>Himantocladium sp.,</i>	8.61369	98.5495	300
W06-1 SPN	C	<i>Leucobryum aduncum Dozy &amp; Molk</i>	8.99510	98.4678	70
W06-2 SPN	E	<i>Barbella asp.</i>	8.99510	98.4678	70
W07 BYB	F	<i>Hyophila cf. involute (Hook. f.) A. Jaeger</i>	10.0651	98.6700	125
W08-1 BK	G	<i>Arthrocorpus schimperi Dozy &amp; Molk</i>	10.3755	98.8567	180
W08-2 BK	G	<i>Arthrocorpus schimperi Dozy &amp; Molk</i>	10.3755	98.8567	180
W08-3 BK	A	<i>Octoblepharum albidum Hedw.</i>	10.3755	98.8567	180
E09-1 KRR	A	<i>Octoblepharum albidum Hedw.</i>	10.3477	99.0891	75
E09-2 KRR	B	<i>Himantocladium sp.</i>	10.3477	99.0891	75
E09-3 KRR	Q	<i>Hypnaceae sp.</i>	10.3477	99.0891	75
E10-1 MT	Q	<i>Hypnaceae sp.</i>	8.75205	99.4355	215
E10-2 MT	B	<i>Himantocladium sp.,</i>	8.75205	99.4355	215

**Table 2.1** (Continue)

Sample sites	Moss code	Moss type	Latitude	Longitude	Altitude a.s.l. (m)
E11-1 PL	H	<i>Leucoloma sp.</i>	8.52734	99.7833	230
E11-2 PL	I	<i>Pyrrhobryum spiniforme</i> (Hedw.) Mitt.	8.52734	99.7833	230
E11-3 PL	J	<i>Thuidium sp.2</i>	8.52734	99.7833	230
E11-4 PL	Q	<i>Hypnaceae sp.</i>	8.52734	99.7833	230
E12-1 KHRR	E	<i>Barbella asp.</i>	8.23808	99.8053	1,010
E12-2 KHRR	F	<i>Hyophila cf. involute</i> (Hook. f.) A. Jaeger	8.23808	99.8053	1,010
E12-3 KHRR	K	<i>Mitthyridium sp.</i>	8.23808	99.8053	1,010
E12-4 KHRR	L	<i>Aerobryopsis sp.</i>	8.23808	99.8053	1,010
E13-1 PW	M	<i>Neckeropsis sp.,</i>	7.36241	99.9608	130
E13-2 PW	N	<i>Syrrhopodon cf. japonicus</i> (Besch.) Broth	7.36241	99.9608	130
E13-3 PW	O	<i>Leucobryum sanctum</i> (Brid.) Hampe	7.36241	99.9608	130
W14-3TT-TT	A	<i>Octoblepharum albidum</i> Hedw.	7.28154	99.8824	130
W14-4TT-TT	E	<i>Barbella asp.</i>	7.28154	99.8824	130
W14-5TT-TT	B	<i>Himantocladium sp.</i>	7.28154	99.8824	130
W14-6TT-TT	F	<i>Hyophila cf. involute</i> (Hook. f.) A. Jaeger	7.28154	99.8824	130
W15-1 YR	N	<i>Syrrhopodon cf. japonicus</i> (Besch.) Broth	6.75827	100.154	130
W15-2 YR	D	<i>Thuidium sp.1</i>	6.75827	100.154	130
W15-3 YR	D	<i>Thuidium sp.1</i>	6.75827	100.154	130
W15-4 YR	H	<i>Leucoloma sp.</i>	6.75827	100.154	130

**Table 2.1** (Continue)

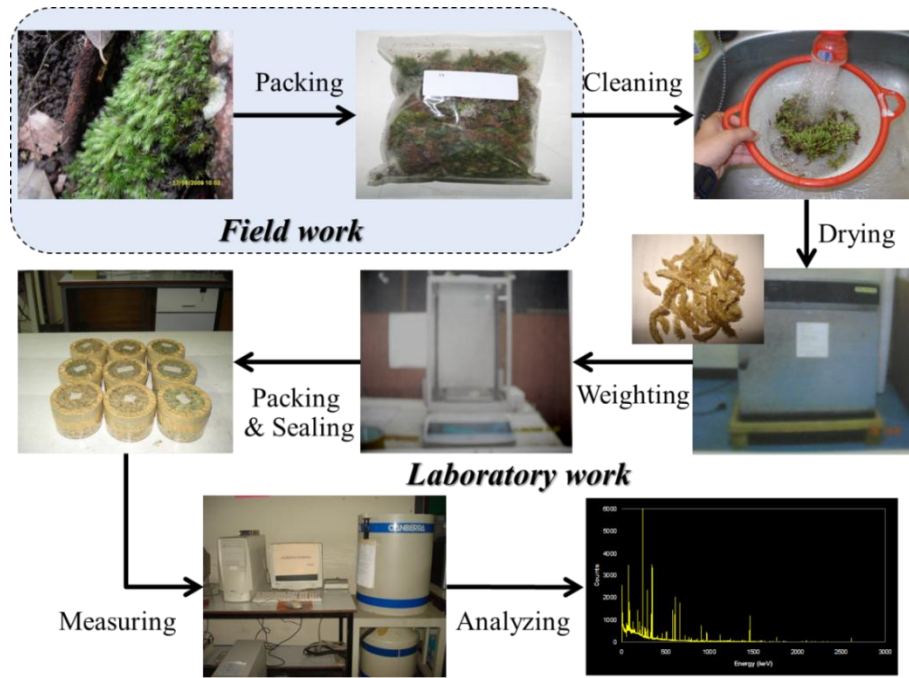
Sample sites	Moss code	Moss type	Latitude	Longitude	Altitude a.s.l. (m)
W15-5 YR	B	<i>Himantocladium sp.</i>	6.75827	100.154	130
W16-1 TLB	H	<i>Leucoloma sp.</i>	6.70919	100.169	160
W16-2 TLB	P	<i>Leucophanes glaucum</i> (Schwaegr.) Mitt.	6.70919	100.169	160
W16-3 TLB	N	<i>Syrrhopodon cf. japonicus</i> (Besch.) Broth	6.70919	100.169	160
W16-4 TLB	J	<i>Thuidium sp.2</i>	6.70919	100.169	160
E17 TYP	O	<i>Leucobryum sanctum</i> (Brid.) Hampe	7.03548	100.525	140

**Notice:****West side of the Peninsular Thailand** (W01 – W08 and W14 – W16):

PSW = Pri Sa Wan waterfall, PJ = Pak Jam waterfall, HT = Hoi Tho waterfall, RCPV = Roi Chan Pan Wung waterfall, TPRV = Ton Parivath waterfall, SPN = Sri Pung Nga National Park, BYB = Boon Ya Ban waterfall, BK = Bok Gluy waterfall, YR = Ya Roy waterfall and TLB = Thale Bun National Park.

**East side of the Peninsular Thailand** (E9 – E12 and E17):

KRR = Khang Roi Ru waterfall, MT = Muang Toud waterfall, PL = Pomlok waterfall, KhRR = Ram Rom Mountain, PR = Pri Wan waterfall, TT-TT = Ton Tok – Ton Tae waterfall and TYP = Ton Ya Plong waterfall.



**Figure 2.3** Mosses sampling, mosses sample preparation and analyzing of radionuclides content in moss samples.

Refer to 2 categories, all moss samples are collected under the similar conditions;

1) They were collected just only 2 – 10 m. beside stream line, due to the difficulty of finding the moss sample grew far from the water.

2) A variety in moss species was collected at the given sampling site because it is difficult to collect an identical moss at all different sampling sites.

3) At a given sampling location, 3 – 5 subsamples of an identical moss were collected around 50x50 m<sup>2</sup> area, and mixed in the field work.

4) The fresh moss samples were collected and kept in the plastic bags, labeled and returned to the laboratory.

### 2.2.3 Moss sample preparation

On return to the laboratory at Department of Physics, Faculty of Science, Prince of Songkla University, the fresh samples were prepared using the following procedure (as shown in **Figure 2.3**):

- 1) Moss samples are washed by tap water to remove soil and all other impurities.
- 2) The brown part of the samples were cut-out, only the green part were kept and dried at 104 °C and 24 hours with electronic oven to a constant weight; the different of fresh and dry weight shows the water content in sample varying between 83% and 94%.
- 3) Approximately 4.7 – 60.0 g of each dried moss sample were homogenized, packed into a cylindrical plastic container with a diameter of 105 mm and height 57 mm. and sealed with PVC tape to prevent the escape of airborne  $^{222}\text{Rn}$  (and  $^{220}\text{Rn}$ ) from the samples.
- 4) The dried moss samples were sent to identify their species by Assist. Prof. Dr. Sahut Chantanaorppint; Biologist & Lecturer of Department of Biology, Faculty of Science, Prince of Songkla University. Their species names and photographs are presented in **Table 2.2**.
- 5) All samples were stored for a month prior to the measurement in order to reach radioactive secular equilibrium between  $^{226}\text{Ra}$ ,  $^{228}\text{Ac}$  and their short – lives progenies.

**Table 2.2** Species names and photographs of moss samples












Moss type	Moss name	Photograph		
A	<i>Octoblepharum albidum</i> Hedw.,			
		W01 PSW	W08-3 BK	W09-1 KRR
				
		W14-3 TT-TT		
B	<i>Himantocladium sp.</i>			
		W02 PJ	W05-3 TPRV	E09-2 KRR
				
		E10-2 MT	W14-2 TT-TT	W14-5 TT-TT
				
		W15-5 YR		



Table 2.2 (Continue)











Moss type	Moss name	Photograph
C	<i>Leucobryum aduncum</i> <i>Dozy &amp; Molk</i>	 <p data-bbox="730 591 890 620">W03 RCPW</p>  <p data-bbox="979 591 1171 620">W05-1 TPRW</p>  <p data-bbox="1219 591 1410 620">W05-2 TPRW</p>  <p data-bbox="730 949 890 978">W06-1 SPN</p>
D	<i>Thuidium sp.1</i>	 <p data-bbox="730 1308 820 1337">W04-1</p>  <p data-bbox="979 1308 1069 1337">W04-2</p>  <p data-bbox="1219 1308 1308 1337">W15-2</p>  <p data-bbox="730 1666 820 1695">W15-3</p>
E	<i>Barbella asp.</i>	 <p data-bbox="730 2040 890 2069">W06-2 SPN</p>  <p data-bbox="979 2040 1155 2069">E12-1 KHRR</p>  <p data-bbox="1219 2040 1410 2069">W14-4 TT-TT</p>

Table 2.2 (Continue)


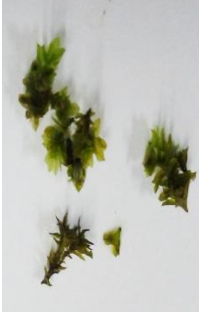















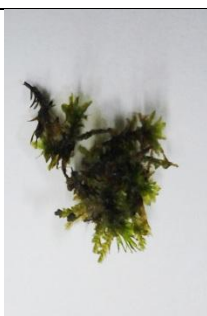






Moss type	Moss name	Photograph		
F	<i>Hyophila cf. involute</i> (Hook. f.) A. Jaeger			
		W07 BYB	E12-2 KHRR	W14-6 TT-TT
G	<i>Arthrocnemum schimperi</i> Dozy & Molk			
		W08-1 BK	W08-2 BK	
H	<i>Leucoloma sp.</i>			
		E11-1 PL	W14-1 TT-TT	W15-4 YR
				
		W16-1 TLB		
I	<i>Pyrrhobryum spiniforme</i> (Hedw.) Mitt.			
		E11-2 PL		

Table 2.2 (Continue)

Moss type	Moss name	Photograph		
J	<i>Thuidium sp.2</i>			
		E11-3 PL	W16-4 TLB	
K	<i>Mitthyridium sp.</i>			
		E12-3 KHRR		
L	<i>Aerobryopsis sp.</i>			
		E12-4 KHRR		
M	<i>Neckeropsis sp.</i>			
		E13-1 PW		
N	<i>Syrrhopodon cf. japonicus (Besch.) Broth</i>			
		E13-2 PW	W15-1 YR	W16-3 TLB

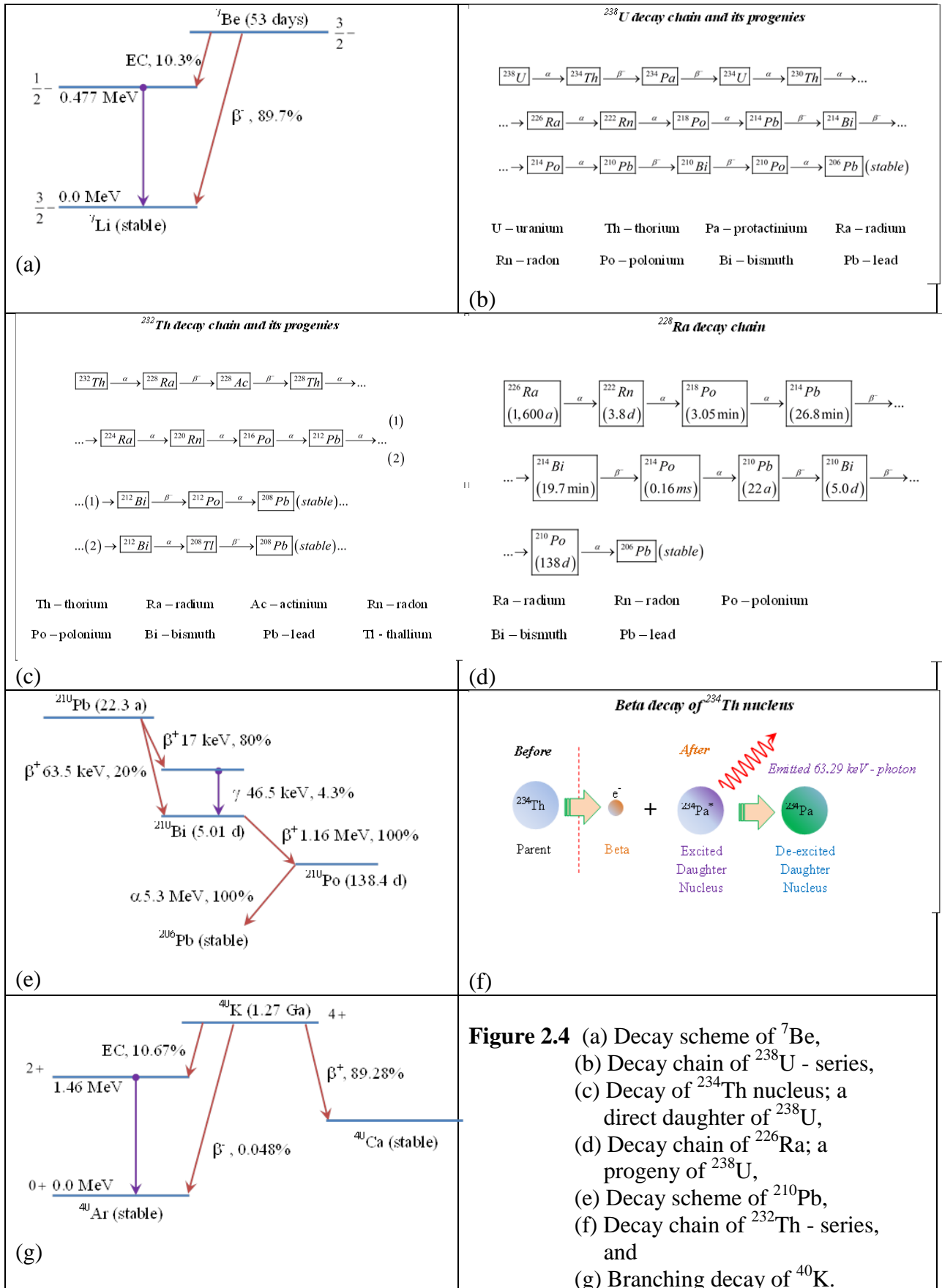
**Table 2.2** (Continue)

Moss type	Moss name	Photograph		
O	<i>Leucobryum sanctum</i> (Brid.) Hampe			
		E13-3 PW	E17 TYP	
P	<i>Leucophanes glaucum</i> (Schwaegr.) Mitt.			
		W16-2 TLB		
Q	<i>Hypnaceae</i> sp.			
		E09-3 KRR	E10-1 MT	E11-4 PL

### 2.3 Instrumentation and moss sample measurement

In order to measure the activity concentration of studied radionuclides, the sealed moss samples (**Figure 2.3**) were transported to Department of Physics, University of Novi Sad, Republic of Serbia. The gamma spectroscopy was carried out using high – resolution hyper purity germanium (HPGe) detector equipped by thin carbon window to allow detection of low energy gamma lines. The ultra-low background, large volume germanium spectrometer has 100% relative efficiency. The detector shield is constructed of layered bulk lead with 15 cm in total thickness. The lining materials are 1 mm low – background tin, and 1.5 mm high purity copper. The shield interior is flushed with nitrogen gas from the Dewar vessel in order reducing the background of  $^{222}\text{Rn}$  (as well as  $^{220}\text{Rn}$ ) and their progenies. The 8,196 channels MCA is used to recorded gamma spectra, and they are analyzed by using Genie 2000 acquisition system (Canberra, USA). The detector efficiency calibration is performed using the NIST standard

reference material 4350B (Columbia River sediment, Table 2.3) in same geometry with moss samples.



**Figure 2.4** (a) Decay scheme of  ${}^7\text{Be}$ , (b) Decay chain of  ${}^{238}\text{U}$  - series, (c) Decay of  ${}^{234}\text{Th}$  nucleus; a direct daughter of  ${}^{238}\text{U}$ , (d) Decay chain of  ${}^{226}\text{Ra}$ ; a progeny of  ${}^{238}\text{U}$ , (e) Decay scheme of  ${}^{210}\text{Pb}$ , (f) Decay chain of  ${}^{232}\text{Th}$  - series, and (g) Branching decay of  ${}^{40}\text{K}$ .

**Table 2.3** NIST – 4350B Standard Reference Materials

NIST-4350B River sediment – Radioactivity Certified Values -		85 g
<sup>241</sup> Am	.....	$1.5 \times 10^{-4}$ Bq/g
<sup>152</sup> Eu	.....	$2.90 \times 10^{-2}$ Bq/g
<sup>238</sup> Pu	.....	$1.3 \times 10^{-5}$ Bq/g
<sup>60</sup> Co	.....	$4.64 \times 10^{-3}$ Bq/g
<sup>154</sup> Eu	.....	$3.78 \times 10^{-3}$ Bq/g
<sup>239</sup> Pu + <sup>240</sup> Pu	.....	$5.08 \times 10^{-4}$ Bq/g
<sup>137</sup> Cs	.....	$2.90 \times 10^{-2}$ Bq/g
<sup>226</sup> Ra	.....	$3.58 \times 10^{-2}$ Bq/g

After background subtraction and peak analysis, activity concentration of radionuclides in moss samples was determined by the following procedure;

1) <sup>7</sup>Be was determined by intensity of 477.6 keV gamma line from it decays to excited state of <sup>7</sup>Li via EC, however after returned to the ground state those gamma is emitted as shown in **Figure 2.4** (a). Due to its short half – life ( $T_{1/2} = 53.3$  days) and delay time between sampling and measurement period, its measured activity concentration must be decay corrected back to moss sampling period by using Eq. (2.1)

$$A_0 = A_t e^{-\lambda t_d} \quad \dots \text{Eq. 2.1}$$

where

$A_0, A_t$  = Measured activity concentration of <sup>7</sup>Be (Bq/kg) at moss sampling period and end – of – measuring period, respectively

$\lambda$  = decay constant of <sup>7</sup>Be (0.013 /day)

$t_d$  = delay time between moss sampling period to measuring period (day)

2) The decay of <sup>238</sup>U is shown in **Figure 2.4** (b), measured activity concentration of <sup>238</sup>U was determined by intensity of 63.29 keV gamma line from decay of <sup>234</sup>Th (a direct daughter of <sup>238</sup>U) to excited state of <sup>234</sup>Pa as shown in **Figure 2.4** (c).

3) The weighted mean by intensity of 352 and 609 keV gamma lines from decay of <sup>214</sup>Pb and <sup>214</sup>Bi, respectively, were used to determine <sup>226</sup>Ra (**Figure 2.4** (d)).

4) Unsupported Lead-210 ( $^{210}\text{Pb}_{\text{ex}}$ ) is carefully calculated under assumption of radioactive equilibrium between the supported  $^{210}\text{Pb}$ ,  $^{214}\text{Bi}$  (and  $^{214}\text{Pb}$ ) and intensity of 46.5 keV gamma line from decay of  $^{210}\text{Pb}$  (**Figure 2.4** (e)).

5) The decay of  $^{232}\text{Th}$  is shown in **Figure 2.4** (f), its activity concentration was determined by weighted mean of  $^{212}\text{Pb}$  and  $^{228}\text{Ac}$  which presented in 238.6 and 911 keV gamma line, respectively.

6) Activity concentration of  $^{40}\text{K}$  is determined by intensity of 1,460 keV gamma line from it decays to excited state of  $^{40}\text{Ar}$  via EC as shown in **Figure 2.4** (g).

7) The intensity of 661.5 keV gamma line (excited state of  $^{137}\text{Ba}$ ) is used to determined activity concentration of  $^{137}\text{Cs}$ .

The activity concentrations (Bq/kg) of radionuclides are determined by the following equation:

$$A = \frac{N_s - N_b}{\varepsilon_\gamma Y t_s m K} \quad \dots \text{Eq. 2.2}$$

where

- A = activity concentration of measured radionuclide (Bq/kg)
- $N_s$  = net peak area of a given gamma energy (count)
- $N_b$  = a corresponding net peak area in background spectrum (count)
- $\varepsilon_\gamma$  = detector efficiency at a given photo-peak (cps/Bq)
- Y = the gamma-ray yield corresponding to a given peak energy
- $t_s$  = counting time (s)
- m = mass of sample (kg)
- K = corrected factors and

$$K = \prod_{i=1}^5 K_i \quad \dots \text{Eq. 2.3}$$

$K_1$  is corresponding to the delayed time ( $t_d$ ) from the time that sample was collected to the time that sample was measured, and half-life of such radionuclide ( $T_{1/2}$ ). It is given by

$$K_1 = e^{-\frac{0.693}{T_{1/2}} t_d} \quad \dots \text{Eq. 2.4}$$

$K_2$  is corrected factor for the radionuclides decay during measuring period ( $t_s$ ) as given by

$$K_2 = \frac{T_{1/2}}{0.693 t_s} \left( 1 - e^{-\frac{0.693}{T_{1/2}} t_s} \right) \quad \dots \text{Eq. 2.5}$$

$K_3$  is corrected factor for the self – attenuation from the bulk of samples, and it is defined by

$$K_3 = \frac{\varepsilon_s(\mu, E)}{\varepsilon_{std}(\mu, E)} \quad \dots \text{Eq. 2.6}$$

where

$\varepsilon_s(\mu_s, E)$  = detector efficiency at a given energy (E) for the sample with linear attenuation coefficient  $\mu_s$

$\varepsilon_{std}(\mu_{std}, E)$  = detector efficiency at a given energy (E) for standard with linear attenuation coefficient  $\mu_{std}$

If the composition or matrix of the sample and standard are the same thus  $K_3 = 1$ .

In the case of high decay rate of the sample, the number of count/counting signal were loss by resolution of the detecting system ( $\tau$ ).  $K_4$  is a factor which is performed for corrected the activity of sample, if R is the mean count rate of sample, thus  $K_4$  is defined by

$$K_4 = e^{-2R\tau} \quad \dots \text{Eq. 2.5}$$

It is noted that, if the sample count rate is low generally, thus  $K_4 = 1$ .



Finally,  $K_5$  is approximately to 1 for the case of there is no cascade of photon decay or photon emission of measured radionuclides. In addition, all gamma spectra were collected for a long time until the statistical uncertainty of Pb gamma line was low enough to provide accuracy of the activity concentration of Pb in moss samples less than 10%.

In addition, the activity concentration of studied radionuclides is limited by background count rate of any given gamma energy ( $R_{b,i}$ ); - minimum detectable activity (MDA). MDA is defined by Currie's equation (Currie, 1989)

$$MDA = \frac{2.71 + 4.65\sqrt{R_{b,i}}}{\varepsilon_{\gamma} \times Y_i \times t_m \times m} \quad \dots \text{Eq. 2.6}$$

In order to reasonable explanation of the results; general and multivariate statistical procedures (Berg and Steinnes, 1997; Faus-Kessler et al., 2001; Smirnov, 2004) were performed for data analysis by using the commercial statistics software package QI Macro 2015 for Windows. Pearson correlations between measured radionuclides were determined in order to clarify their relationship. Principal component analysis (PCA) is used to analyze for the patterns variables of elements that correlate and may be associated with their similar behaviors origin along the studied areas (Grodzinska et al., 2003; Frontasyeva et al., 2004; Pesch and Schroeder, 2006; Barandovski et al., 2008; Astel et al., 2008). PCA with VARIMAX normalized rotation was applied. Its principal factors were retained from the activity concentration of radionuclides when eigenvalue larger than unity as suggested by Kaiser Criteria (Kaiser, 1960). The PCA can be used to reduce the number of dimensions, while there is no loss of information (Krzanowski, 2000; Seddeek et al., 2009). Furthermore it can be also used to identify the sources of heavy metal pollutions (Culicov et al., 2002; Frontasyeva et al., 2004; Viet et al., 2010) as well as radionuclides (Tsikritzis, 2005; Popovic et al., 2008; Gordo et al., 2015). The cluster analysis (CA) with Ward's method is also applied in order to obtain the degree of association by a dendrogram showing clusters of radionuclides concentration as a function of their similarity. The distance axis displays the degree of association between groups of, i.e., the lower the value indicates the more significant correlation (Dragović and Mihailović, 2009; Elena et al., 2013). The PCA and CA were applied to activity concentration of measured radionuclides in moss samples collected; the results were presented and discussed. The brief of PCA and CA are presented in **Appendix A2**.

## Chapter Three

### Results and discussions

In order to meet the purpose of this study, the activity concentrations of studied radionuclides are measured by means of HPGe spectrometry with an ultra – low background configuration at the Department of Physics, University of Novi Sad, Republic of Serbia. The radionuclide contents in moss samples are determined, presented and discussed in this chapter.

#### 3.1 Activity concentration of $^7\text{Be}$ , $^{210}\text{Pb}_{\text{ex}}$ , $^{226}\text{Ra}$ , $^{232}\text{Th}$ and $^{40}\text{K}$ in moss samples collected around Hatyai City, Songkhla Province.

The several prominent gamma lines of studied radionuclides in 9 moss samples collected from sampling sites around Hatyai City can be observed after background subtraction consequently peak analysis, radionuclides contents in moss samples are shown in [Table 3.1](#). The airborne radionuclides,  $^7\text{Be}$  ranged from 130 – 340 Bq/kg with low variability in its activity concentration (mean =  $226 \pm 73$  Bq/kg), and  $^{210}\text{Pb}_{\text{ex}}$  ranged from 199 – 660 Bq/kg (mean =  $351 \pm 176$  Bq/kg). In contrast to both  $^7\text{Be}$  and  $^{210}\text{Pb}_{\text{ex}}$ , activity concentrations of terrestrial radionuclides ( $^{226}\text{Ra}$ ,  $^{232}\text{Th}$  and  $^{40}\text{K}$ ) have more variability and widely scatter.  $^{226}\text{Ra}$ ,  $^{232}\text{Th}$  and  $^{40}\text{K}$  ranged from 9 – 300 Bq/kg (mean =  $63 \pm 99$  Bq/kg), 3 – 327 Bq/kg (mean =  $67 \pm 111$  Bq/kg) and 21 – 109 Bq/kg (mean =  $55 \pm 29$  Bq/kg) respectively. It can be seen that, the lowest activity concentrations of studied radionuclides have been measured in moss samples collected from Kho – Numkhang Nation Park (M1 – KNN for  $^7\text{Be}$ ,  $^{226}\text{Ra}$  and  $^{232}\text{Th}$ , and M2 – KNN for  $^{210}\text{Pb}_{\text{ex}}$ ), and a moss sample collected from Tone – Nga – Chang waterfall (M6 – TNC for  $^{40}\text{K}$ ). The highest activity concentrations have been measured in moss samples collected from Tone – Nga – Chang waterfall (M6 – TNC for  $^{210}\text{Pb}_{\text{ex}}$ , M7 – TNC for  $^{226}\text{Ra}$  and  $^{232}\text{Th}$ , and M8 – TNC for  $^7\text{Be}$ ), and from Kho – Numkhang Nation (M3 – KNN). Furthermore, the higher value of mean activity concentrations of radionuclides (except  $^{40}\text{K}$ ) have been found in moss samples collected from Tone – Nga – Chang waterfall compared to the other sites.

There was no any previous study about the using terrestrial growing mosses as a promising media to monitor the natural radionuclides in Southern Thailand, it is difficult to compare the radionuclides content in moss samples of this study with their values measured

before. However, some initial notification and conclusions can be archived by the followed discussions.

**Table 3.1** Activity concentrations of studied radionuclides in moss samples collected around

Hatyai City.						
Sample location	Moss type	Activity concentration $\pm 1\sigma$ (Bq/kg)				
		$^7\text{Be}$	$^{210}\text{Pb}_{\text{ex}}$	$^{226}\text{Ra}$	$^{232}\text{Th}$	$^{40}\text{K}$
M1 – KNN	R	130±17	213±19	MDA < 9	3±14	59±23
M2 – KNN	C	216±28	199±18	MDA < 9	10±17	72±22
M3 – KNN	C	290±40	271±25	MDA < 14	18±26	109±12
	Mean	212±80	228±38	11±3	11±8	80±26
M4 – TYP	R	225±30	250±23	MDA < 10	19±21	29±8
M5 – TYP	R	142±24	231±22	16±2	30±27	35±10
	Mean	184±59	241±13	13±4	25±8	32±4
M6 – TNC	C	260±30	660±50	32±6	10±12	21±8
M7 – TNC	R	153±28	490±40	300±19	327±16	77±20
M8 – TNC	C	340±40	580±50	150±14	175±12	31±8
M9 – TNC	C	280±40	269±25	30±5	11±19	65±10
	Mean	258±78	500±169	128±128	131±152	49±27
All sampling sites	Mean	226±73	351±176	63±99	67±111	55±29

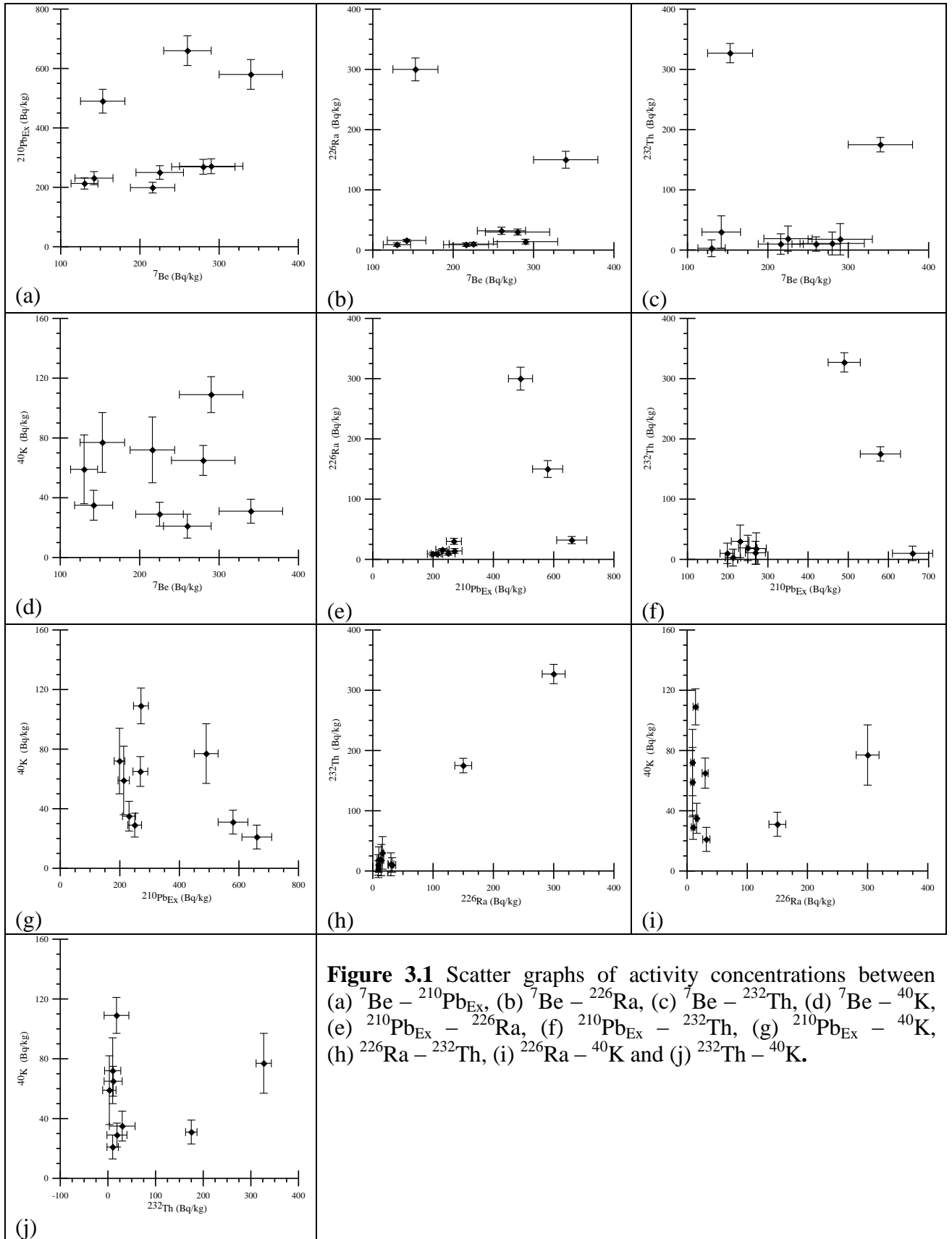
**Remark:** KNN = Kho – Numkhang Nation Park, TYP = Tone – Ya – Plong waterfall  
TNC = Tone – Nga – Chang waterfall, R = *Leucobrym arfakianum* C. Muell (M1, M4, M5 and M7), C = *Leucobrym aduncum* Dozy & Molk (M2, M3, M6, M8 and M9)

The measured activity concentration of radionuclides in a moss sample represents the average value of the whole moss samples of an area about 2,500 m<sup>2</sup> (50x50 m<sup>2</sup>) at a given sampling location. For this fact, it can be expected that the growing mosses were exposed with the approximately equal atmospheric depositions and re – suspension of soil dust particles. Thus both airborne and terrestrial radionuclides content in an identical moss should be the same. In contrary, if moss types are different, the different in radionuclides content should be observed, this due to the different in mosses morphology, uptake mechanism, retentions and leaching processes of radionuclides. It can be supported by the significant different of radionuclide contents in mosses collected from Kao – Numkhang Nation Park (M1 – KNN (*Leucobrym*

*arfakianum* C. Muell) and M2 – KNN (*Leucobrym aduncum* Dozy & Molk)) or from Ton – Nga – Chang waterfall (M7 – TNC (*Leucobrym arfakianum* C. Muell) and M8 – TNC (*Leucobrym aduncum* Dozy & Molk)).

The mean value of activity concentration of  $^7\text{Be}$  in this study is relative low compared the mean values from the measured value in literatures: 360 Bq/kg (England; [Sumerling, 1984](#)), 680 Bq/kg (India, 14°51'08"N; [Karunakara et al., 2003](#)) and 363 Bq/kg (Republic of Serbia, 42°26' – 45°23'N; [Krmr et al., 2007](#)). It can be expect that  $^7\text{Be}$  content in identical moss samples collected from a given sampling location should be the same. However, [Table 3.1](#) shows the different in  $^7\text{Be}$  contents in identical moss samples (M2 – KNN and M3 – KNN; M4 – TYP and M5 – TYP; M6 – TNC and M8 – TNC) are observed. This can explain by the screening of  $^7\text{Be}$  by moss covered plants; due to mosses M2 – KNN, M5 – TYP and M6 - TNC were collected under the treetops and exposed to the atmosphere in some period of daytime, thus amount of  $^7\text{Be}$  is screened by the plants grew over the moss. In addition, there was no precipitation during sampling period this mean that there was no any new incoming of  $^7\text{Be}$  contained aerosol was wash out from atmosphere and from moss covered plants into the moss samples. These may be a possible reason to explain the different measured values of  $^7\text{Be}$  in identical mosses are observed.

It is generally known that  $^7\text{Be}$  is reached into moss by dry and wet deposition, thus it should has no any significant correlation with other terrestrial radionuclides as shown in scatter graph ([Figure 3.1\(b\) – \(d\)](#)). For example,  $^{226}\text{Ra}$  content in moss samples was determined by weighted mean intensity of 358 and 609 keV gamma lines ( $^{214}\text{Pb}$  and  $^{214}\text{Bi}$ ) which are results of decay from  $^{238}\text{U}$ , while the decaying from  $^{222}\text{Rn}$  in atmospheric aerosol during sampling period can be neglected. In addition, [Figure 3.1 \(h\)](#) shows strong correlation between  $^{226}\text{Ra}$  and  $^{232}\text{Th}$  which is implied that they were transported to moss samples by the similar processes via re – suspension and re – deposition of surrounded soil dust particles. Although, the present of  $^{40}\text{K}$  in moss sample was came from surrounding soil dust however, however it was also present in moss sample by decaying of moss covered plants ([Belivermiş and Çotuk, 2010](#)) this can be supported by there was no correlation between  $^{40}\text{K}$  with  $^{226}\text{Ra}$  and  $^{232}\text{Th}$  as shown in [Figure 3.1 \(i\) and \(j\)](#).



The activity concentration of  $^{210}\text{Pb}$  is determined by using the detector with high efficiency in the low energy region the intensity of 45.6 keV gamma line. Although a part of

$^{210}\text{Pb}$  was deposited in mosses from  $^{238}\text{U}$  (and its daughters) contained soil – dust particle, however under the assumption of radioactive equilibrium in  $^{226}\text{Ra}$  and its progenies, activity concentration of supported  $^{210}\text{Pb}$  and unsupported  $^{210}\text{Pb}_{\text{ex}}$  in moss samples were carefully calculated. It can be seen that the mean value of activity concentration of  $^{210}\text{Pb}_{\text{ex}}$  in moss was higher than  $^{226}\text{Ra}$  in all moss samples with a factor of 5. The different in the mean value of measured activity concentration of  $^{226}\text{Ra}$  (and  $^{232}\text{Th}$ ) from 3 sampling sites can be observed (**Table 3.1**). For  $^{226}\text{Ra}$  content in 3 mosses collected from Kho – Numkhang Nation Park and one moss collected from Tone – Ya – Plong waterfall (M4 – TYP) were at under detection limit, while the its activity concentration in mosses collected from Tone – Nga – Chang waterfall ranged from 30 – 300 Bq/kg with mean value about  $131 \pm 152$  Bq/kg. Activity concentration of  $^{232}\text{Th}$  in moss samples exhibit similar trend as  $^{226}\text{Ra}$ , the lower values presented in the moss samples collected from Tone – Ya – Plong while the higher values from Tone – Nga – Chang waterfall. If uranium and thorium are originated from soil and deposited into moss by dry deposition of dust particles, their content in moss collected in sampling sites surrounded by cultivating soil dominant were generally high. This mean that soil dust is may be a significant source of natural radionuclide in moss (**Krmar et al., 2013**). Lower level of  $^{226}\text{Ra}$  (as well as  $^{238}\text{U}$ ) and  $^{232}\text{Th}$  (and its progenies) in mosses reflected their lower uptake the soil dust particles. In addition, it is difficult to find mosses far from the water because the moisture is a very necessary condition for their growing, furthermore there was frequently raining in Southern Thailand and it is possible that soil dust particles were washed from moss samples. This mean that almost of lead – 210 presented in moss is  $^{210}\text{Pb}_{\text{ex}}$  and activity concentration of  $^7\text{Be}$  and  $^{210}\text{Pb}_{\text{ex}}$  in moss samples shown the similar trend as presented in **Figure 3.1 (a)**, this may be implied that  $^{210}\text{Pb}_{\text{ex}}$  was probably deposited in moss samples by the aerosol deposition like  $^7\text{Be}$ .

Although the strong correlation between  $^{226}\text{Ra}$  and  $^{232}\text{Th}$  (**Figure 3.1 (h)**) was observed, however  $^{226}\text{Ra}$  content in moss samples are slightly lower than  $^{232}\text{Th}$ . In moss collected from sampling areas when the cultivated soil is dominant  $^{238}\text{U}$  (as well as  $^{226}\text{Ra}$ ) content in soil is slightly higher than  $^{232}\text{Th}$  and their content in moss samples exhibit the similar trend (**Bikit et al., 2005; Krmar et al., 2013**). Moss sampling sites in this study located in mountain areas where those mosses sit onto the sedimentary rock and metamorphic rock are dominant which the measured activity concentrations of  $^{226}\text{Ra}$  and  $^{232}\text{Th}$  are 16 and 40 Bq/kg for sedimentary (shale), 26 and 31 Bq/kg for metamorphic, 260 and 116 Bq/kg for granite (**Bhongsuwan, 2010**). This can be concluded that the measured activity concentration of  $^{226}\text{Ra}$  and  $^{232}\text{Th}$  in moss samples may associated to their activities in bed rock where moss samples sit on and gives a reasonable explanation why activity concentration of  $^{226}\text{Ra}$  is slightly lower than  $^{232}\text{Th}$  in moss samples.

The elevated values of  $^{226}\text{Ra}$  and  $^{232}\text{Th}$  (compared to their mean) in moss samples M7 – TNC and  $^{210}\text{Pb}_{\text{ex}}$  in moss sample M6 – TNC can be seen. Due to the difficult to find mosses; just only 2 – 10 meters beside the stream, however mosses collected from Kho – Numkhang Nation Park and Tone – Ya – Plong waterfall were far from the water or small stream line, in contrast to the those two moss samples collected from Tone – Nga – Chang waterfall were sit too close the big water fall and big stream line. Moss samples were exposed the moist air through the year before sampling and water from the water fall may contain the dissolved  $^{226}\text{Ra}$  and  $^{232}\text{Th}$  and even trough  $^{222}\text{Rn}$  and its progenies. Furthermore, the elevated of  $^{210}\text{Pb}_{\text{ex}}$  in moss M6 – TNC was not following the high value of  $^{226}\text{Ra}$  this mean that there was elimination of dissolved  $^{222}\text{Rn}$  in stream water around the stream line, consequently it was accumulated in this area and this may be the source of that lead – 210 in moss samples.

### **3.2 Activity concentration of $^7\text{Be}$ , $^{210}\text{Pb}_{\text{ex}}$ , $^{226}\text{Ra}$ , $^{232}\text{Th}$ and $^{40}\text{K}$ in moss samples collected around Peninsular Thailand.**

#### **3.2.1 General statistic of activity concentration of studied radionuclides**

The measured activity concentrations of both atmospheric and terrestrial radionuclides in all mosses samples collected in Peninsular Thailand are presented in **Table 3.2**. For statistical analysis, the means, median, standard derivations, skewness and kurtosis values are presented in **Table 3.2** and **Figure 3.2(a) – (f)**. Scatter graphs and Pearson's coefficients for correlation analysis of various radionuclides are also presented in **Figure 3.2** and **Table 3.3**.

It can be seen from **Table 3.2** that the measured activity concentrations are widely scattered;  $^7\text{Be}$  ranged MDA – 1,220 Bq/kg (mean = 295 Bq/kg),  $^{40}\text{K}$  ranged 34 – 1,157 Bq/kg (mean = 384 Bq/kg),  $^{226}\text{Ra}$  ranged 9 – 432 Bq/kg (mean = 145 Bq/kg),  $^{232}\text{Th}$  ranged 4 – 422 Bq/kg (mean = 97 Bq/kg),  $^{238}\text{U}$  ranged 16 – 406 Bq/kg (mean = 102 Bq/kg) and  $^{210}\text{Pb}$  ranged 135 – 1,630 Bq/kg (mean = 656 Bq/kg). The highest activity concentrations of  $^{40}\text{K}$ ,  $^{232}\text{Th}$  and  $^{238}\text{U}$  in moss sample W16 – 1 collected from Thalaie Bun National Park, while highest values of  $^7\text{Be}$ ,  $^{226}\text{Ra}$  and  $^{210}\text{Pb}$  are found in moss samples W04 – 1, W15 – 5 and W06 – 1 collected from

**Table 3.2** Activity concentrations ( $\pm 1\sigma$  interval) of radionuclides presented in moss samples.

Sample Site	Moss type	D.W. (g)	Activity concentration (Bq/kg) $\pm 1\sigma$ interval					
			<sup>7</sup> Be	<sup>40</sup> K	<sup>226</sup> Ra	<sup>232</sup> Th	<sup>238</sup> U	<sup>210</sup> Pb
W01 PSW	A	20.0	46±18	228±16	69±10	50±16	56±5	200±20
W02 PJ	B	15.0	201±29	163±17	56±26	31±6	37±4	201±19
W03 RCPW	C	15.8	260±30	135±16	15±18	13±22	50±30	135±12
W04-1 HT	D	20.0	1,220±80	233±17	190±40	58±28	96±6	143±17
W04-2 HT	D	25.0	730±50	318±16	67±22	51±3	56±4	711±29
W05-1 TPRV	C	18.0	210±30	386±23	210±40	90±10	113±6	573±21
W05-2 TPRV	C	20.0	96±26	357±18	175±23	88±7	106±6	1,490±30
W05-3 TPRV	B	20.0	74±17	369±15	164±29	79±4	94±4	1,350±40
W06-1 SPN	C	20.0	211±28	309±19	39±20	72±25	58±4	1,630±40
W06-2 SPN	E	20.0	156±24	160±15	30±30	33±6	16±3	1,580±40
W07 BYB	F	50.0	269±21	501±12	120±30	104±3	98±3	740±30
W08-1 BK	G	20.0	MDA ±70	34±10.0	25±14	17±17	40±26	758±20
W08-2 BK	G	8.2	MDA ±170	145±27	75±26	47±4	44±7	900±22
W08-3 BK	A	4.7	170±60	140±40	150±50	68±4	63±6	1,050±30
E09-1 KRR	A	18.5	BDL±80	86±11	13±13	15±16	40±26	853±23
E09-2 KRR	B	30.0	145±21	316±13	63±6	76±7	67±4	961±28
E09-3 KRR	Q	20.0	190±30	335±18	52±7	70±4	40±3	980±40
E10-1 MT	Q	20.0	390±40	320±21	330±30	59±6	105±6	710±25
E10-2 MT	B	30.0	192±25	395±15	259±25	66±19	93±4	1,180±40
E11-1 PL	H	30.0	800±50	210±13	90±50	81±10	72±4	307±15
E11-2 PL	I	20.0	510±50	532±21	90±50	62±5	57±4	440±20
E11-3 PL	J	20.0	220±30	191±15	30±50	29±7	38±4	309±19
E11-4 PL	Q	25.0	750±60	679±21	300±70	310±30	308±8	370±15
E12-1 KHRR	E	16.8	350±40	241±17	50±30	19.6±13	19±6	1,000±30
E12-2 KHRR	F	40.0	760±50	405±13	100±30	31±12	41±27	580±30
E12-3 KHRR	K	40.0	650±40	56±8	9±29	4.1±8	22±13	900±30
E12-4 KHRR	L	20.0	740±60	153±14	30±40	8.4±8	40±25	752±24
E13-1 PW	M	20.0	600±60	324±20	250±60	140±30	157±6	587±24
E13-2 PW	N	30.0	870±60	262±15	280±50	150±30	123±4	679.0±28
E13-3 PW	O	15.0	150±50	634±27	190±50	121±9	137±7	307±19
W14-1TT-TT	H	40.0	263±29	364±14	190±30	200±50	169±5	321±13
W14-2TT-TT	B	25.0	370±40	146±14	80±50	70±18	87±5	265±19
W14-3TT-TT	A	30.9	MDA ±80	549±17	139±16	112±10	107±4	444±24
W14-4TT-TT	E	22.9	MDA ±100	194±13	90±25	93±6	76±4	446±25
W14-5TT-TT	B	20.0	200±30	125±14	13±20	7.5±22	40±23	306±25
W14-6TT-TT	F	60.0	81±17	844±17	155±15	143±9	151±4	710±28
W15-1 YR	N	24.6	390±50	358±19	200±50	116±18	111±6	409±20
W15-2 YR	D	17.9	80±50	1,150±30	413±16	290±40	301±10	870±30
W15-3 YR	D	20.7	190±40	711±26	260±24	144±27	171±7	511±28
W15-4 YR	H	35.8	330±40	704±20	270±40	196±23	166±6	581±20
W15-5 YR	B	40.0	220±30	796±20	432±15	340±40	329±8	355±22
W16-1 TLB	H	40.0	156±29	1,157±27	428±23	422±21	406±10	590±23
W16-2 TLB	P	23.4	MDA ±100	424±19	130±14	52.2±22	61±4	676±17
W16-3 TLB	N	59.0	107±17	830±17	173±12	128±8	144±4	230±20
W16-4 TLB	J	23.7	80±30	364±17	135±10	52±6	67±4	400±40



**Table 3.2**  
(Continues)

Sample Site	Moss type	D.W. (g)	Activity concentration (Bq/kg) $\pm 1\sigma$ interval					
			<sup>7</sup> Be	<sup>40</sup> K	<sup>226</sup> Ra	<sup>232</sup> Th	<sup>238</sup> U	<sup>210</sup> Pb
E17 TYP	O	15.0	160±50	327±21	28±29	38±5	26±4	780±40
<b>Max</b>			1,220	1,157	432	422	406	1,630
<b>Min</b>			MDA	34.0	9	4	16	135
<b>Median</b>			201	326	125	70	74	589
<b>Mean</b>			295	384	145	97	102	656
<b>SD</b>			282	266	115	91	85	374
<b>Skewness</b>			1.352	1.287	0.950	1.928	1.960	0.908
<b>Kurtosis</b>			1.427	1.450	0.282	3.870	3.937	0.503

MDA = Minimum detectable activity

Hoi Tho waterfall, Ya Roi waterfall and Sri – Phung – Nga National Park, respectively. Furthermore, the highest values of measured activity concentration of <sup>7</sup>Be, <sup>40</sup>K, <sup>226</sup>Ra, <sup>232</sup>Th and <sup>238</sup>U are higher than their mean values by factor of 5, except <sup>210</sup>Pb the factor was about 3.

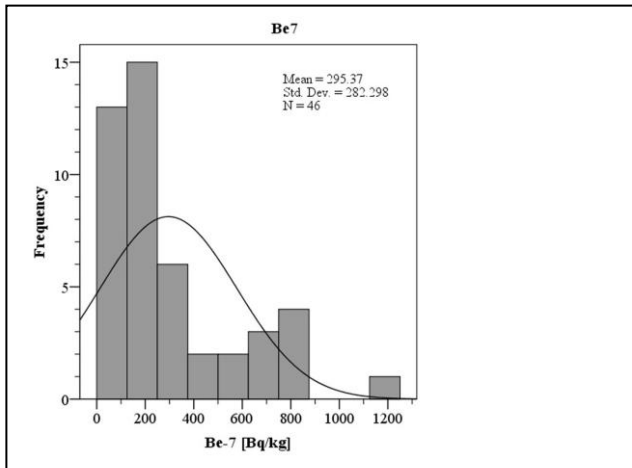
It should be noted that, the activity concentration of <sup>7</sup>Be in moss samples W08 – 1, W08 – 2, E09 – 1, W14 – 3, W14 – 4, and W16 – 2 (below MDA: < 70 Bq/kg, < 170 Bq/kg, < 80 Bq/kg, < 80 Bq/kg, < 100 Bq/kg and < 100 Bq/kg, respectively). The half – life of <sup>7</sup>Be is about 53 days and there is a long delay from field sampling to sample analysis (over 4 months). After field sampling in early March 2012, it took two weeks with sample preparation in the laboratory (Prince of Songkla University, Thailand), it was about a month later for samples transportation to Novi Sad (Rep. of Serbia), and finally it was about 2 months later for the sample analysis (June – July 2012). Consequently, if <sup>7</sup>Be had accumulated in the moss that was sampled, on measurement about 4 months later its activity had decayed to below MDA.

The radionuclide contents in different species of moss samples collected in the same sampling location are observed to vary (Table 3.2) as similar as the Section 3.1. Additional example, in moss samples W08 – 1 and W08 – 2 (*Arthrocnemum schimperi* Dozy & Molk.), W14 – 2 and W14 – 5 (*Himantocladium sp.*), most radionuclides contents differ significantly. On the other hand, there are the different of <sup>7</sup>Be and <sup>210</sup>Pb in samples W05 – 1 and W05 – 2 (*Leucobryum aduncum* Dozy & Molk.) but the <sup>40</sup>K, <sup>226</sup>Ra, <sup>232</sup>Th and <sup>238</sup>U are almost the same.

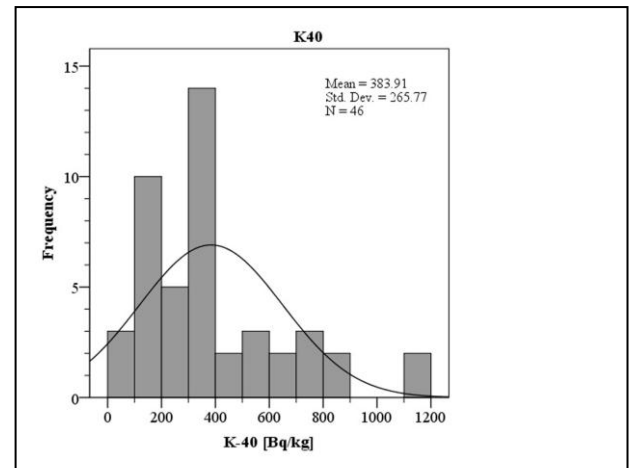
These study results have been similar to those observed in the literatures (Mietelski et al., 2000; Al-Masri et al., 2005; Dragović et al., 2010), and this can be confirmed that the radionuclides content in mosses can be significantly different depending on their species, which is explained by the difference of morphological structures in moss samples. The different in their

species could have diverse uptake mechanisms; interception and retention of airborne radionuclides are mainly affected by the surface morphology and degree of local shelter (moss covered plants), level of saturation and adsorption at different concentration intervals and competition between mosses and their covered plants (Boileau et al., 1982; Zechmeister, 1995; Denayer et al., 1999). The difference in  $^7\text{Be}$  and  $^{210}\text{Pb}$  content between identical mosses at the same particular sampling location can be explained by the difference of growth strategies of the bryophytes. As the previous results in Section 3.1, another good example is moss sample W05 – 1 and W05 – 2, the first one grows on a rock, under the tree trunk and directly exposed to the atmosphere all daytimes, while the other one grows on the top soil, covered by higher plants and it was exposed to the atmosphere for a few period of daytime (as similar as moss sample W08 – 1 and W08 – 3). In general, in most sampling sites, mosses were covered by a number of vascular plants which have ability to retain the aerosols from atmospheric deposition processes (Sugihara, 2008). These mean that atmospheric aerosols may be attached onto the plant leaves by wax or resin and ability for retaining the rain water in the process of ‘wet deposition’. In addition, during a sampling period the moss samples were collected in an area about 2,500 m<sup>2</sup> (50x50 m<sup>2</sup>), it can be expected that identical mosses (as well as different) are exposed to a similar atmospheric depositions and re-suspension of soil dust particles in the same habitat, then the radionuclide contents are generally different probably due to the growth strategy of the bryophytes. It can be also supposed that the different covering mosses will have a significant effect of the concentration of airborne radionuclide in them. The mosses samples grown in open field areas were exposed directly to the atmospheric deposition of airborne radionuclides. In contrast, trees or covered-plants will significantly affect the uptake of airborne radionuclides for underlying mosses samples.

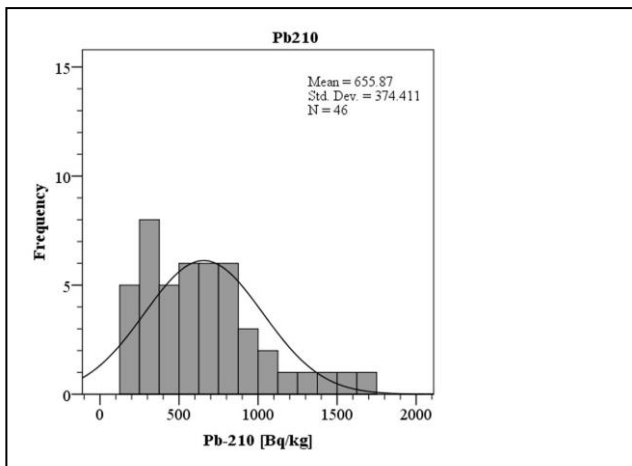
The frequency distributions of  $^7\text{Be}$ ,  $^{40}\text{K}$ ,  $^{226}\text{Ra}$ ,  $^{232}\text{Th}$ ,  $^{238}\text{U}$  and  $^{210}\text{Pb}$  content in moss samples are presented in Figure 3.2, their skewness and kurtosis are also presented in Table 3.2. Table 3.2 shows the low positive value of kurtosis coefficients, it can be seen that only  $^{226}\text{Ra}$  and  $^{210}\text{Pb}$  follow normal pattern approximately, and  $^7\text{Be}$ ,  $^{40}\text{K}$ ,  $^{232}\text{Th}$  and  $^{238}\text{U}$  show non – normal distribution. In addition, the highest measured values of  $^{40}\text{K}$  and  $^{226}\text{Ra}$  are within  $3\sigma$  - interval about the mean values while the highest measured values of  $^{232}\text{Th}$  and  $^{238}\text{U}$  are within  $4\sigma$  - interval about their mean values. Pearson’s coefficients presented in Table 3.3 show a strong correlation between terrestrial radionuclides,  $^{238}\text{U} - ^{232}\text{Th}$  ( $r = 0.978$ ,  $p < 0.05$ ),  $^{226}\text{Ra} - ^{238}\text{U}$  ( $r = 0.885$ ,  $p < 0.05$ ),  $^{210}\text{Pb} - ^{210}\text{Pb}_{\text{ex}}$  ( $r = 0.961$ ,  $p < 0.05$ ), intermediate correlation between  $^{226}\text{Ra} - ^{40}\text{K}$  ( $r = 0.750$ ,  $p < 0.05$ ), however the correlation between  $^{226}\text{Ra}$  and  $^{210}\text{Pb}$  (as well as  $^{210}\text{Pb}_{\text{ex}}$  and  $^7\text{Be}$ ) was not observed.



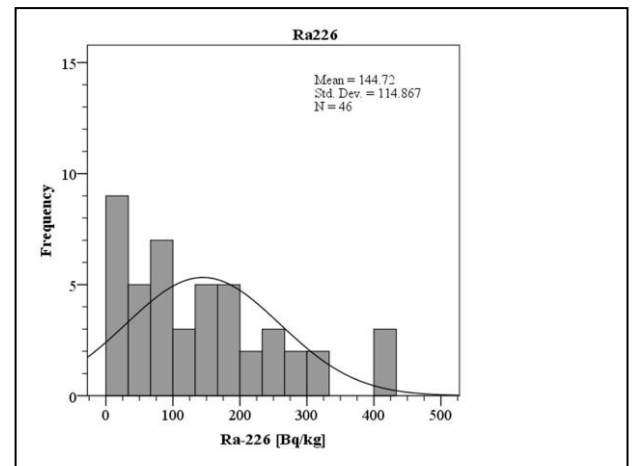
(a)



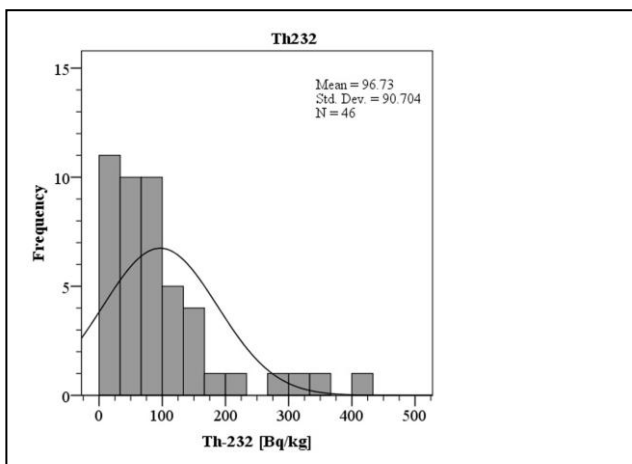
(b)



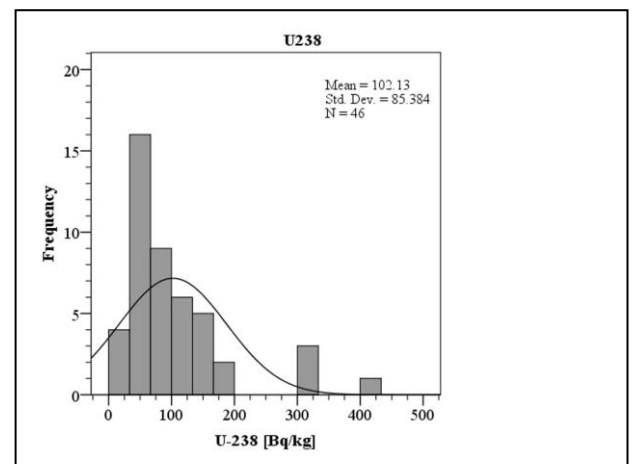
(c)



(d)



(e)



(f)

**Figure 3.2** Frequency distributions of measured radionuclides (a)  $^7\text{Be}$ , (b)  $^{40}\text{K}$ , (c)  $^{210}\text{Pb}$ , (d)  $^{226}\text{Ra}$ , (e)  $^{232}\text{Th}$  and (f)  $^{238}\text{U}$ .

In this study, PCA with VARIMAX rotation is applied to determine the relationship between studied radionuclides. The processes affecting in moss samples, **Table 3.4** presents the total variances of seven components, by using Kaiser's criteria which accepted only eigenvalues more than unity. The first two PC were selected and explained about 81.34% in total variances of dataset, the factor loadings of radionuclides contents were calculated and shown in **Table 3.5**.

A high positive loading value in each components class of the variables can be observed. They indicate that PC1 (accounted for 52.42%) included the terrestrial radionuclides with high positive loadings 0.973 ( $^{238}\text{U}$ ), 0.964 ( $^{232}\text{Th}$ ), 0.914 ( $^{226}\text{Ra}$ ) and 0.908 ( $^{40}\text{K}$ ). The PC2 (28.92%) contained the lead – 210 with high positive loading 0.957 ( $^{210}\text{Pb}$ ) and 0.913 ( $^{210}\text{Pb}_{\text{ex}}$ ), and  $^7\text{Be}$  with intermediate negative loading (-0.499). **Figure 3.3 (a)** illustrates the factor score plot (component 1 vs. component 2) that reveals the two clearly different groups. The x-axis represents PC1 while the y-axis is the PC2; therefore the closest variables to each axis will be associated with the first and the second factors, respectively. In agreement with PCA, CA results are illustrated in a dendrogram (**Figure 3.3 (b)**). The studied radionuclides were grouped into 3 statistically significant separated clusters, where  $^{238}\text{U}$ ,  $^{232}\text{Th}$ ,  $^{226}\text{Ra}$  and  $^{40}\text{K}$  are combined in the first branch (Cluster 1),  $^{210}\text{Pb}$  and  $^{210}\text{Pb}_{\text{ex}}$  are grouped in the second one (Cluster 2) and  $^7\text{Be}$  is clustered in the last branch (Cluster 3). The radionuclides composed in PC1 (in CA as well) is a factor that links the local surrounding soil dust. This may indicate that they are accumulated into mosses by the similar sources and atmospheric deposition processes and it can be called “**Factor of soil dust origin**”. On the other hand, the  $^{210}\text{Pb}$ ,  $^{210}\text{Pb}_{\text{ex}}$  and  $^7\text{Be}$  are composed together in PC2 which can be called “**Factor of atmospheric aerosol origin**”. However, these atmospheric radionuclides are laid in two separated clusters; it is due to the fact that  $^7\text{Be}$  and  $^{210}\text{Pb}$  possess the different atmospheric origins even though they are presented in moss samples by similar processes (i.e., atmospheric wet/dry depositions). It is supported by (1) there is no correlation between  $^7\text{Be}$  and  $^{210}\text{Pb}$  ( $r = -0.238$ ) and (2) their opposite factor loading score. This implies that there are other atmospheric processes as well as other geographic conditions affecting radionuclide content in moss samples, the results will be discussed in **Section 3.2.3**.

In addition, if  $^{210}\text{Pb}$  originates from the soil dust or bed rock where mosses are seated, it should deposit into moss by the same processes as  $^{226}\text{Ra}$ ; however, there is no correlation between  $^{226}\text{Ra}$  and  $^{210}\text{Pb}$  (as well as  $^{210}\text{Pb}_{\text{ex}}$ ). Because of the unsupported lead – 210 is calculated under the assumption that secular equilibrium between  $^{226}\text{Ra}$ ,  $^{214}\text{Pb}$  and  $^{214}\text{Bi}$  are maintained while a strong correlation between  $^{210}\text{Pb}$  and  $^{210}\text{Pb}_{\text{ex}}$  ( $r = 0.961$ ) is observed, these may imply that the most of lead – 210 presented in moss samples are unsupported and occurred by the decay of radon in air around the sampling site.

**Table 3.3** Pearson's correlation analysis of studied radionuclides.

	Altitude	<sup>7</sup> Be	<sup>40</sup> K	<sup>226</sup> Ra	<sup>232</sup> Th	<sup>238</sup> U	<sup>210</sup> Pb	<sup>210</sup> Pb <sub>ex</sub>
Altitude	1.000	0.365	-0.200	-0.225	-0.279	-0.247	0.100	0.156
<sup>7</sup> Be		1.000	-0.149	0.073	-0.015	0.004	-0.238	-0.237
<sup>40</sup> K			1.000	0.750	0.821	0.830	-0.101	-0.306
<sup>226</sup> Ra				1.000	0.848	0.885	-0.102	-0.372
<sup>232</sup> Th					1.000	0.978	-0.146	-0.371
<sup>226</sup> Ra						1.000	-0.191	-0.423
<sup>210</sup> Pb							1.000	0.961
<sup>210</sup> Pb <sub>ex</sub>								1.000

**Table 3.4** Total variance explained for the analyzing of moss samples.

Component	Initial Eigenvalues			Extraction Sums of Squared Loadings			Rotation Sums of Squared Loadings		
	Total	% of Variance	Cumulative %	Total	% of Variance	Cumulative %	Total	% of Variance	Cumulative %
1	3.860	55.136	55.136	3.860	55.136	55.136	3.670	52.423	52.423
2	1.835	26.207	81.343	1.835	26.207	81.343	2.024	28.920	81.343
3	0.898	12.823	94.167						
4	0.227	3.245	97.412						
5	0.164	2.336	99.748						
6	0.017	0.246	99.994						
7	0.000	0.006	100.000						

**Extraction Method:** Principal Component Analysis.

**Table 3.5** Factor loadings for the analyzing of moss samples.

	Component	
	PC1	PC2
<sup>7</sup> Be	-0.101	-0.499
<sup>40</sup> K	0.908	0.018
<sup>226</sup> Ra	0.914	-0.081
<sup>232</sup> Th	0.964	-0.069
<sup>238</sup> U	0.973	-0.118
<sup>210</sup> Pb	-0.094	0.957
<sup>210</sup> Pb <sub>ex</sub>	-0.342	0.913

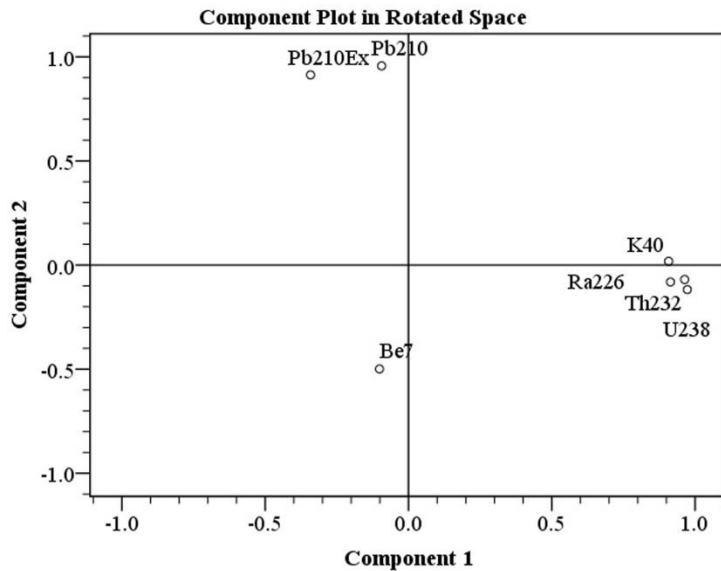
**Extraction Method:** Principal Component Analysis.

**Rotation Method:** Varimax with Kaiser Normalization.

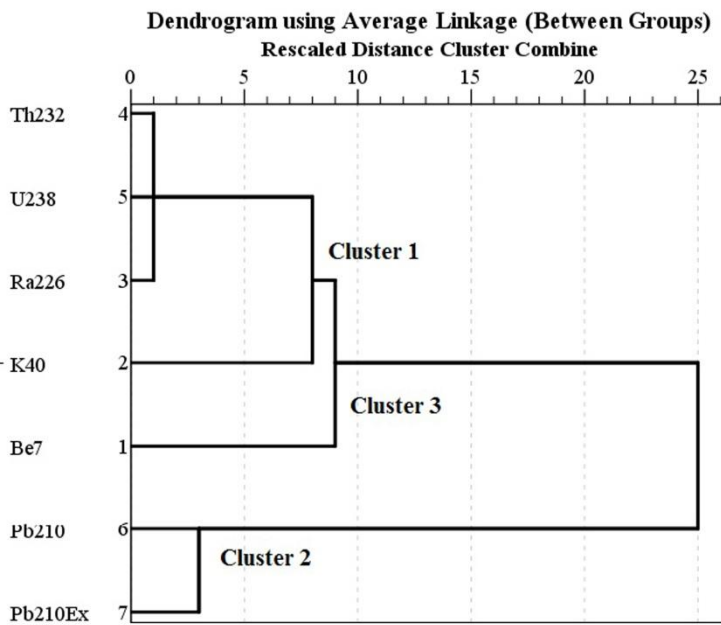
### 3.2.2 Spatial distribution, correlation and probable factors affecting to the activity concentration of terrestrial radionuclides; $^{40}\text{K}$ , $^{226}\text{Ra}$ , $^{232}\text{Th}$ and $^{238}\text{U}$ .

**Figure 3.4(a)** shows a strong correlation between  $^{238}\text{U}$  and  $^{232}\text{Th}$  in selected moss samples with  $r = 0.978$  ( $p < 0.05$ ), and ratio of  $^{232}\text{Th}$  and  $^{238}\text{U}$  ( $^{232}\text{Th}/^{238}\text{U}$ ) is ranged from 0.2 to 2.1 and it is approximately unity. Correlation between  $^{226}\text{Ra}$  and  $^{238}\text{U}$  concentrations is also strong with  $^{226}\text{Ra}/^{238}\text{U}$  ranged from 0.3 to 3.1, but  $^{226}\text{Ra}$  concentration is generally slightly higher than  $^{238}\text{U}$  as shown in **Figure 3.4(b)**. This means a low degree of secular equilibrium in uranium-238 series in moss samples. In general disequilibrium may be affected by a number of factors such as degrees of rock weathering, oxidation/reduction processes which correspond to occurrence and physical and chemical behavior of uranium and radium (Psichoudaki and Papaefthymiou, 2008). In fact almost moss samples are collected not far from the water stream or close to a waterfall, a possible explanation for the disequilibrium of radium and uranium in the moss samples is their respective solubility in natural water. It is generally known that in a similar fashion to the alkaline earth elements, radium presents only one valence state (+H), and the  $\text{Ra}^{2+}$  ion is moderately soluble in natural water while its isotopes are strongly absorbed onto riverine particles and tend to bind with sediment in a river (Silva et al., 2006). Radium solubility increases with salinity due to desorption and diffusion from estuarine and coastal sediments and river-borne suspended particulates (Moore, 1969; Moore, 1981). The solubility of uranium depends on its valence state, and it forms various soluble complexes with carbonate, phosphate, sulfate, fluoride and silicate ions, and adsorbs onto organic compounds (Ivanovich and Harmon, 1992). The most often encountered complex in natural waters is the soluble uranyl carbonate complex ( $\text{U}^{6+}$ , oxidizing condition) linked with organic matter in riverine, estuarine and coastal sediments (Langmuir, 1978). As with radium, uranium is also more soluble in saline water than in fresh water (Mlakar and Branica, 1994; Djogić et al., 2001), but Landais suggested that dissolved uranium in fresh water is low due to its sorption onto particulate organic matter and carbonate particles (Landais, 1996). In this study, the sampling sites are located in mountain areas far from human communities, so the main sources of dissolved uranium and radium are probably bed rocks and soil dust. Almost all the moss samples were collected close to a stream or waterfall, for example W01 PSW, W02 PJ, W04 HT on the west side and E10 MT, E13 PW on the east side, and the measured activity concentration of  $^{226}\text{Ra}$  was higher than of  $^{238}\text{U}$  (or  $^{226}\text{Ra}/^{238}\text{U}$  larger than unity), reflecting the slightly greater solubility of radium compared to uranium in fresh water. The additional  $^{226}\text{Ra}$  ( $^{226}\text{Ra}_{\text{excess}}$ ) could be dissolved into water and transported to the mosses. Moreover, this can also explain the significantly elevated level (over 4 fold the mean values) of activity concentration of  $^{226}\text{Ra}$  and  $^{232}\text{Th}$  in sample sites W15 – 5 (B,

*Himantocladium sp.*) and W16 – 1 (*H. Leucoloma sp.*) where moss sampling areas located near the big waterfall.



(a)



(b)

**Figure 3.3** (a) Component plot in a rotated space for 7 radionuclides and (b) A dendrogram is obtained by cluster analysis for activity concentrations in moss samples; the degrees of correlation between variables are related to the distances.

As well as  $^{238}\text{U}$ ,  $^{232}\text{Th}$  is showing a strong correlation with  $^{226}\text{Ra}$  as shown in [Figure 3.4\(c\)](#), but radium content in moss samples is generally higher than thorium. It is contrary when

compared with the pilot results from [Section 3.1](#). Krmar suggested that the difference of bedrock (mostly shale and granite) at the sampling site is a possible reason to explain why thorium is slightly higher than radium (and uranium) (Krmar et al., 2013). Thus the sampling sites number E17 (Ton Yha Plong Waterfall) in this study is at the same place as sampling area analyzed in [Section 3.1](#), it is interesting to compare the obtained results. Clearly the activity concentrations of  $^{226}\text{Ra}$  and  $^{232}\text{Th}$  in moss samples from this site are comparable with the previous study. However, the previous results were obtained from a small number of sampling sites (3 sampling sites) and with short distances between the sites (not more than 50 km from site-to-site), while in this current study there were 17 sampling sites covering about 800 km distance of peninsular Thailand. The measured activities of  $^{226}\text{Ra}$  and  $^{232}\text{Th}$  in various rocks from peninsular Thailand were reported as 260 and 116 Bq/kg for granite rock, 16 and 40 Bq/kg for sedimentary rock, and 26 and 31 Bq/kg for metamorphic rock (Bhongsuwan, 2010). Analogous to the discussion by Krmar (Krmar et al., 2013), radium will be generally higher than thorium when the bedrock in the sampling site is granite, and less than thorium for sites where the bedrock is sedimentary or metamorphic.

The mean value of  $^{40}\text{K}$  in moss samples is higher than the means of  $^{232}\text{Th}$  and  $^{238}\text{U}$ . It is known that the average activity concentration of  $^{40}\text{K}$ :  $^{232}\text{Th}$ :  $^{238}\text{U}$  in soil is about 400: 35: 30 Bq/kg (UNSCEAR, 2000). Both activity concentrations of thorium and uranium are in good correlations with measured  $^{40}\text{K}$  values with  $r = 0.821$  for  $^{40}\text{K} - ^{232}\text{Th}$  ( $p < 0.05$ ) and  $r = 0.830$  for  $^{40}\text{K} - ^{238}\text{U}$  ( $p < 0.05$ ). Thus the geological information should be considered. Activity concentrations of  $^{238}\text{U}$  ( $^{232}\text{Th}$ ,  $^{40}\text{K}$  and  $^{226}\text{Ra}$ ) in moss samples and a simplified geological map are shown in [Figure 3.5\(a\) – \(f\)](#). The mean activity concentrations of radionuclides collected in different particular sampling sites and classification of bedrock are presented in [Table 3.6](#). Although their uncertainties are large due to the variety in moss species, it can be seen that the sampling area located on the Triassic granitic zones correspond with the higher activity concentration of  $^{40}\text{K}$ ,  $^{232}\text{Th}$  and  $^{238}\text{U}$  (as well as  $^{226}\text{Ra}$ ) (i.e. sampling sites E13, W14, W15) when comparing with Mesozoic sedimentary zone as well as the older Paleozoic sedimentary zone (sample sites W01, W03, W04). It could be due to the degree of decomposition and porosity of the rock which depended on their age; Triassic granite is older than the other ones and it is intruded and baked by the magma of the younger granites. For a long period of times, the decomposed (and high porosity) granites are exposed to the earth surface and started to weather and erode (transport) like soil-dust by wind and accumulated in moss samples by dry deposition. Some older granite in peninsular Thailand was intruded by aplite dike and quartz veins under the influences of pneumatolytic and hydrothermal activities. It decomposed to soil, leaving the



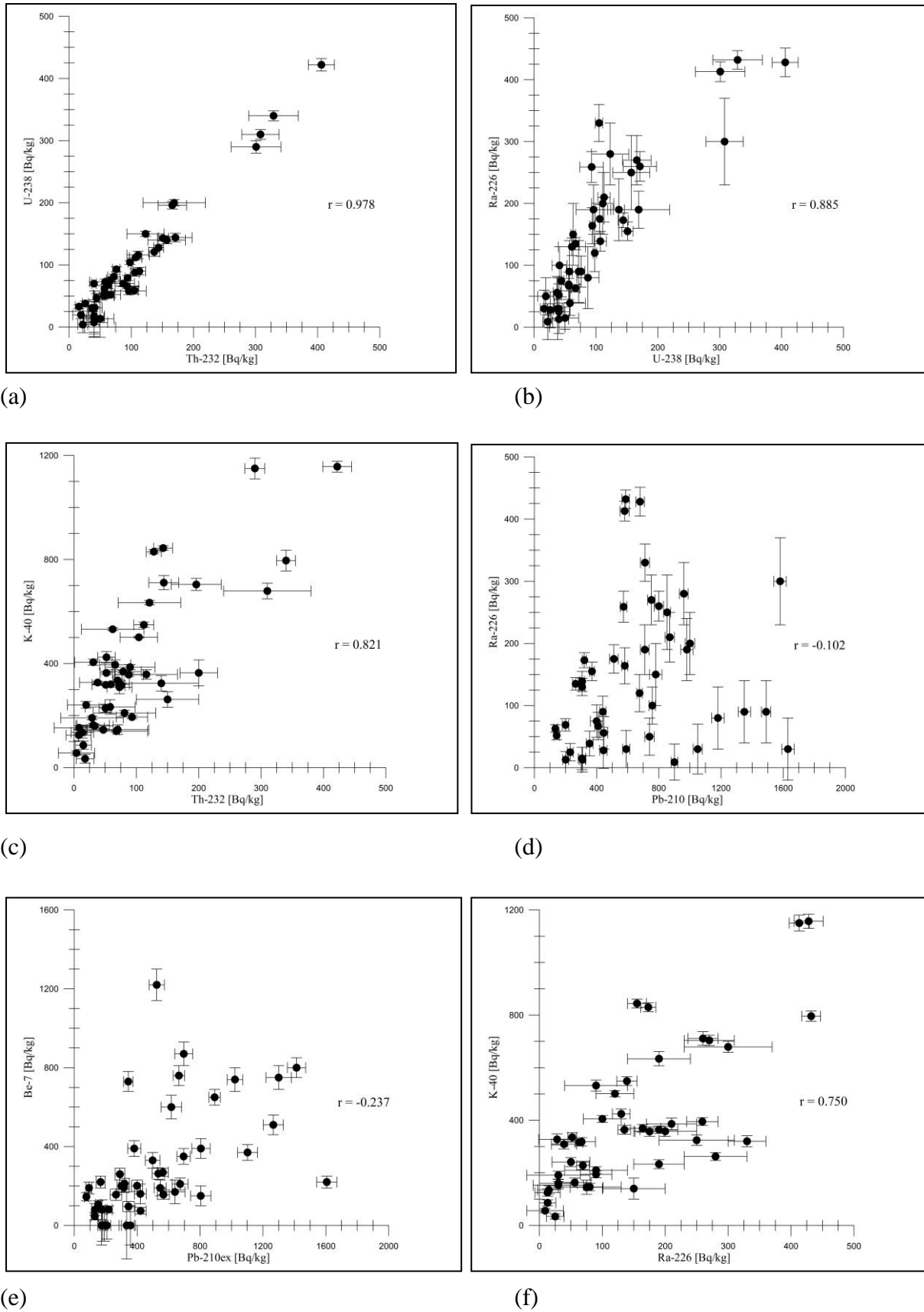
elements dissolved. Torbernite and monazite, highly radioactive minerals, were discovered in some areas, for example in dikes and joints of granite and in quartz, quartzite and decomposed granite (Pungrassami, 1984). Faults in the rock cause dissolution of heavy metals in underground water, including radium, an important daughter element of uranium. Over a longer period, the decomposed (highly porous) granites are exposed on the earth surface and start to weather and erode (transport) forming soil-dust carried by winds, and accumulate in moss samples by dry deposition.

In addition, it can be seen the intermediate correlation between  $^{226}\text{Ra}$  and  $^{40}\text{K}$  as shown in **Figure 3.4(f)**. It is probably due to the fact that both  $^{40}\text{K}$  and  $^{226}\text{Ra}$  are transported to mosses and eventually captured by the same mechanism. However there is another aspect that should be mentioned. Potassium (and also calcium) is a necessary element for metabolic processes of the plants. Good  $^{40}\text{K} - ^{226}\text{Ra}$  correlation could be partly due to the similar chemical behavior of calcium and radium. Necessary elements (potassium) and calcium (as well as  $^{226}\text{Ra}$ ) are deposited up taken on mosses collected and measured in this study (Karunakara et al., 2003; Belivermiş and Çotuk, 2010).

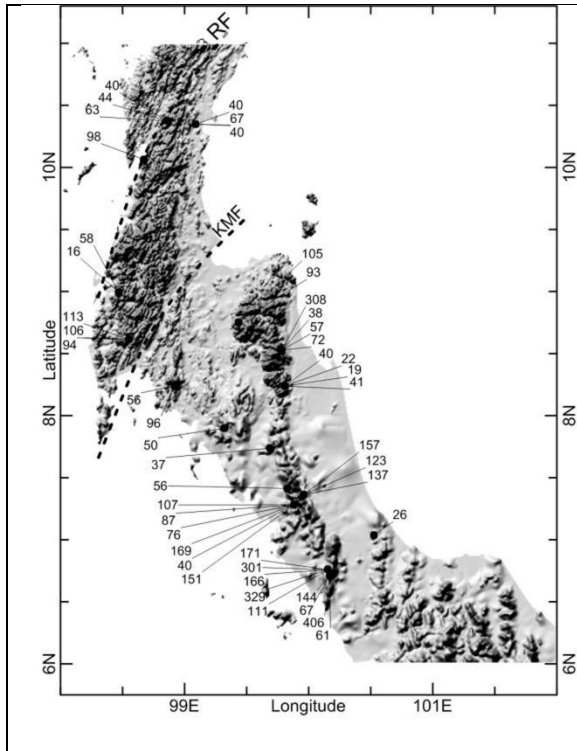
**Table 3.6** Average activity concentrations of  $^{40}\text{K}$ ,  $^{210}\text{Pb}_{\text{ex}}$ ,  $^{232}\text{Th}$  and  $^{238}\text{U}$  and types of bedrock where sampling sites located on.

Rock	Average activity concentrations (Bq/kg)				Sampling sites
	$^{40}\text{K}$	$^{210}\text{Pb}_{\text{ex}}$	$^{232}\text{Th}$	$^{238}\text{U}$	
C	106±63	393±223	44±25	49±12	W08
C, CP	206±120	195±158	50±29	43±17	E09 and E17
C, P, Gr	336±250	447±298	91±61	88±53	W06 and W14
K-J Gr	293±166	775±478	60±76	75±72	W01, W03, W04, E10, E11 and E12
P	371±15	480±172	86±6	104±10	W05
TrGr	598±312	428±251	163±113	165±108	W02, W07, E13, W15 and W16

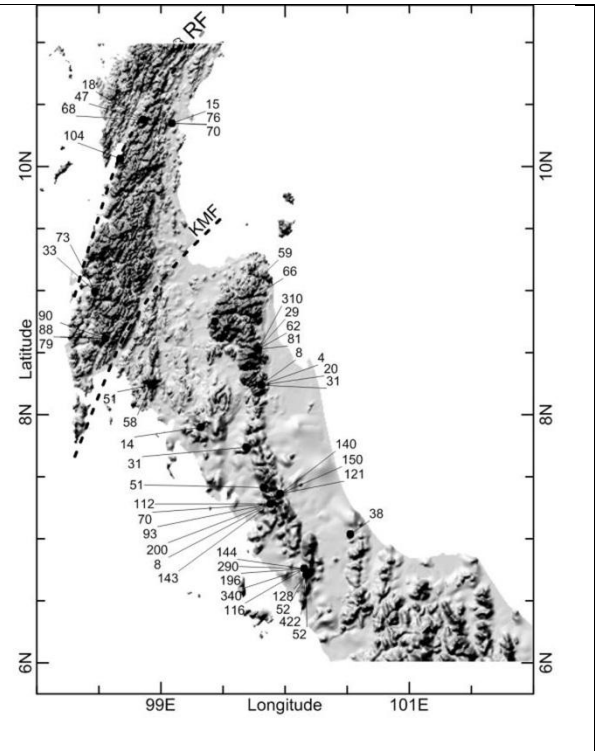
**Remark:** C, CP = Pebbly mudstone  
P = Permian limestone  
O = Ordovician limestone  
KGr = Cretaceous granite  
JGr = Jurassic granite  
TrGr = Triassic granite



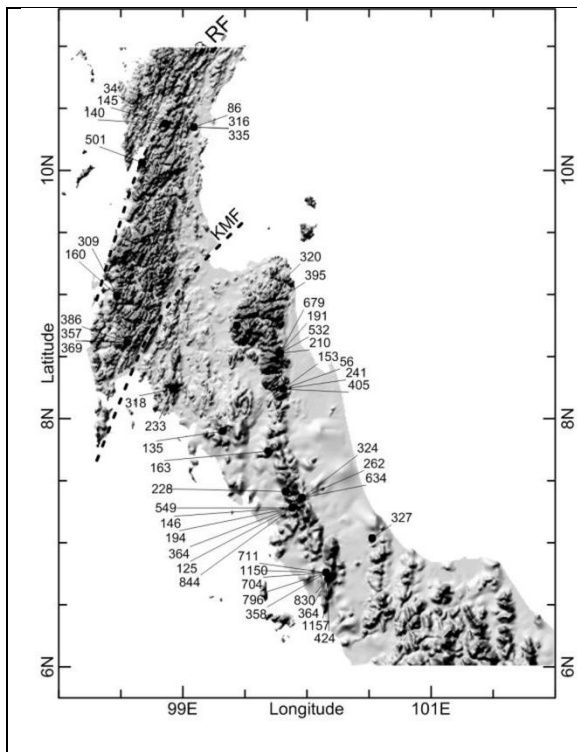
**Figure 3.4** the scatter graph of activity concentrations measured in moss samples  
 (a)  $^{238}\text{U}$  -  $^{232}\text{Th}$ , (b)  $^{226}\text{Ra}$  -  $^{238}\text{U}$ , (c)  $^{40}\text{K}$  -  $^{232}\text{Th}$ , (d)  $^{226}\text{Ra}$  -  $^{210}\text{Pb}$ , (e)  $^7\text{Be}$  -  $^{210}\text{Pb}_{\text{ex}}$  and  
 (f)  $^{40}\text{K}$  -  $^{226}\text{Ra}$ .



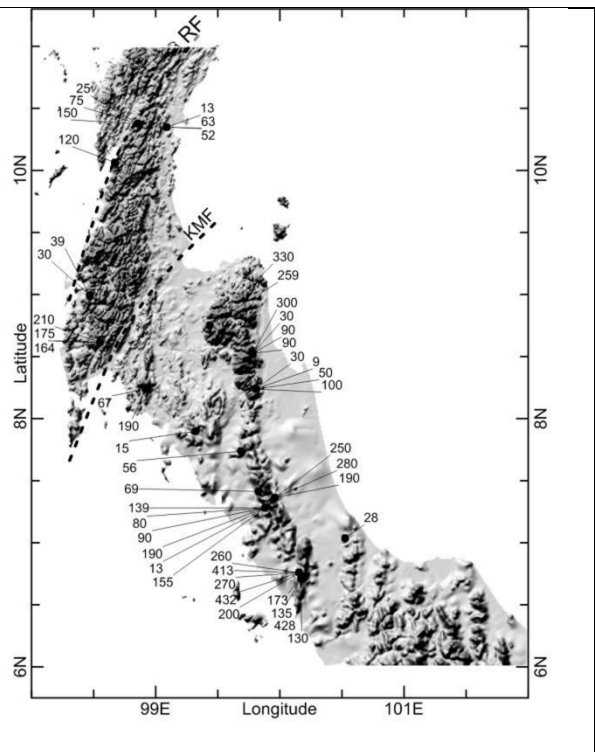
(a)



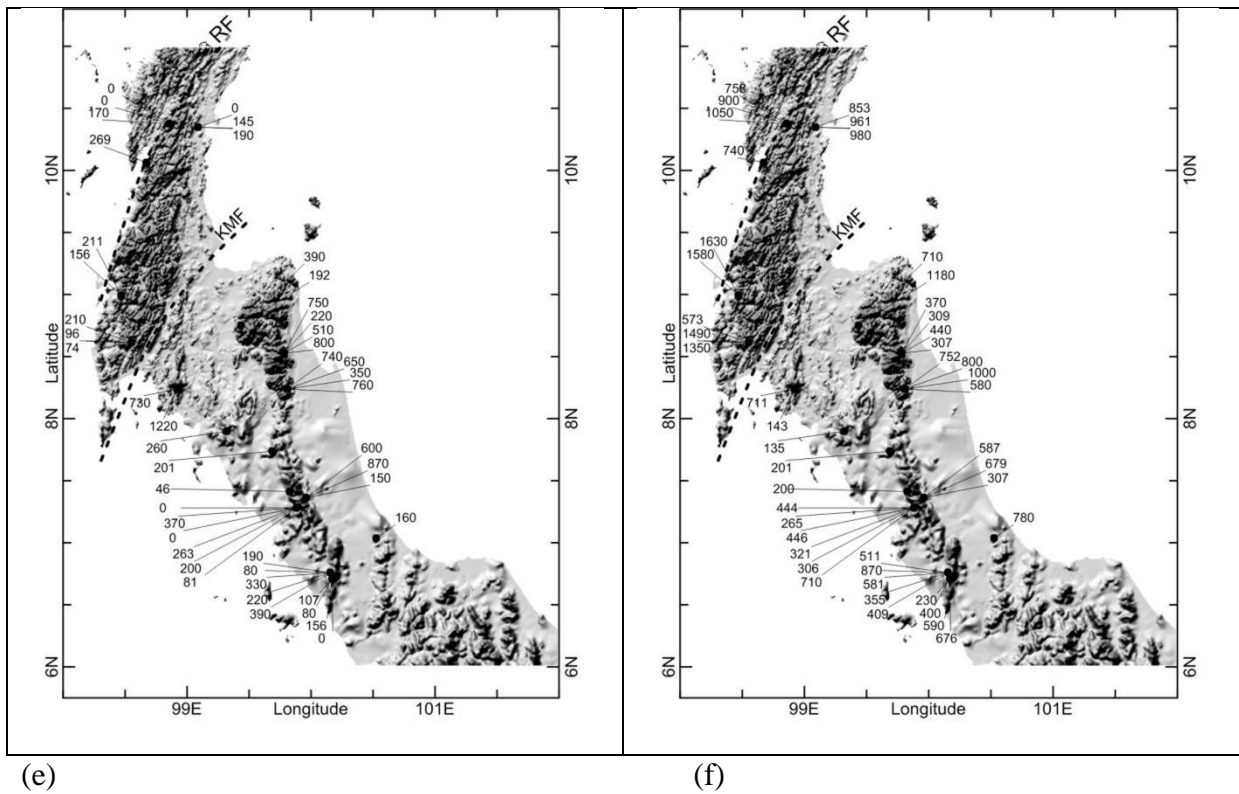
(b)



(c)



(d)



**Figure 3.5** Activity concentrations of radionuclides at various geographic of studied areas; (a)  $^{238}\text{U}$ , (b)  $^{232}\text{Th}$ , (c)  $^{40}\text{K}$ , (d)  $^{226}\text{Ra}$ , (e)  $^7\text{Be}$  and (f)  $^{210}\text{Pb}$ .

### 3.2.3 Spatial distributions, correlation and probable factors affecting to the activity concentration of airborne radionuclides; $^7\text{Be}$ and $^{210}\text{Pb}$ .

#### 3.2.3.1 Beryllium - 7

The activity concentration of  $^7\text{Be}$  in moss samples in this study vary from MDA to 1,220 Bq/kg. Its mean value (295 Bq/kg) is significantly higher than that value obtained in Section 3.1, however it is slightly lower than that observed in England (360 Bq/kg, Sumerling, 1984), Rep. of Serbia (363 Bq/kg, Krmar et al., 2007; 314 Bq/kg, Krmar et al., 2013) and Kaiga, India (Karunakara et al., 2003) as shown in Table 3.7. This result supported the fact that a higher value of  $^7\text{Be}$  in mosses is generally found in region of mid – latitude of upper hemisphere due to higher deposition rate of  $^7\text{Be}$  concentration in surface air with increasing latitude (Kulan et al., 2006). One exception is the activity concentration of  $^7\text{Be}$  measured in mosses collected in Kaika, India where the mean value was about 680 Bq/kg, which is very high compared with those from the other region suggesting the high deposition rates of  $^{210}\text{Pb}$ ,  $^{210}\text{Po}$  and  $^{137}\text{Cs}$  (Karunakara et al., 2003). However, it can be concluded that the activity concentrations of  $^7\text{Be}$  in moss samples in this study do not significantly differ from the worldwide measured values (Table 3.7).

**Table 3.7** Range and mean values of activity concentrations of  $^7\text{Be}$ ,  $^{40}\text{K}$ ,  $^{226}\text{Ra}$ ,  $^{210}\text{Pb}$ ,  $^{232}\text{Th}$  and  $^{238}\text{U}$  from those reported literatures comparing to this study.

		Location	Activity concentrations (Bq/kg)					
			$^7\text{Be}$	$^{40}\text{K}$	$^{226}\text{Ra}$	$^{210}\text{Pb}$	$^{232}\text{Th}$	$^{238}\text{U}$
Kaiga, India [Tree mosses]	(Karunakara et al., 2003)	14°51'08"N, 74°26'40"E	234.5- 1,061 [680.1]	12.01- 40.1 [22.1]	BDL- 2.2 [1.5]	-	-	-
Coastal Syrian mountain (Along sea coast)	(Al-Marsi et al., 2005)	-	-	-	165- 2,392 [-]	-	-	-
Belarus and Slovakia (Aleksiayenak et al., 2012)								
-Belarus		48°12'- 49°20'N 17°05'- 22°05'E	-	-	-	163-572 [312]	-	-
-Slovakia					330- 1,521 [771]			
Marmara region, Turkey	(Belivermiş and Çotuk, 2010)	-	-	17.1- 181.1	-	-	1.51-6.17	0.87-6.70
Novi Sad, Rep. of Serbia		42°14'45"N, 19°51'35"E	100-900 [248] [340]	-	-	347-885 [-]	-	-
-Jan-Feb 2007								
-Jan-Feb 2008								
Nine semi-natural highland in Rep. of Serbia	(Dragović et al., 2010)	-	-	60-537 [207]	7.3-29 [16]	-	-	-
Zlatibor Mountain, Western Serbia	(Dragović et al., 2010)	43°31'- 43°51'N 19°28'- 19°56'E	-	44-692 [-]	0.9- 25.8 [-]	-	0.8-13.7 [-]	1.7-25.1 [-]
Northern Province of Vovvodina to Southern border of Rep. of Serbia	(Krmr et al., 2007)	42°26'- 45°23'N 19°58'- 22°13'E	195-560 [363]	30-800 [281]	-	-	-	-

**Table 3.7 (Continues)**

	Location	Activity concentration (Bq/kg)					
		<sup>7</sup> Be	<sup>40</sup> K	<sup>226</sup> Ra	<sup>210</sup> Pb	<sup>232</sup> Th	<sup>238</sup> U
South of Serbia (Čučulović et al., 2014)	-	41-122 [-]	100-500 [-]	5-50 [-]	-	5-50 [-]	-
This study [2012]	6°71'-10°37'N 98°46'- 100°53'E	0-1,220 [295]	34-1,157 [384]	9-432 [145]	135- 1,630 [656]	4.1-422 [97]	16-406 [102]

*Remark*      BDL = below detection limit,      [ ] = mean value

The spatial distributions of <sup>7</sup>Be contents in moss samples collected from each particular sampling site are shown with simplified geological map in **Figure 3.5(e)**. Unfortunately, there was no prior systematic study of <sup>7</sup>Be concentration in surface air, top soils or terrestrial plants (including mosses) in overlarge area in Southern Thailand; however, the measured values of <sup>7</sup>Be in moss samples in the study area confirm an abundant atmospheric deposition flux of <sup>7</sup>Be. The maximum of <sup>7</sup>Be deposition flux in China are reported on January to April, which was due to

1) The seasonal stratosphere – troposphere air exchange in mid – latitude of northern hemisphere (Cho et al., 2007; Du et al., 2008; Petrova et al., 2009).

2) The vertical air mass convection from lower stratosphere – upper troposphere and 3) The transportation of air mass from Chinese continent have also affected the variation of <sup>7</sup>Be concentration in air in Japan (Momoshima et al., 2006; Sato et al., 2003; Ueno et al., 2003).

Beryllium-7 deposition flux is increasing with both altitude and latitude; the highest production rate of <sup>7</sup>Be was found at around 50°N and decreases toward the equator (Nagai et al., 2000). The activity concentration of <sup>7</sup>Be in this study shows a large variation, not only depending on variety of moss species but also depending on difference in geography of study sites. Pearson's coefficient (**Table 3.3**) between activity concentrations of <sup>7</sup>Be and altitude of the sampling sites shows a weak correlation between them with  $r = 0.365$  ( $p < 0.05$ ). It implies that activity concentrations of <sup>7</sup>Be in moss samples are slightly increased with altitude of the sampling site.

The  $^7\text{Be}$  concentration in ground level air is influenced by meteorological factors such as change in production rate due to solar heating, stratosphere – troposphere exchange, and advection of air mass containing  $^7\text{Be}$  at different latitude (Aldahan et al., 2001; Pham et al., 2011). Not only these meteorology factors, but the morphology of the study area is also an important factor affecting the activity concentration of  $^7\text{Be}$  as shown in Figure 3.5(e). In mid – latitude countries; such as China,  $^7\text{Be}$  is accumulated in air over continental area. During the sampling period in this study (March, 2012), the North – East monsoon coming from China continent, a high  $^7\text{Be}$  content in cold and dry air mass is transported to Thailand, this may give an increased deposit of  $^7\text{Be}$  through over large area in the Peninsular Thailand by both (1) dry deposition by wind and (2) wet deposition by rain; because there had been raining during the sampling time. It is possible that the new additional precipitation of airborne radionuclides may be washed by rain from the atmosphere onto moss samples.

However, our measurements failed to confirm this hypothesis due to high variation of the measured activity concentrations of  $^7\text{Be}$  in the mosses collected from peninsular Thailand. The mean value of  $^7\text{Be}$  activity in sampling sites located along the east side is higher than in those on the west side of the peninsula,  $440\pm 285$  and  $211\pm 248$  Bq/kg, respectively. This difference is statistically significant (independent Student's t-test,  $F = 4.098$ , sig. level = 0.049,  $t = -2.756$ , sig. level = 0.01). A possible explanation of this result is an effect of regional topography, as the north – south mountain range separates peninsular Thailand into the western and eastern low lands. During the sampling period the east side of peninsular Thailand faced cold and dry air masses coming from higher latitudes over continental China, enriching  $^7\text{Be}$  in the atmosphere. For example, 0.11 (January, 2005) – 2.93 (February, 2005) Bq/m<sup>2</sup>/day (Yi et al., 2007) and 0.02 (December, 2006) – 15.0 (April, 2006) Bq/m<sup>2</sup>/day (Du et al., 2008), respectively. The west side of peninsular Thailand was under the influence of air masses from the Andaman Sea and Indonesia, with comparatively lower  $^7\text{Be}$  concentrations in air from lower latitudes. While there is no systematic report on  $^7\text{Be}$  in ground surface air over Indonesia and Andaman Sea, the measured  $^7\text{Be}$  concentrations in surface air in Oceania (0.5 – 46.4 °S) range from  $1.4\pm 0.3$  Bq/m<sup>2</sup>/day (0.5 °S) to  $4.9\pm 1.2$  Bq/m<sup>2</sup>/day (27.5 °S) as reported by Doering and Akber (2008) (Doering and Akber, 2008).. The  $^7\text{Be}$  production rates in the atmosphere, as well as the increment in its measured concentrations, depend on latitude (Lavrenchuk et al., 1962, Larin et al., 2014). This may imply that the  $^7\text{Be}$  concentration in surface air over areas located in lower latitudes (Northern – Southern Hemisphere) such as Indonesia and Andaman Sea should be low. These provide plausible reasons for the differences in  $^7\text{Be}$  concentration in mosses collected

from the east and the west side of peninsular Thailand, and future studies could further address these phenomena.

Other evidence supporting a high  $^7\text{Be}$  in cold air mass coming from Chinese continent is an elevated  $^7\text{Be}$  concentration in moss samples W04 ( $1,220 \pm 80$  Bq/kg). This sampling sites located on the west side of the Peninsula, the measured value of  $^7\text{Be}$  content in moss is contrary to what we have observed at other sampling sites located on the west side. This sampling location is probably facing to the cold air masses affected by North – East monsoon in the sampling period, similar as the sampling sites located on the East – Side (E09 – E13 and E17 in [Figure 3.1](#)). Considering that this sampling site located near a hill summit surrounded by a channel of low land connecting eastern and western seas and is not sheltered by any high mountain ridge, whereas sampling sites W01, W02, W14 – W16 and W06 – W08 located in Ban – Thud and Ta – Now – Wa – Sri Mountain Range and sheltered by a long North – South mountain ridges. It can be a reason why the activity concentrations of  $^7\text{Be}$  in moss samples collected in the west side are slightly lower than the sample collected from the East – side of the Peninsular Thailand.

#### **- Lead - 210**

$^{210}\text{Pb}$  (supported and unsupported Lead – 210) is be observed in all moss samples, their activity concentrations varied significantly from 135 to 1,630 Bq/kg with mean value is  $656 \pm 374$  Bq/kg. They are slightly higher than those of mosses collected in Belarus ([Aleksiayenak et al., 2013](#)), Novi Sad ([Krmr et al., 2009](#)), West Antarctica ([Mietelski et al., 2000](#)). In the cases of low content of  $^{226}\text{Ra}$  (as well as  $^{238}\text{U}$ ) in soil and dust, low concentration of  $^{210}\text{Pb}$  should be expected, if there is no abundant atmospheric deposition of  $^{210}\text{Pb}$ . The high  $^{210}\text{Pb}$  content in mosses were observed in some sampling sites associate with human activities; 900 Bq/kg from the nuclear power station ([Sumerling, 1984](#)), 1,898 Bq/kg from the coal-fired power stations ([Delfanti et al., 1999](#)), and areas with high level of  $^{222}\text{Rn}$  emanations from soil air to surface air, for example, in fault zone ([Al-Masri et al., 2005](#)). However, in this study almost moss samples were collected under tree leaves, topsoil and rock exposures closet to flowing water or stream side located in the mountain areas, relatively far from any human, industrial communities and coal-fired power stations with exception for site W07 that is located close to the local road, whereas sites E09 and E17 are surrounded by cultivated areas. Furthermore, activity concentrations of  $^{210}\text{Pb}$  in moss samples are significantly higher than  $^{226}\text{Ra}$  (as similar as Section



3.1), with no correlation between them as shown in **Figure 3.4(d)**. This means that secular equilibrium of  $^{226}\text{Ra}$  and its decay products is broken;  $^{210}\text{Pb}$  is not in equilibrium with  $^{214}\text{Bi}$  (or  $^{226}\text{Ra}$ ) and other short-lived daughters of  $^{222}\text{Rn}$ . Therefore, the contribution of unsupported lead-210 ( $^{210}\text{Pb}_{\text{ex}}$ ) in samples is significant. The levels of  $^{210}\text{Pb}_{\text{ex}}$  are carefully calculated from  $^{214}\text{Bi}$ ,  $^{214}\text{Pb}$  and  $^{210}\text{Pb}$  gamma lines, however its value were not shown except  $^{210}\text{Pb}$  values are presented in **Table 3.2** and **Figure 3.5(f)**.

In Section 3.1 and previous study (Krmár et al., 2013), relatively low  $^{226}\text{Ra}$  content in mosses samples was observed, however those results were obtained from 3 sampling sites around Hat Yai City, Songkhla Province only. This fact can be supported a conclusion that most of  $^{210}\text{Pb}$  content in moss samples do not relate to  $^{226}\text{Ra}$  in ground soil, but significant portion of  $^{210}\text{Pb}$  is deposited from aerosols. In contrast to previous study, the higher  $^{210}\text{Pb}$  concentration in this study may be associated, not only to deposition of aerosol, however it was not similar to  $^7\text{Be}$  with  $r = -0.238$  ( $p = 0.112$ ) as shown in **Figure 3.4(e)** and **Table 3.3**, but also a consequence of high  $^{222}\text{Rn}$  emanation from ground over sampling areas. The sampling sites W05 and W06 – W08 are located near the active faults of the Peninsular Thailand, the Khlong Marui fault (KMF) and Ranong fault (RF) as shown in **Figure 2.1** and **Figure 3.5(f)** respectively. This can be expected that the levels of  $^{222}\text{Rn}$  and  $^{210}\text{Pb}$  concentrations in air near those sites are higher than the other sites (Al-Masri et al., 2005).

In contrary, sampling sites E09, E12, W15, W16 and E17 are located far from any fault zones; however their activity concentrations of  $^{210}\text{Pb}$  in moss samples are slightly elevated values, especially in site E09 and E12. The higher values of  $^{210}\text{Pb}$  are not correlated with relatively low values of both  $^{226}\text{Ra}$  and  $^{238}\text{U}$  in these samples. Sampling site E09 and E17 are located in the areas where the limestone is dominated (lower concentration of  $^{238}\text{U}$ ,  $^{232}\text{Th}$  and  $^{40}\text{K}$ ). In addition, they are surrounded by cultivated areas (Oil Palm plantation, E09, and Para-rubber plantation, E17). However, if phosphate fertilizers were used in this area, it could elevate  $^{238}\text{U}$  only without significant presence of other radionuclides from its chain. Furthermore, all moss samples are collected on the topsoil beside the stream side thus moss samples may be exposed to the moist air. However, the high activity concentrations of  $^{210}\text{Pb}$  in moss samples are not followed by the high values of  $^{238}\text{U}$  (as well as  $^{226}\text{Ra}$ ). It can be indicated that water droplet in moist air may contain dissolved  $^{222}\text{Rn}$ ; more than  $^{226}\text{Ra}$  and after uptake and decay of radon, its progenies are accumulated in moss samples. It can be a possible reason to explain the higher activity concentration of  $^{210}\text{Pb}$  collected in these areas.

There was no correlation between  $^{210}\text{Pb}_{\text{ex}}$  and  $^7\text{Be}$ , and that these radionuclides have distinct sources;  $^{210}\text{Pb}$  is produced by the decay of  $^{222}\text{Rn}$  from the land surface, while  $^7\text{Be}$  is produced in the upper atmosphere and transported by stratosphere – troposphere exchange processes. The vertical transport of air mass mixes them in the troposphere (Kuroda et al., 1962, Hirose et al., 2004), so they are mainly transported from remote areas through the upper troposphere (Church et al., 1992), and finally, they are deposited on the Earth surface by similar processes. Consequently, in the atmosphere they are significantly correlated as reported by several authors (Baskaran et al., 1993; Baskaran 1995; Kim et al., 2000; Hirose et al., 2004; Du et al., 2008). In this study the moss samples were collected at the end of winter and in early summer, when solar heating warms the surface air – not only at the ground surface air of peninsular Thailand that may contain aerosols enriched in  $^{210}\text{Pb}$ , but also within the marine air in the Gulf of Thailand that may contain aerosols depleted in  $^{210}\text{Pb}$  (Hirose et al., 2004; Du et al., 2008). Both the heated air masses move upward and mix with cold air from China, and then get transported to the peninsula by the North – East Monsoon. However, unlike the activity concentration of  $^7\text{Be}$  in surface air, the activity concentration of  $^{210}\text{Pb}$  is controlled by “local meteorological conditions”, such as temperature, rainfall amount, and relative humidity (Kim et al., 2000; Pham et al., 2011; Bourcier et al., 2011; Gordo et al., 2015). Since it rains often in peninsular Thailand, the washout may influence some control over the activity concentration of  $^{210}\text{Pb}$  in the aerosols. In this way, both the mixing processes and the local meteorological conditions are important factors controlling the activity concentration of  $^{210}\text{Pb}$  in the surface air of peninsular Thailand, which provides a possible explanation for the lack of correlation between  $^7\text{Be}$  and  $^{210}\text{Pb}$ .

At sampling site E12, the activities concentration of airborne radionuclides in all moss samples here are generally high; however there is no correlation between  $^{210}\text{Pb}$  and  $^7\text{Be}$ . It can be explained by the fact that this site is located on the top of a granitic mountain (Figure 2.1) at elevation around 1,000 m above mean sea level. All bryophytes growing on the top soil are covered by the grasses and small trees which are direct exposed to the atmospheric influences all the time. It is well known that the local meteorological conditions can affect the ground surface air, and the concentration of radionuclides in air (Pham et al., 2011). During the sampling period, it was the end of rain season and start early summer time. In the lack of raining or any precipitation airborne radionuclide can be enriched by solar heating;  $^7\text{Be}$  can be accumulated in

hot air while the presence of elevated  $^{210}\text{Pb}$  coincides with hot ground (earth) surface which can increase  $^{222}\text{Rn}$  emanations rate.

In addition, if we expected that both radionuclides were directly deposited into moss samples as the similar atmospheric processes, the occurrence of the atmospheric temperature inversion of the surface air layer may be a possible explanation of the disagreement between their concentrations in moss samples. Temperature inversion layers (stable condition) are significant to meteorology and air pollutions because they block atmospheric flow which causes the air over an area experiencing an inversion to become stable. More importantly though, areas with radon in air are prone to increase its concentration when an inversion is present because they trap the radon gas at ground level where it originated instead of circulating them diluted away. Stable atmospheric conditions most commonly develop at evening to early morning when the ground rapidly cools as well as the surface air layer. An inversion occurs when air temperature increases with altitude. This situation occurs frequently and generally confined to a relatively shallow layer near ground surface and block atmospheric flow which causes the air over an experiencing area. During daytime, the solar heats the ground; the ground rapidly absorbs heat and transfers some of that heat to the surface air layer. There may be one buoyant air mass if the thermal properties of the surface are uniform, or there may be numerous parcels if the thermal properties vary. The air warms, becomes less dense than the surrounding air and rises and it lets the near surface air mass move upward, and also increases the concentration of radon and its progenies in that air. While cool air mass contains high concentration of  $^7\text{Be}$  from the higher altitude air masses cannot reach to the mosses due to the prevention of inversion layer and  $^7\text{Be}$  is accumulated in this layer. However, during late evening till early morning the ground surface temperature decreased faster than the air and temperature inversion built up again cause the cold air masses from the higher altitude to move downward to earth surface and increase the aerosol concentration in the air mass which can reach the moss and cause  $^7\text{Be}$  accumulation in the bryophytes.

## Chapter Four

### Conclusion, suggestions and future works

#### 4.1 Conclusion

This preliminary study uses moss technique as a suitable medium for the measurement of activity concentrations of terrestrial radionuclides  $^{40}\text{K}$ ,  $^{226}\text{Ra}$ ,  $^{232}\text{Th}$  and  $^{238}\text{U}$  and airborne radionuclides  $^7\text{Be}$  and  $^{210}\text{Pb}$  in the Peninsular Thailand. It can be concluded that;

1. Almost moss samples are collected beside the water streams located in mountain areas of the National Parks and Wildlife Sanctuaries, due to the moisture is an important factor for growing of mosses in Thailand.

2. The biological variety of bryophytes in particular sampling sites; different in sampling sites, different in moss species, can be reasons in order to explain the large variation of radionuclides content in moss samples. In addition, the variation in radionuclides content at a given sampling site may be associated with the degree of local shelter and moss covered – plants to prevent mosses or retain the airborne radionuclides from atmospheric depositions as well as re – suspensions of soil and dust.

3. The PCA and CA analyses have implied the origin of the studied radionuclides into two PCs and three separated clusters, the terrestrial radionuclides ( $^{226}\text{Ra}$ ,  $^{232}\text{Th}$ ,  $^{238}\text{U}$  and  $^{40}\text{K}$ ) contained in the first PCs which is called *factor of soil dust origin*. The airborne radionuclides ( $^{210}\text{Pb}$ ,  $^{210}\text{Pb}_{\text{ex}}$  and  $^7\text{Be}$ ) contained in the second PCs and called *factor of atmospheric origin*.

##### 4.1.1 Terrestrial radionuclides;

1) Geology of sampling sites has an influence in radionuclides content in bryophytes;

- It can be implying that  $^{40}\text{K}$ ,  $^{226}\text{Ra}$ ,  $^{232}\text{Th}$  and  $^{238}\text{U}$  have similar origin and accumulated to moss samples via dry depositions of soil and dust particles; this can be supported by the observed strong correlations between their contents in moss samples. The higher values of their content in mosses are probably associated with the rock formations; mostly Triassic weathered granite, while the lower values correspond to sedimentary and metamorphic rocks; mostly pebbly mudstone and shale.

2) Disequilibrium in uranium chains can be observed;

- Activity concentrations of  $^{226}\text{Ra}$  are slightly higher than  $^{238}\text{U}$  (as well as  $^{232}\text{Th}$ ); there are two possible reasons for explanation. The first one is the diffusion of water droplets which may contain dissolved radium beside the sampling areas, considering that almost all moss samples are collected near the stream lines and waterfalls, radium and other radionuclides in them can be transported and increase its activity concentration in moss samples. The second, one is the radium's solubility in fresh water is slightly higher than uranium due to uranium has more various complex ions and strongly adsorbed onto organic compounds than radium in fresh water.

- There are no correlations between these terrestrial radionuclides and  $^{210}\text{Pb}$  (as well as  $^{210}\text{Pb}_{\text{ex}}$ ) and it can be clear evidence that they reached the moss samples from the different origin. In addition, the high values of activity concentration of  $^{210}\text{Pb}$  (not following the high values of those two) are observed and good correlation between  $^{210}\text{Pb}$  and  $^{210}\text{Pb}_{\text{ex}}$  should be mentioned, it probably corresponds to the high emanation rate of  $^{222}\text{Rn}$  such as in area of fault zones.

#### 4.1.2 Airborne radionuclides;

1) The mean activity concentration of  $^7\text{Be}$  is in agreement and slightly lower than those in the studies worldwide. There is a significant difference in its values of moss samples collected from the east side and the west side of the Peninsular Thailand, this corresponds to the topographic feature of the sampling sites and the influence of the seasonal North – Eastern monsoon; the cold and dry air masses containing a high concentration of  $^7\text{Be}$  from the north, the China mainland.

2) The interesting result can be noticed, the high activity concentration of  $^7\text{Be}$  and  $^{210}\text{Pb}$  in moss collected from sample site E12 which is located at 1,000 m elevated from mean sea level. This may be associated with the atmospheric stability of inversion type. The enrichment of  $^{222}\text{Rn}$  and  $^7\text{Be}$  may occur during daytime and nighttime, respectively, and thus increase the activity concentrations accumulated in the moss samples during the sampling period. Although  $^7\text{Be}$  and  $^{210}\text{Pb}$  are belonging to the same PC2 which can be implied that they reached to the moss samples via an aerosol deposition, but the morphology, geographic location of study areas and temperature inversion may affect the variation of their activity concentrations and give a reason

why there is no significant correlation between them and why they were separated into two distinguish clusters.

#### **4.2 Suggestion and future works**

This thesis has presented measurement and analysis of the activity concentration of naturally occurring radionuclides in moss samples collected from natural systems located in Peninsular Thailand. The study was limited by a variety of bryophytes; due to the difficult to find mosses far from the water as similar as the difficult to find identical mosses in different sampling sites, however the measured radionuclide contents in moss samples were compared to other previous worldwide studies, the spatial distribution and some significant correlation between activities concentrations of this studied radionuclides can be observed, explained and discussed based on the reasonable knowledge in previous studies of geography, geology and meteorology in Thailand, worldwide and neighboring countries.

The future research is to use the moss techniques for measuring the natural radionuclides for assessment of environmental problems. One area is to use mosses as the bio – monitor for investigation of an anomaly of terrestrial radionuclides in some suspicious sampling sites; such as near active faults or eroding rocks areas. In fact, Thai's mosses growths in natural environment areas; close to water stream surrounded by mountain areas and locate in National Parks and Wildlife Sanctuaries, these areas often belong to the water sources for human communities. Consequently, it is necessary to evaluate the degree of radioactive pollutants or their contaminations levels in natural environments for radiation hazards or guidelines of naturally radiation protection for human communities. The second area is investigation of seasonal variation of airborne  $^7\text{Be}$  in Southern Thailand, which may have probably influenced to N – E monsoon from Chinese mainland (although this study is missing to prove the influence to W – S monsoon from Andaman Sea). Some particular sampling sites may be perform for this purpose; W01, W04 – W07, W14 – W15 for the west – side of Peninsula while E9, E12, E13 and E17 for the east – side. However, the planted mosses may be more appropriate than natural growing mosses in future study as it is easy to restrict the variation in their species. In addition, the last one may be linked to air pollution by transportation of heavy metals content in air masses from mainland (Chinese continent, or Middle and East part of Thailand; full of heavy industrial companies) to Southern Thailand.

## References

- Abdullah, M., Z., B., Saat, A. B., Hamzah, Z., B., 2012. Assessment of the impact of petroleum and Petrochemical industries to the surrounding areas in Malaysia using mosses as bioindicator Supported by multivariate analysis. *Environ Monit Assess* 184, 3959-3969.
- Aldahan, A., Possnert, G., Vintersved, I., 2001. Atmospheric interactions at northern high latitudes from weekly Be-isotopes in surface air. *Applied Radiation and Isotopes* 54, 345-353.
- Aleksiayenak, Y. V., Frontasyeva, M. V., Florek, M., Sykora, I., Holy, K., Masarik, J., Brestakova, L., Jeskovsky, M., Steinnes, E., Faanhof, A., Ramatlhabe, K. I., 2013. Distributions of  $^{137}\text{Cs}$  and  $^{210}\text{Pb}$  in mosses collected from Belarus and Slovakia. *Journal of Environmental Radioactivity* 117, 19-24.
- Anicic, M., Frontasyeva, M. V., Tomasevic, M., Popovic, A., 2007. Assessment of atmospheric deposition of heavy metals and other elements in Belgrade using the moss biomonitoring technique and neutron activation analysis. *Environ Monit Assess* 129, 207-219.
- Al-Masri, M. S., Mamish, S., Al-Haleem, M. A., Al-Shamali, K., 2005. *Lycopodium cernuum* and *Funaria hygrometrica* as deposition indicators for radionuclides and trace metals. *Journal of Radioanalytical and Nuclear Chemistry* 266, 49-55.
- Astel, A., Astel, K., Biziuk, M., 2008. PCA and multidimensional visualization techniques united to aid in the bioindication of elements from transplanted *Sphagnum palustre* moss exposed in the Gdańsk City Area. *Environmental Science and Pollution Research* 15, 41-50
- Azahra, M., López-Peñalver, J. J., Camacho-García, M. A., González-Gómez, C., ardouni, T. El., Boukhal, H., 2004. Atmospheric concentrations of  $^7\text{Be}$  and  $^{210}\text{Pb}$  in Granada, Spain. *Journal of Radioanalytical and Nuclear Chemistry* 261, 401-405.
- Barandovski, L., Cekova, M., Frontasyeva, M., V., Pavlov, S., S., Stafilov, T., Steinnes, E., 2008. Atmospheric deposition of trace element pollutants in Macedonia studied by the moss biomonitoring technique. *Environ Monit Assess* 138:107–118
- Barci-Funel, G., Dalmaso, J., Andrisson, G., 1989. Radioactive pollution in the Nice region after the Chernobyl accident. *Pollt. Atmos.* 121, 94-98.

Belivermiş, M., Çotuk, Y., 2010. Radioactivity measurements in moss (*Hypnum cupressiforme*) and lichen (*Cladonia rangiformis*) samples collected from Marmara region of Turkey. *Journal of Environmental Radioactivity* 101, 945-951.

Bhongsuwan, T., 1993. Palaeomagnetic Investigations in Thailand. Doctoral's Thesis. Department of Applied Geophysics, Luleå University of Technology. 9-17.

Bhongsuwan, T., 2010. Is tin tailing sand the source of a high natural gamma background in Na Mom district, Songkhla Province, Southern Thailand?. NORM VI March 22-26, 2010, Marrakech, Morocco.

Boileau, L. J. R., Beckett, P. J., Lavoie, P., Richardson, D. H. S., Neiboer, E., 1982. Lichens and mosses as monitors of industrial activity associated with uranium mining in Northern Ontario, Canada-Part 1. Field procedures, chemical analysis and interspecies comparisons. *Environ. Pollut.* 4, 69-84.

Bourcier, L., Masson, O., Laj, P., Pichon, J. M., Paulat, P., Freney, E., Sellegri, K., 2011. Comparative trends and seasonal variation of  $^7\text{Be}$ ,  $^{210}\text{P}$  and  $^{137}\text{Cs}$  at two altitude sites in the central part of France. *Journal of Environmental Radioactivity* 102, 294-301.

Berg, T., Steinnes, E., 1997. Use of mosses (*Hylocomium splendens* and *Pleurozium Schreberi*) as biomonitors of heavy metals deposition from relative to absolute deposition values. *Environmental Pollution* 98:61-71.

Bunopas, S., 1981. Paleogeographic history of western Thailand and adjacent parts of Southern Asia – A plate tectonics interpretation. Ph.D. Thesis, Victoria University of Wellington, New Zealand. 810p; reprinted 1982, Geological Survey paper no. 5, Geological Survey Division, Department of Mineral Resources, Thailand.

Cho, Y. H., Lee, W., Chung, H., Choi, G. S., Lee, C. W., 2007. Seasonal variation and activity size distribution of  $^7\text{Be}$  in ambient air. *Journal of Radioanalytical and Nuclear Chemistry* 274, 531-538.

Čučulović, A., 1, M. Sabovljević, M., Veselinović, D., 2014. The activity concentrations of  $^{40}\text{K}$ ,  $^{226}\text{Ra}$ ,  $^{232}\text{Th}$ ,  $^{238}\text{U}$  and  $^7\text{Be}$  in moss from Spas in Eastern Serbia in period 2000 – 2012. *Arch. Biol. Sci., Belgrade*, 66 (2), 691 – 700.



- Culicov, O. A., Frontasyeva, M. V., Steinnes, E., Okina, O. S., Santa, Zs., Todoran, R., 2002. Atmospheric deposition of heavy metals around the lead and copper-zinc smelters in Baia Mare, Romania, studied by moss biomonitoring technique, neutron activation analysis and flame atomic absorption spectrometry. *Journal of Radioanalytical and Nuclear Chemistry* 254, 109-115.
- Denayer, F. O., Van Haluwyn, C., De Foucault, B., Schumacker, R., Colein, P., 1999. Use of bryological communities as a diagnostic tool of heavy metal soil contamination (Cd, Pb, Zn) in northern France. *Plant Ecol.* 140, 191-201.
- Delfanti, R., Papucci, C., Benco, C., 1999. Mosses as indicators of radioactivity deposition around a coal-fired power station. *Science of the Total Environment* 227, 49-56.
- Dragović, S., Mihailović, N., 2009. Analysis of mosses and topsoils for detecting sources of heavy metal pollution: Multivariate and enrichment factor analysis. *Environ Monit Assess.* 157, 383-390.
- Dragović, S., Mandić, Lj. J., 2010. Transfer of radionuclides to ants, mosses and lichens in semi-natural ecosystems. *Radiat Environ Biophys* 49, 625-634.
- Dragović, S., Mihailović, N., Gajić, B., 2010. Quantification of transfer of  $^{238}\text{U}$ ,  $^{226}\text{Ra}$ ,  $^{232}\text{Th}$ ,  $^{40}\text{K}$  and  $^{137}\text{Cs}$  in mosses of a semi-natural ecosystems. *Journal of Environmental Radioactivity* 101, 159-164.
- Du, J., Zhang, J., Wu, Y., 2008. Deposition patterns of atmospheric  $^7\text{Be}$  and  $^{210}\text{Pb}$  in coast of East China Sea, Shanghai, China. *Atmospheric Environment* 42, 5101-5109.
- Elena, C., Rafael, P., Víctor, P., 2013. Statistical analysis of the spatial distribution of radionuclides in soils around a coal-fired power plant in Spain. *Journal of Environmental Radioactivity* 124, 84-92.
- Ermakova, E.V., Frontasyeva, M.V., Steinnes, E., 2004. Air pollution studies in Central Russia (Tula Region) using the moss biomonitoring technique, INAA and AAS. *Journal of Radioanalytical and Nuclear Chemistry* 259, 51-58.
- Faus-Kessler, T., Dietl, C., Tritschler, J., & Peichl, L., 2001. Correlation patterns of metals in the epiphytic moss *Hypnum cupressiforme* in Bavaria. *Atmospheric Environment*, 35, 427-439.

- Frontasyeva, M. V., Smirnov, L. I., Steinnes, E., Lyapunov, S. M., Cherchintsev, V. D., 2004. Heavy metal atmospheric deposition study in the South Ural Mountains. *Journal of Radioanalytical and Nuclear Chemistry* 259, 19-26.
- Gramatica, P., Battaini, F., Giani, E., Papa, E., Jones, R.J.A., Cenci, R.M. 2006. Multivariate analysis of heavy metal concentrations in soils and mosses of two North – Italy regions. *Fresenius Environmental Bulletin* 15, 731-737.
- Gordo, E., Dueñas, C., Fernández, M. C., Liger, E., Cañete S., 2015. Behavior of ambient concentrations of natural radionuclides  $^7\text{Be}$ ,  $^{210}\text{Pb}$ ,  $^{40}\text{K}$  in the Mediterranean coastal city of Málaga (Spain). *Environ. Sci. Pollut. Res.* 22, 7653–7664.
- Grodzińska, K., Frontasyeva, M., Szarek-Łukaszewska, G., Klich, M., Kucharska-Fabiś, A., Gundorina, S.F., Ostrovnaya, T.M., 2003. Trace element contamination in industrial regions of Poland studied by moss monitoring. *Environmental Monitoring and Assessment* 87. 255-270.
- Hirose, K., Honda, T., Yagishima, S., Igarashi, Y., Aoyama, M., 2004. Deposition behaviors of  $^{210}\text{Pb}$ ,  $^7\text{Be}$  and thorium isotopes observed in Tsukuba and Nagasaki, Japan, *Atmospheric Environment* 38, 6601-6608.
- Jenkins, C. E., Wogman, N. A., Rieck, H. G., 1972. Radionuclide distribution on Olympic National Park, Washington. *Water, Air and Soil Pollution* 2, 181-204.
- Kaiser, H., F., 1960. The application of electronics computer to factor analysis. *Educational and Physiological Measurement* 20, 141-151.
- Karunakara, N., Somashekarappa, H. M., Narayana, Y., Avadhani, D. N., Mahesh, H. M., Siddappa, K., 2003.  $^{226}\text{Ra}$ ,  $^{40}\text{K}$  and  $^7\text{Be}$  activity concentrations in plants in the environment of Kaiga, India. *Journal of Environmental Radioactivity* 65, 255-266.
- Kirchner, G., Daillant, O., 2002. The potential of lichens as long-term biomonitors of natural and artificial radionuclides. *Environ. Pollut.* 120, 145-150.
- Krmar, M., Radnović, D., Rakic, S., Matavuly, M., 2007. Possible use of terrestrial mosses in detection of atmospheric deposition of  $^7\text{Be}$  over large areas. *Journal of Environmental Radioactivity* 95, 53-61.

- Krmar, M., Radnović, D., Mihailović, D. T., Lalić, B., Slivka, J., Bikit, I., 2009. Temporal variations of  $^7\text{Be}$ ,  $^{210}\text{Pb}$  and  $^{137}\text{Cs}$  in moss samples over 14 month period. *Applied Radiation and Isotopes* 67, 1139-1147.
- Krmar, M., Wattanavatee, K., Radnović, D., Slivka, J., Bhongsuwan, T., Frontasyeva, M.V., Pavlov, S. S., 2013. Airborne radionuclides in mosses collected at different latitudes. *Journal of Environmental Radioactivity* 117, 45-48.
- Krzanowski, W., 2000. *Principal of Multivariate Analysis: A User's Perspective*. Oxford University Press, Oxford.
- Kulan, A., Aldahan, A., Possnert, G., Vintersved, I., 2006. Erratum to "Distribution of  $^7\text{Be}$  in surface air of Europe". *Atmospheric Environment* 40, 3855-3868.
- McCartney, M., Davidson, C. M., Howe, S. E., Keating, G. E., 2000. Temporal changes in the distribution of natural radionuclides along the Cumbrian coast following the reduction of discharge from phosphoric acid production plant. *Journal of Environmental Radioactivity* 49, 279-291.
- Mietelski, J. W., Gaca, P., Olech, M. A., 2000. Radioactive contamination of lichens and mosses collected in South Shetlands and Antarctic Peninsula. *Journal of Radioanalytical and Nuclear Chemistry* 245, 527-537.
- Momoshima, N., Nishio, S., Kusano, Y., Fukuda, A., Ishimoto, A., 2006. Seasonal variations of atmospheric  $^{210}\text{Pb}$  and  $^7\text{Be}$  concentrations at Kumamoto, Japan and their removal from the atmosphere as wet and dry depositions. *Journal of Radioanalytical and Nuclear Chemistry* 268, 297-304.
- Nagai, H., Tada, W., Kobayashi, T., 2000. Production rates of  $^7\text{Be}$  and  $^{10}\text{Be}$  in the atmosphere. *Nucl. Instrum. Methods Phys. Res., Sect. B*, 172, 796-801.
- Nifontova, M. G., 2006. Long term dynamics of technogenic radionuclide concentrations in moss-lichen cover. *Russian Journal of Ecology* 37, 247-250.
- Paatero, J., Hatakka, J., Viisanen, Y., 2001. Trajectory analysis of  $^{210}\text{Pb}$  and  $^7\text{Be}$  in ground – level air in Southern Finland. *Radiochemistry* 43, 475-481.

- Papastefanou, C., Manlopoulou, M., Sawidis, T., 1989. Lichens and mosses: biological monitors of radioactive fallout from Chernobyl reactor accident. *Journal of Environmental Radioactivity* 9, 199-207.
- Pham, M. K., Betti, M., Nies, H., Povinec, P. P., 2011. Temporal changes of  $^7\text{Be}$ ,  $^{137}\text{Cs}$  and  $^{210}\text{Pb}$  activity concentrations in surface air at Monaco and their correlation with meteorological parameters. *Journal of Environmental Radioactivity* 102, 1045-1054.
- Pesch, R., Schroeder, W. (2006). Mosses as bioindicators for metal accumulation: statistical aggregation of measurement data to exposure indices. *Ecological Indicators*, 6, 137–152.
- Petrova, T. B., Mikljaev, P. S., Vlasov, V. K., Afinogenov, A. M., Kirjukhin, O. V., 2009. Variations in the  $^7\text{Be}$  content in the ground layer of the atmosphere at middle latitudes. *Moscow University Chemistry Bulletin* 64, 317-321.
- Pettersson, H. B. L., Hallstadius, L., Redvall, R., Holm, E., 1988. Radioecology in the vicinity of prospected uranium mining sites in a subarctic environment. *Journal of Environmental Radioactivity* 6, 25-40.
- Popovic, D., Todorovic, D., Frontasyeva, M. V., Ajtic, J., Tasic, M., Rajsic, S., 2008. Radionuclides and heavy metals in Borovac, Southern Serbia. *Environ. Sci. Pollut. Res.* 15, 509-520.
- Psichoudaki, M., Papaefthymiou, H., 2008. Natural radioactivity measurements in the city of Ptolemais (Northern Greece). *Journal of Environmental Radioactivity* 99, 1011-1017.
- Ritchie, S. W., Nguyen, H. T., Holaday, A. S., 1990. Leaf water content and gas-exchanges parameters of two wheat genotypes differing in drought resistance. *Crop. Sci.*, 30, 105-111.
- Rühling, Å., Tyler, G., 1973, Heavy metal deposition in Scandinavia. *Water, Air and Soil Pollution* 2, 445-455.
- Sato, S., Koike, Y., Saito, T., Sato, J., 2003. Atmospheric concentration of  $^{210}\text{Pb}$  and  $^7\text{Be}$  at Sarufutsu, Hokkaido, Japan. *Journal of Radioanalytical and Nuclear Chemistry* 225, 351-353.
- Seddeek, M. K., Kozae, A. M., Sharshar, T., Badran, H. M., 2009. Reduction of the dimensionality and comparative analysis of multivariate radiological data. *Applied Radiation and Isotopes* 67, 1721-1728.

- Sert, E., Uğur, A., Özden, B., Saç, M. M., Camgöz, B., 2011. Biomonitoring of  $^{210}\text{Po}$  and  $^{210}\text{Pb}$  using lichens and mosses around coal-fired power plants in Western Turkey. *Journal of Environmental Radioactivity* 102, 535-542.
- Smirnov, L.I., Frontasyeva, M.V., Steinnes, E., Lyapunov, S.M., Cherchintsev, V.D., Romanov, S.A., Samosadnyj, V.T., 2004. Multidimensional statistical analysis of the concentration of heavy metals and radionuclides in moss and soil in southern Urals. *Atomnaya Energiya* 97, 68-74.
- Sugihara, S., Efrizal, Osaki, N., Momoshima, N., Maeda, Y., 2008. Seasonal variation of natural radionuclides and some elements in plant leaves. *Journal of Radioanalytical and Nuclear Chemistry* 278, 419-422.
- Sumerling, T. J., 1984. The use of mosses as indicators of airborne radionuclides near a major nuclear installation. *The Science of the Total Environment* 35, 251-265.
- Szczepaniak, K., Biziuk, M., 2003. Aspects of the biomonitoring studies using mosses and lichens as indicators of metal pollution. *Environmental Research* 93, 221-230.
- Tipayamongkholgul, M., Fang, C. T., Klinchan, S., Liu, C. M., King, C. C., 2009. Effects of the El Niño-Southern Oscillation on dengue epidemics in Thailand, 1996-2005. *BMC Public Health* 9, 422.
- Tsikritzis, L. I., 2005. Chemometrics of the distribution and origin of  $^{226}\text{Ra}$ ,  $^{228}\text{Ra}$ ,  $^{40}\text{K}$ , and  $^{137}\text{Cs}$  in plants near the West Macedonia Lignite Center (Greece). *Journal of Radioanalytical and Nuclear Chemistry* 264, 651-656.
- Ueno, T., Nagao, S., Yamazawa, H., 2003. Atmospheric deposition of  $^7\text{Be}$ ,  $^{40}\text{K}$ ,  $^{137}\text{Cs}$  and  $^{210}\text{Pb}$  during 1993 – 2001 at Tokai-mura, Japan. *Journal of Radioanalytical and Nuclear Chemistry* 255, 335-339.
- Uğur, A., Özden, B., Saç, M. M., Yener, G., 2003. Biomonitoring of  $^{210}\text{Po}$  and  $^{210}\text{Pb}$  using lichens and mosses around a uraniferous coal-fired power plant in Western Turkey. *Atmospheric Environment* 37, 2237-2245.
- UNSCEAR, 2000. United Nations Scientific Committee on the Effects of Atomic Radiation Report. Ionizing Radiation: Sources and Biological Effects. United Nation, New York.

Viet, H., N., Frontasyeva, M. V., Thi T., M., T., Gilbert, D., Bernard, N., 2010. Atmospheric heavy metal deposition in Northern Vietnam: Hanoi and Thainguayen case study using the moss biomonitoring technique, INAA and AAS. *Environ. Sci. Pollut. Res.* 17, 1045-1052.

Wangwongchai, A., Zhao, S., Zeng, Q., 2005. A case study on a strong tropical disturbance and record heavy rainfall in Hat Yai, Thailand during the winter monsoon. *Advances in Atmospheric Sciences.* 22, 436-450.

Zechmeister, H. G., 1995. Correlation between altitude and heavy metal deposition in the Alps. *Environ. Pollut.* 89, 73-80.

## **Appendices**

## Appendix A1

### Radioactive decay and radioactivity

Radioactive decay; an unstable nuclide or “parent” is transformed into a more stable (or unstable) nuclide called “daughter”, if daughter is still unstable and continue decay until a stable product is reached; which is called “decay chain or series decay”. The radioactive nuclide is defined by nucleus give off radiant energy in the form of particles (alpha, beta) or gamma rays, by the spontaneous disintegration of atomic nuclei: such as plutonium, radium, thorium, and uranium and their products, these phenomena of spontaneous emission of radiation from these atomic nucleus is called radioactivity. Naturally occurring and artificially nuclei, radioactivity are alpha active, beta active or both and emit a combination of alpha, beta and gamma radiation.

#### A1.1 Alpha emission

Alpha particle is the helium nucleus consisted of 2 protons and 2 neutrons combined together by strong nuclear interaction. Many natural occurring, heavy nuclei with  $82 < Z < 92$  and artificially produced transuranic elements ( $Z > 92$ ) decay by alpha emission as shown in eq.

A1.1 and energy released ( $Q_\alpha = E_{k,\alpha} + E_{k,Y} = \text{decay energy}$ ) in the decay is shown in eq. A.1.2



$$Q_\alpha = \left[ M({}^A_Z X) - M({}^4_2 \text{He}) - M({}^{A-4}_{Z-2} Y) \right] c^2 = E_{k,\alpha} \left[ 1 + \frac{M({}^4_2 \text{He})}{M({}^{A-4}_{Z-2} Y)} \right] \dots \text{A1.2}$$

where  $M({}^A_Z X)$ ,  $M({}^4_2 \text{He})$ ,  $M({}^{A-4}_{Z-2} Y)$  = unified mass of “parent”, “alpha” and

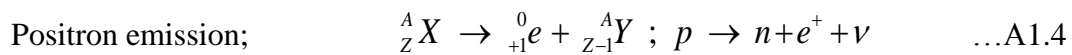
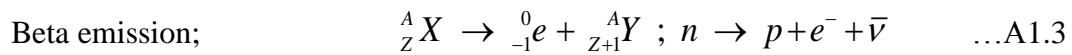
“daughter” respectively.

$c$  = speed of light in vacuum ( $3 \times 10^8$  m/s).



## A1.2 Beta emission and electron capture

Unstable nuclei as either neutron rich or proton rich decay toward the “stability line” into other isobaric nuclei; for neutron rich nucleus, electron (negative beta particle) emission while positron (positive beta particle) emission or electron capture emission from proton rich nucleus decays. The beta emissions are shown in eq. A1.3 – A1.4,

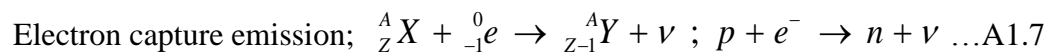


Although alpha particles are emitted with discrete spectrum of energies, however due to weak interaction between decay produced particle (lepton;  $e^- - \nu, e^+ - \bar{\nu}$ ), beta energy of beta decay are continuous spectrum, ranged from 0 to  $Q_\beta$  (Decay energy or “End – Point”) with the most probable energy is about  $Q_\beta/3$ . The decay energies of beta decays are

$$\text{Beta emission; } \quad Q_{\beta^-} = \left[ M \left( {}^A_Z X \right) - M \left( {}^A_{Z+1} Y \right) \right] c^2 \quad \dots\text{A1.5}$$

$$\text{Positron emission; } \quad Q_{\beta^+} = \left[ M \left( {}^A_Z X \right) - M \left( {}^A_{Z+1} Y \right) - 2m_e \right] c^2 \quad \dots\text{A1.6}$$

An alternative to positron emission, in proton rich nuclei with the different between parent and daughter is less than 2 times of electron mass, electron capture in which proton and atomic electron (mostly probably from K – shell) are transformed into a neutron and a neutrino, as shown in eq. A1.7 and energy released as same as eq. A1.5



## A1.3 Gamma emission and internal conversion

After alpha and/or beta emissions parent nucleus transformed to a certain (or more) excited states of daughter nucleus, most of the transition energy which is the energy different between initial and final state may appear in the form of gamma ray or photon. If  $E^*$  and  $E$  are energy of initial and final states of daughter nucleus, thus frequency of emitted photon is

$$\nu = \frac{E^* - E}{h} \quad \dots A1.8$$

Alternatively, the nucleus may de – excite by ejecting an atomic electron in process called “internal conversion” where the total energy of ejected electron ( $E_{e^-}$ ) is equal to the energy different between photon and binding energy of an electron ( $E_B$ ), as

$$E_{e^-} = h\nu - E_B \quad \dots A1.9$$

In addition, both of decay modes are due to the action of electromagnetic interaction, if energy of photon has sufficiently high enough ( $> 1.02$  MeV), the “internal pair production” decay is possible observed

$$h\nu \rightarrow e^+ + e^- \quad \dots A1.10$$

The activity of a radioisotope source is defined by its rate of decay; where N is number of nuclei,  $\lambda$  is decay constant (/s) and  $T_{1/2}$  is physical half – life (s), and is given by the “radioactive decay law” as

$$A = -\frac{dN}{dt} = \lambda N = \frac{N \ln 2}{T_{1/2}} \quad \dots A1.11$$

Unit of activity is Bq where 1 Bq = 1 disintegration per second (dps) =  $2.703 \times 10^{-11}$  Ci

By decay law, both of number of nuclei and activity decreased exponentially with respect to time from  $A_0$ ,  $N_0$  (initial activity and initial number of nuclei at time  $t = 0$ ) as

$$A = \lambda N = A_0 e^{-\lambda t} = \lambda N_0 e^{-\lambda t} \quad \dots A1.12$$

Mean life – time ( $\tau$ ) is defined as an average lifetime of a radioactive nucleus. From eq. A11 the number of nucleus which decay between  $t \rightarrow t + dt$  is  $dN = -\lambda N dt = -\lambda N_0 e^{-\lambda t} dt$ , thus

$$\tau = \frac{\int t dN}{\int dN} = \frac{\int_0^{\infty} t e^{-\lambda t} dt}{\int_0^{\infty} e^{-\lambda t} dt} = \frac{1}{\lambda} \quad \dots A1.13$$

### A1.4 Radioactive decay chains and Secular equilibrium

Consider a chain of decays;  $A \xrightarrow{\lambda_A} B \xrightarrow{\lambda_B} C$  etc. it can be seen that

$$\frac{dN_A}{dt} = -\lambda_A N_A \Rightarrow N_A(t) = N_{A,0} e^{-\lambda_A t} \quad \dots A1.14$$

$$\frac{dN_B}{dt} = -\lambda_A N_A + \lambda_B N_B \Rightarrow N_B(t) = \left( \frac{\lambda_A}{\lambda_B - \lambda_A} \right) N_{A,0} [e^{-\lambda_A t} - e^{-\lambda_B t}] \quad \dots A1.15$$

$$\frac{dN_C}{dt} = -\lambda_B N_B \Rightarrow N_C(t) = \left( \frac{1}{\lambda_B - \lambda_A} \right) N_{A,0} [1 + \lambda_A e^{-\lambda_A t} - \lambda_B e^{-\lambda_B t}] \quad \dots A1.16$$

If C is unstable, another chain of decays is  $A \xrightarrow{\lambda_A} B \xrightarrow{\lambda_B} C \xrightarrow{\lambda_C} \dots \rightarrow N$ , the Bateman's equation is calculated for the number of  $n^{\text{th}}$  nuclei in chain, following eq. A1.17

$$N_n(t) = \sum_{i=1}^n \left[ N_{i,0} \cdot \prod_{j=i}^{n-1} \lambda_j \cdot \sum_{j=i}^n \left( \frac{e^{-\lambda_j t}}{\prod_{p=i, p \neq j}^n (\lambda_p - \lambda_j)} \right) \right] \quad \dots A1.17$$

From eq. A1.15, if the daughter has relatively short – life compared with the parent ( $T_B \lll T_A$  or  $\lambda_B \ggg \lambda_A$ ),  $N_B$  is grows rapidly and, after long time enough ( $e^{-\lambda_A t} \ggg e^{-\lambda_B t}$ ), eq. A1.15 become

$$N_B(t) \approx \left( \frac{\lambda_A}{\lambda_B} \right) N_{A,0} e^{-\lambda_A t} \Rightarrow A_B(t) \approx A_A(t) \quad \dots A1.18$$

Eq. A1.18 is call “Radioactive secular equilibrium”; it means that “If parent and daughter are in secular equilibrium, their actual activities are approximately equal”. This phenomenon is generally useful in field of environmental radiation measurements.

## Appendix A2 Short brief of general statistic, principle component analysis (PCA) and cluster analysis (CA)

### A2.1 Characterization of measuring data

For N – independent measurements the activity of radioactive source;  $x_1, x_2, \dots, x_i, \dots, x_N$ , thus the “experimental mean” is

$$\bar{x}_{\text{exp}} \equiv \frac{\sum_{i=1}^N x_i}{N} \quad \dots \text{A2.1}$$

It is often appropriate to represent the data set by a corresponding “frequency distribution function F(x)” with is normalized  $\sum_{x=0}^{\infty} F(x) = 1$ , by definition

$$F(x) \equiv \frac{\text{number of occurrences of value "x"}}{N} \quad \dots \text{A2.2}$$

So, it is possible to calculate the  $\bar{x}_{\text{exp}}$  by using F(x) as

$$\bar{x}_{\text{exp}} = \sum_{x=0}^{\infty} x \cdot F(x) \quad \dots \text{A2.3}$$

The sample deviation is amount by it's different from  $\bar{x}_{\text{exp}}$  and defined by  $\varepsilon_i = x_i - \bar{x}_{\text{exp}}$  so that  $\sum_{i=1}^N \varepsilon_i = 0$ . As long as  $N \rightarrow \infty$ , thus the sample variance ( $s^2$ ) is served to quantify the average value of squared deviation of each data point from their mean value (internal spread in data set), as

$$s^2 = \frac{1}{N-1} \sum_{x=0}^{\infty} \varepsilon_i^2 \quad \dots \text{A2.4}$$

### A2.2 Statistical model

#### Poisson and Gaussian Distributions

In nuclear counting experiments associate with a large number of decay of nuclei (in order of Avogadro's number), it make up the sample or number of trials, which is a relative

small fraction of these give rise to recorded counts. If  $n$  is the number of count for which each counting event has a success probability  $p$ , for this phenomenon  $p \ll 1$ , and by using eq. A2.3 thus  $\bar{x} = n \cdot p$ . The Poisson and Gaussian distributions are more appropriated than other distribution for nuclear counting statistic; Poisson distribution is defined by

$$P(x) \equiv \frac{(\bar{x})^x e^{-\bar{x}}}{x!} \quad \dots A2.5$$

This equation is a very useful simplification in order to reconstruct its amplitude at all other values of the argument. That is a great help to estimate the mean value which have no idea of either the individual probability or the sampling size of the measurement. It can calculate mean value of measurement;

$$\bar{x} = \sum_{x=0}^{\infty} x \cdot P(x) = n \cdot p \quad \dots A2.6$$

The prediction of sample variance can be calculate by

$$\sigma^2 \equiv \bar{x} = \sum_{x=0}^{\infty} (x - \bar{x})^2 \cdot P(x) = n \cdot p \quad \dots A2.7$$

From eq. A2.6 – A2.7, the predicted sample standard (uncertainty of counting) is

$$\sigma \equiv \sqrt{\bar{x}} \quad \dots A2.8$$

However, Poisson distribution holds in the limit  $p \ll 1$ , and the distribution curve is not symmetry for  $N < 3 - 10$ , if the mean value of distribution is large ( $>20$ ) the curve is approximated symmetry, thus the additional simplifications can generally be carried out which lead to the Gaussian distribution;

$$P(x) \equiv \frac{1}{\sqrt{2\pi\bar{x}}} e^{-\left[\frac{(x-\bar{x})^2}{2\bar{x}}\right]} \quad \dots A2.9$$

This is again, the calculated mean value of measurement, predicted sample variance and predicted sample standard are similar as eq. A2.6 – A2.9 respectively. However, because of  $\sigma \equiv \sqrt{\bar{x}}$  thus, (i) the integral of Gaussian curve is used to determine the uncertainty of counting in the term of “percentage of confidence level” or (ii) in order to reduce the uncertainty

the increasing the measurement time is used or using of the higher efficiency of radiation detector.

### A2.3 Principle component analysis and cluster analysis

#### A2.3.1 Principle component analysis (PCA)

In multivariate analysis, it is often starts out with a number of data involving a substantial number of correlated variables. Principle component analysis is a technique for simplifying a dataset (sample) or by finding a new set of variables (smaller than the original set – also called dimension reducing), that the sample's information is reserved

PCA is also “*an orthogonal linear transformation that transfers the observed data to a new coordinate system that the largest variance by any projection of the data lie on the first coordinate (first principal component, PC1), the second largest variance lies on the second coordinate (second principal component, PC2), and so on.*”

If  $m$  is number of variables, a sample matrix ( $\mathbf{X}_i$ ) is represented by  $1 \times m$  matrix as shown in Eq. A2.10. If  $n$  is number of samples, the Data matrix  $\mathbf{X}$  is represented by  $n \times m$  matrix and it is represented by Eq. A2.11

$$\begin{aligned} X_1 &= (x_{11}, x_{12}, \dots, x_{1m}) \\ &\vdots \\ X_n &= (x_{n1}, x_{n2}, \dots, x_{nm}) \quad ; \text{where } 1 \leq i \leq n, 1 \leq j \leq m \end{aligned} \quad \dots \text{A2.10}$$

and

$$X = \begin{bmatrix} x_{11} & \dots & x_{1m} \\ \vdots & \ddots & \vdots \\ x_{n1} & \dots & x_{nm} \end{bmatrix} \quad \dots \text{A2.11}$$

For  $j^{\text{th}}$  column, mean value of ( $\bar{x}_j$ , where  $1 \leq j \leq m$ ) and sample variance ( $\text{var}_j$ ) are calculated by

$$\bar{x}_j = \frac{1}{n} \sum_{i=1}^n x_{ij} = \frac{1}{n} (x_{1j} + x_{2j} + \dots + x_{nj}) \quad \dots \text{A2.12}$$

$$\text{var}_j = \frac{1}{n-1} \sum_{k=1}^n (x_{jk} - \bar{x}_j)^2 \quad \dots \text{A2.13}$$

It is generally known that the square root of  $\text{var}_j$  is “standard derivation of samples,  $\sigma_j$ ”

The covariant matrix ( $\mathbf{S}$ ) is performed by

$$S = \begin{bmatrix} \text{COV}_{11} & \text{COV}_{12} & \cdots & \text{COV}_{1n} \\ \text{COV}_{21} & \text{COV}_{22} & \cdots & \vdots \\ \vdots & \vdots & \ddots & \vdots \\ \text{COV}_{n1} & \cdots & \cdots & \text{COV}_{nn} \end{bmatrix} \quad \dots \text{A2.14}$$

; Where covariance (cov<sub>ij</sub>) are defined by

$$\text{cov}_{ij} = \frac{1}{n-1} \sum_{k=1}^n (x_{ik} - \bar{x}_i)(x_{jk} - \bar{x}_j) \quad \dots \text{A2.15}$$

Noted, if covariance is (i) positive, both dimensions increase together, (ii) negative, as one increases, the other decreases, and (iii) zero: it is independent of each other.

By negligible of theory, PCA is considered by following procedure

**Step 1** Test correlation between variables by using Pearson's correlation coefficient and testing the KMO's coefficient (Kaiser – Mayer – Olkin).

Let R is "correlation matrix" and defined by Eq.2.16

$$R = \begin{bmatrix} 1 & r_{12} & \cdots & r_{1n} \\ r_{21} & 1 & \cdots & \vdots \\ \vdots & \cdots & \ddots & \vdots \\ r_{n1} & \cdots & \cdots & 1 \end{bmatrix} \quad \dots \text{A2.16}$$

; Where 
$$r_{ij} = \frac{\text{COV}_{ij}}{\sigma_i \sigma_j} \quad \dots \text{A2.17}$$

Given r<sub>ij</sub> is Pearson's correlation coefficient between x<sub>i</sub> and x<sub>j</sub>, if it closes to 1 reflects they should belonging to a same component. From presented correlation coefficients, the KMO was also test before PCA; KMO coefficient is defined by

$$KMO = \frac{\sum_{\substack{i,j=1 \\ i \neq j}}^n r_{ij}^2}{\sum_{\substack{i,j=1 \\ i \neq j}}^n r_{ij}^2 + \sum (\text{partial correlation})^2} \quad \dots \text{A2.18}$$

In fact, if  $0.0 < KMO < 1.0$  the PCA is appropriated for analyzing the measured data. Although the calculated value is about 0.544 (in **Table 3.3**) – it is close to its lower limit, however this may be due to a variety of moss samples collected in this study, it should be note that PCA is suitable for the analyzing.

**Step 2** Factor extraction method by using of “PCA – whose groups the variables into separated components (PCs), which the number of components are minimized as possible and uncorrelated (some time called orthogonal) to each other’s”.

The PCA method is performed by calculation the eigenvalues ( $\lambda$ ) and eigenvectors ( $\mathbf{u}$ ); if  $\mathbf{I}$  is the identity matrix, they are calculated from the characteristic equation

$$\det(\lambda \mathbf{I} - \mathbf{S}) = 0 \quad \dots \text{A2.19}$$

Let  $\lambda_1 \geq \lambda_2 \geq \lambda_3 \geq \dots \geq \lambda_m > 0$  be the eigenvalues of  $\mathbf{S}$  with corresponding orthogonal eigenvectors ( $\vec{u}_1, \vec{u}_2, \dots, \vec{u}_m$ ), the important notification is T (called total variance) that is summation of its eigenvalues as

$$T = \lambda_1 + \lambda_2 + \dots + \lambda_m. \quad \dots \text{A2.20}$$

**Step 3** Choosing the sufficient principal components to account for a great percentages (over 75%) of total variability in dataset with Kaiser’s criteria

The eigenvectors are called the principal components of data set ( $PC_1, PC_2, \dots, PC_m$ ) and can be rewritten by

$$PC_m = \sum_{k=1}^p w_{mk} x_k \quad \dots \text{A2.21}$$

Let m is number of the component (and  $m < p$ ) and  $w_{mk}$  is the factor loading; - if the calculated value of any variables have to closes +1 or -1, they are grouped in the same particular PCs. Refer to Eq. **A2.21**, For example, the 1<sup>st</sup> principal components ( $PC_1$ ) is

$PC_1 = w_{11}x_1 + w_{12}x_2 + \dots + w_{1p}x_p$  and  $w_{11}^2 + w_{12}^2 + \dots + \dots + w_{1p}^2 = 1$ , the remaining PCs (2<sup>nd</sup>, 3<sup>rd</sup> ...) are chosen in this similar constraint.

Kaiser’s criteria is the generally used to selecting the number of components; - *The more variables that load onto a particular component, the more important the factor is in summarizing the data. An eigenvalue indicates how good a component is as a summary of the data, if it is unity means that “the factor contains the same amount of information as a single variable”.*

However, it is ambiguous if at least two components have the closed value of loading factors, thus the “*Varimax rotation*” (Kaiser, 1958); - a most popular rotation method to simplify the interpretation, is applied. This rotation method means that each factor has a small number of large loadings and a large number of zero (or small) loadings, the interpretation is simplified because, each original variable tends to be associated with one (or a small number) of factors, and each factor represents only a small number of variables. In addition, the factors can often be interpreted from the opposition of few variables with positive loadings to few variables with



negative loadings. Formally Varimax searches for a rotation (i.e., a linear combination) of the original factors such that the variance of the loadings is maximized, which amounts to maximizing.

#### Step 4 Forming of new variables, labeling and interpretation

By meaning of PCA and Varimax rotation, the original variables ( $X_1, \dots, X_n$ ) is replaced by the new ones ( $Z_i$ ), which is performed as linear combination of  $PC_m$  as shown in Eq. **A2.22**

$$Z_i = \sum_{m=1}^p I_{im} (PC_m) \quad \dots \text{A2.22}$$

; Where  $I_{im}$  are any loading constants

After suitable interpretation of new variables ( $Z_i$ ) are already to for another statistical method such as t – test, Z – test, ANOVA or Linear regression etc. for further studies.

#### A2.3.2 Cluster analysis (CA)

Cluster analysis is a multivariate method *which is applied to divides the observation variables into homogeneous or distinguished groups*. Although there are a number of different methods which are used to carry out a CA, however the Agglomerative – Hierarchical with Ward's methods is almost popular.

Agglomerative methods, in which all variables start in their own separated clusters (*n variables with n clusters*). Then the two 'closest clusters' are combined and this is done repeatedly until all variables are in one cluster. At the end, the number of clusters is then chosen out of all cluster solutions. While the Ward's method is main method, in all possible pairs of clusters are combined and are summed over all clusters. The chosen clusters are in the way that the increasing of the summation of the squared distances within each cluster is minimized or the combination that gives the lowest summation of squares is chosen.

Let

$$\begin{aligned} X_1 &= (x_{11}, x_{12}, \dots, x_{1m}) \\ &\vdots \\ X_n &= (x_{n1}, x_{n2}, \dots, x_{nm}) \quad ; \text{where } 1 \leq i \leq n, 1 \leq j \leq m \end{aligned}$$

In CA, the *Euclidean distance* is calculated to measure the distance between variables (called measuring of the 'Similarity' or 'Dissimilarity'), and it is defined by

$$d(i, j) = \sqrt{\sum_{k=1}^n (X_{ki} - X_{kj})^2} \quad \dots \text{A2.23}$$

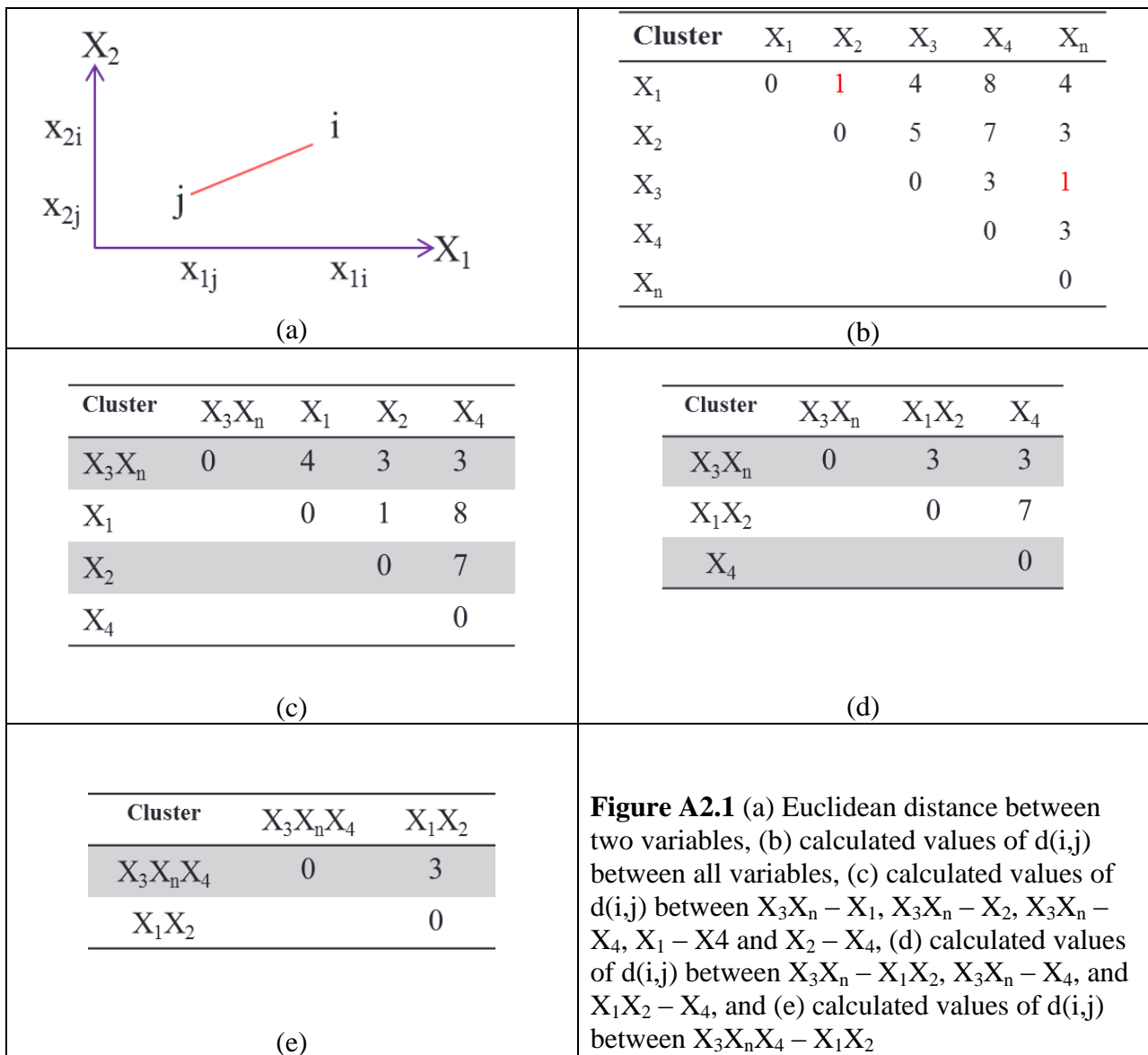
For example, the Euclidean distance of the  $n$  – variables  $X_1 - X_n$  are shown in **Figure A2.1(a)**, their calculated values of  $d(i,j)$  are shown in **Figure A2.1(b)**. Then, it can be seen that the minimum distance between  $X_1, X_2$  is 1.0 as similar as  $X_3, X_n$ , thus they are belonging into the 2 separated clusters (1<sup>st</sup> Cluster is consisted of  $X_1, X_2$ , 2<sup>nd</sup> Cluster is consisted of  $X_3, X_n$ ).

From **Figure A2.1(b)** it can be seen that

$$d(X_3X_n, X_1) = \min \{d(X_3, X_1), d(X_n, X_1)\} = \min \{4, 4\} = 4$$

$$d(X_3X_n, X_2) = \min \{d(X_3, X_2), d(X_n, X_2)\} = \min \{5, 3\} = 3$$

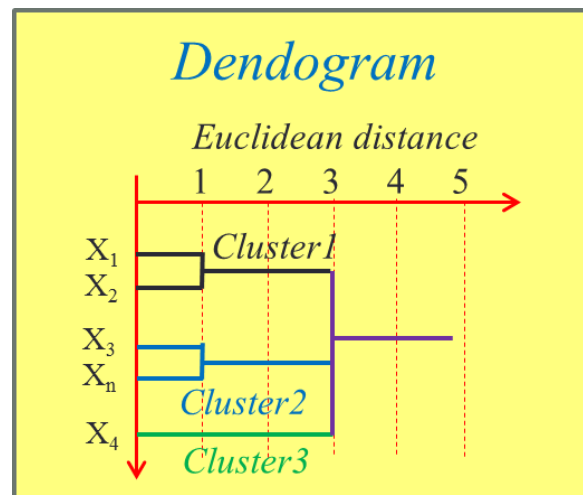
and 
$$d(X_3X_n, X_1X_2) = \min \{d(X_3X_n, X_1), d(X_3X_n, X_2)\} = \min \{5, 3\} = 3$$



Thus the distance between 1<sup>st</sup> cluster and 2<sup>nd</sup> cluster is 3.0; the calculated values are shown in **Figure A2.1 (c) and (d)**. From **Figure A2.1 (d)**, it can be seen that  $X_4$  is separated into 3<sup>rd</sup> cluster with distance of 3.0 as shown in **Figure A2.1 (e)**.

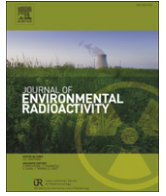
$$d(X_3X_nX_4, X_1X_2) = \min\{d(X_3X_n, X_1X_2), d(X_4, X_1X_2)\} = \min\{5, 3\} = 3$$

As stated above, when carrying out a hierarchical cluster analysis, the process can be represented on a *dendrogram*; - A diagram illustrates which clusters have been joined at each stage of the analysis and the distance between clusters. If there is a small distance between clusters means they are relatively close together, whereas the large ones is suggested that at one stage clusters were joined were relatively far apart. This implies that the optimum number of clusters may be the number present just before those large values of Euclidean distance. This is easier to understand by actually looking at a dendrogram. The dendrogram of the example is presented in **Figure A2.2**



**Figure A2.2** The dendrogram of  $X_1, X_2, X_3, X_4$  and  $X_n$

**Appendix A3** First publication “Airborne radionuclide in different latitude”



## Airborne radionuclides in mosses collected at different latitudes

M. Krmar<sup>a,\*</sup>, K. Wattanavatee<sup>b</sup>, D. Radnović<sup>a</sup>, J. Slivka<sup>a</sup>, T. Bhongsuwan<sup>b</sup>, M.V. Frontasyeva<sup>c</sup>, S.S. Pavlov<sup>c</sup>

<sup>a</sup> Faculty of Science, University Novi Sad, Trg Dositeja Obradovica 4, 21000 Novi Sad, Serbia

<sup>b</sup> Department of Physics, Faculty of Science, Prince of Songkla University, Thailand

<sup>c</sup> Frank Laboratory of Neutron Physics, Joint Institute for Nuclear Research, Dubna, Moscow Region, Russian Federation

### ARTICLE INFO

#### Article history:

Received 27 December 2010

Received in revised form

29 July 2011

Accepted 9 August 2011

Available online 30 August 2011

#### Keywords:

Airborne radionuclides

Atmospheric deposition

Biomonitors

Low-background gamma spectroscopy

### ABSTRACT

Terrestrial mosses are a promising medium for investigation and monitoring of airborne radionuclide depositions due to their widespread occurrence, ease of sampling, and the possibility of high-resolution gamma spectrometry measurements without preparatory chemical treatment of samples. The overall objective of the present study was to compare <sup>7</sup>Be, <sup>210</sup>Pb and <sup>137</sup>Cs activity concentrations (in Bq/kg) in moss samples collected at two different climate zones: the south of Thailand (7 °N) and in Serbia (~45 °N) in order to examine deposition of airborne radionuclide in these distant areas. Significant difference of the <sup>210</sup>Pb content (almost a factor of 2) in mosses was observed. The mean value of <sup>7</sup>Be activity in samples from Serbia was almost 40% higher than activity of those collected in Thailand. Level of <sup>137</sup>Cs in Thailand mosses was below the detection limit. It was shown that air transport of water droplets in the area of waterfalls and strong turbulence can deposit U and Th daughter nuclei.

© 2011 Elsevier Ltd. All rights reserved.

### 1. Introduction

Naturally occurring <sup>7</sup>Be and <sup>210</sup>Pb together with <sup>137</sup>Cs released in the atmosphere can be used as tracers in investigations of atmospheric processes (Koch et al., 1996; Rehfield and Heimann, 1995). Deposition of airborne radionuclides depends on several factors and one can expect that different content of radionuclides should be deposited at different places. Beryllium-7 is formed by spallation reaction between cosmic rays and nuclei of oxygen and nitrogen in the stratosphere and upper troposphere (Masarik and Beer, 1999). By following the <sup>7</sup>Be atmospheric deposition (not altered by anthropogenic activities) it is possible to investigate stratospheric intrusions in the troposphere (Dib et al., 1994), vertical transport and residence time of aerosol particles in the troposphere (Papastefanou and Ioannidou, 1995), horizontal movement of air masses, etc. The production of cosmogenic isotopes also depends on intensity of the geomagnetic field; it was established that <sup>7</sup>Be concentrations in surface air decreases with increasing latitude (Kulan et al., 2006).

Lead-210 is a member of <sup>238</sup>U chain and comes into atmosphere from the soil mostly. After alpha decay of <sup>226</sup>Ra in soil, product <sup>222</sup>Rn, as a noble gas, escapes from all chemical bounds and spreads in the atmosphere. After three alpha and two beta subsequent

decays, long-living ( $T_{1/2} = 22$  years) <sup>210</sup>Pb is formed. Radon-222 daughter nuclei are chemically active, so they are attached to aerosol particles and consequently transported and deposited together with them. Whereas crustal minerals containing <sup>238</sup>U are source of <sup>222</sup>Rn, presence of <sup>210</sup>Pb and other radon daughters depends on geological features and permeability of the rocks and sediments at ground surface and below, distribution of continent and sea areas, general conditions of surface layer, etc. However, <sup>210</sup>Pb is also released from industrial processes such as the sintering of ores containing some amount of <sup>238</sup>U, the burning of coal (Delfanti et al., 1999) or the production and use of agricultural phosphate fertilizers.

The great majority of <sup>137</sup>Cs was released in atmosphere in nuclear accident in Chernobyl and more than 400 atmospheric nuclear weapon tests. Local atmospheric conditions were decisive for the deposition pattern in the first several weeks after accident or weapon test. Since there were no significant <sup>137</sup>Cs emissions after Chernobyl accident, atmospheric <sup>137</sup>Cs was exposed to physical decay ( $T_{1/2} = 26.6$  years) as well as wet and dry deposition. Further deposition of <sup>137</sup>Cs was determined by atmospheric transport and possible soil re-suspension (Todorović et al., 1999).

Terrestrial mosses have shown to be as a promising medium in investigation and monitoring of airborne radionuclide deposition (Steinnes and Njåstad, 1993; Nifontova, 1997; Florek et al., 2001; Krmar et al., 2007, 2009). Mosses do not have a rooting system, so uptake of the nutrients from the substrate is insignificant. They obtain water and most nutrients directly from air by precipitation

\* Corresponding author.

E-mail address: [krmar@df.uns.ac.rs](mailto:krmar@df.uns.ac.rs) (M. Krmar).

and dry deposition. The absence or strong reduction of the cuticle and thin leaves allows easy uptake from the atmosphere. Another significant advantage of the moss technique is that they are growing in different climatic zones, sample collection is very simple and much higher sampling density can be achieved than with the conventional precipitation analysis or air sampling. Accumulation of elements taken from the air in measurable concentrations makes mosses a superior sampling medium for trace elements (Rühling and Tyler, 1973). The results from moss surveys allow examination of both spatial and temporal trends of trace elements deposition and identification of areas exposed to different levels of deposition (Buse et al., 2003).

The objective of this pilot study is to compare measured activities of several radionuclides in moss samples taken from two distant places: Serbia and Thailand. Serbia is located at mid latitudes of northern hemisphere, about 45° north. Southern Thailand is geographically located close to Equator line, about 7° North. Very different climate, wind direction and precipitation can result in different deposition of airborne radionuclides and consequently different level of activity of airborne radionuclides in the moss samples.

## 2. Sampling and measurement

Samples of *Hypnum cupressiforme* were collected from 9 sampling sites in Serbia, distributed along the one direction starting from the northern province of Vojvodina to the southern border of the Republic Serbia. The sampling sites were located from 42.43° North to 45.38° North and from 19.58° East to 22.13° East. The altitude smoothly increases from north to south across the sampling line from 80 to 350 m above the mean sea level. All samples of fresh plant material were collected in a short time interval during the summer 2008. During two days of sampling there was no rain which avoided the complication that some sample could have been exposed to additional precipitation and extra component of airborne radionuclides by rain washing of the atmosphere. Open regions far from treetops and other obstacles were chosen. All sampling sites were carefully selected to avoid possible contact of mosses with surface waters. Samples were dried at 104 °C to a constant weight. Soil and all other mechanical impurities were manually removed and samples were packed into two cylindrical plastic containers, diameter 67 mm and height 31 mm. The minimum mass of dry moss was 25.6 g and the maximum was 38.4 g.

Low-background extended range HPGe detector equipped with a Be window to get evidence about  $^{210}\text{Pb}$  concentration was used in measurements. Relative efficiency of detector is 32%. Background count was reduced by passive shield (18 cm of lead, 1 mm of tin and 1.5 mm of copper) which do not interfere with gamma photons emitted from sample. Gamma spectrum of each sample was collected until statistical uncertainty of the 477.6 keV  $^7\text{Be}$  line up to 5% was achieved and statistical uncertainty of 46.5 keV  $^{210}\text{Pb}$  line was up to 5%. The longest sample counting time was 66 ks. The detection efficiency was established using NIST Standard Reference Material 4350B (Columbia River sediment) packed in same geometry. The source self-attenuation due to different chemical composition and density of sample were corrected with computer program based on Moens et al. (1981). Attenuation properties of samples were measured in narrow beam geometry with calibration set of point sources. Relatively small variation found for the samples originated from the density variation, e.g. mass attenuation coefficients of dry mosses were roughly constant. Accuracy of efficiency calibration was tested using IAEA source made from dry grass.

Nine samples of *Leucobrym aduncum* Dozy & Molk and *Leucobrym arfakianum* C. Muell, from 3 sites around Hatyai City, Songkhla

Province, Southern Thailand: Khonumkang Nation Park (6.56°N 100.59°E), Ton – Ya Plong waterfall (7.00°N 100.46°E) and Ton – Nga – Chang waterfall (7.23°N 100.46°E) were taken. Sample materials were collected on January 2009 within the period of 2 days. During sampling period there was no rain to avoid the additional precipitation and extra component of airborne radionuclide by rain wash. However, the sampling in Thailand is quite different from sampling in Rep. of Serbia, in 3 ways,

1. All materials were collected not far from the stream side, just only 2–10 m. It is very difficult to find the mosses far from the water. This means that the moisture is an important factor in the sampling in Thailand.
2. Samples number 1, 3, 5, 7 and 8 were collected on the rock or roof under treetops, which are exposed to sunshine in some period of the daytime.
3. Samples number 1–5 and 6–9 were collected in the mountainous area between the elevation of 800–850 m and 1200–1250 m above mean sea level, respectively.

It is noted that during the sampling in Ton–Nga–Chang (Sample number 6–8), a large volume of water fall made re-suspension of water droplets in air that may affect radionuclides content in mosses samples if mosses have been exposed to such moist air.

The fresh plants material samples were collected and kept in the plastic bags and returned to the laboratory. The samples were washed by tap water to remove soil and all other mechanical impurities, and dried at 104 °C to a constant weight; the different of fresh and dry weight shows the water content in sample varying between 83% and 94%. The 100 g of each sample were packed into a cylindrical plastic container with a diameter 105 mm and height 57 mm.

Gamma spectroscopy measurements of moss samples taken in Thailand were carried out using extended range high-resolution HPGe detector equipped by thin carbon window to allow detection of low energy gamma lines. This ultra-low background, large volume germanium spectrometer has 100% relative efficiency. The detector shield is constructed of layered bulk lead. The total thickness of the lead shield is 15 cm. The lining materials are 1 mm low-background tin, and 1.5 mm high purity copper. The shield interior is flushed with nitrogen gas from the Dewar vessel in order to reduce the background from radon and its progenies. The detector was calibrated by NIST Standard Reference Material 4350B IAEA source made from dry grass as described earlier. In all spectra, the 477.6 keV gamma line was observed. Spectral data were collected about 150 ks until the statistical uncertainty of  $^{210}\text{Pb}$  gamma line was low enough to provide accuracy of the activity of  $^{210}\text{Pb}$  per unit mass (in Bq/kg) less than 10%. Thailand samples were almost three times longer measured because of the relative lower level of  $^7\text{Be}$  activity. Namely, due to transport delay, moss samples from Thailand were measured almost three months after sampling (Berilium-7 has relative short half-life (53.3 days)).

## 3. Results and discussion

Several prominent gamma lines appeared in all spectra. After background subtraction and peak analysis, intensities of 477.6 keV and 46.5 keV gamma lines were obtained and concentrations of  $^7\text{Be}$  and  $^{210}\text{Pb}$  activities in moss samples were calculated. The results of measurements of samples from 9 locations from Thailand and 9 locations from Serbia are shown in Table 1. Standard error ( $1\sigma$ ) related to counting statistic is presented in parenthesis in Table 1 and further in text.

It can be seen that measurable concentrations of  $^7\text{Be}$  and  $^{210}\text{Pb}$  were observed in moss samples taken in Thailand and Serbia. The

**Table 1**

Activity concentrations of  $^7\text{Be}$  and  $^{210}\text{Pb}$  detected in dried moss samples ( $1\sigma$  statistic uncertainty in parenthesis).

Sample No	Thailand		Serbia	
	Be-7 [Bq/kg]	Pb-210 [Bq/kg]	Be-7 [Bq/kg]	Pb-210 [Bq/kg]
1	130(17)	213(19)	380(30)	526(45)
2	216(28)	199(18)	238(25)	548(46)
3	290(40)	271(25)	412(28)	630(50)
4	225(30)	250(23)	242(23)	881(72)
5	142(24)	231(22)	259(20)	691(45)
6	260(30)	660(50)	200(25)	834(64)
7	153(28)	490(40)	385(30)	840(76)
8	340(40)	580(50)	217(18)	577(47)
9	280(40)	269(25)	494(39)	728(57)
Mean	226(73)	351(175)	314(104)	695(134)

concentration of  $^7\text{Be}$  is slightly higher in Serbian samples than those collected in Thailand. The mean value of  $^7\text{Be}$  activity measured in Thailand samples is about 40% lower than mean activity of samples taken in Serbia. Papers referring to activity concentrations of  $^7\text{Be}$  in mosses are not so abundant. Our measurements at both locations can be compared with values of  $^7\text{Be}$  activity concentration of moss samples obtained by Sumerling (1984). Although the mean value of 360 Bq/kg measured in England and reported in mentioned reference mach the mean value of  $^7\text{Be}$  measured in mosses collected in study conducted in Serbia, for some more general comparison larger number of samples collected from broader area should be measured (radius of sampling area in England was just 10 km). It is interesting to notice that in both sets of samples, in Serbia as well in Thailand; the smallest and the highest value of  $^7\text{Be}$  differ by a factor of 2.5.

Mean activity concentration of  $^{210}\text{Pb}$  detected in samples taken in Serbia was almost two times higher than that measured in Thailand. The difference between the lowest and the highest  $^{210}\text{Pb}$  concentration in Serbian mosses was about 70%. However the highest value of  $^{210}\text{Pb}$  concentration measured in Thailand moss sample was higher than the lowest one by a factor of 3.3. Values of  $^{210}\text{Pb}$  activity concentrations referred in literature, show relative high variability. The lowest values, between 17.3 and 149.8 Bq/kg of  $^{210}\text{Pb}$  in moss samples were measured in the South Shetland Archipelago (Godoy et al., 1998). The highest published values originated from the moss samples collected in areas having some industrial sources of  $^{210}\text{Pb}$ . For example, near the coal-fired power plants in western Turkey the values of  $^{210}\text{Pb}$  activity concentrations from 200 to 650 Bq/kg were measured (Uğur et al., 2003). The maximal value of  $^{210}\text{Pb}$ , ever measured in moss samples was 1898 Bq/kg (Delfanti et al., 1999). These authors collected mosses in area around a coal-fired power station located in the central Italy. Nuclear power stations can be a source of  $^{210}\text{Pb}$  as well. In West Cumbria near a nuclear installation, more than 900 Bq/kg of  $^{210}\text{Pb}$  was measured at some places (Sumerling, 1984). The sampling sites in Serbia and Thailand were relatively far from coal-fired or nuclear power stations.

To check the level of unsupported  $^{210}\text{Pb}$  in moss samples, concentration of  $^{226}\text{Ra}$  was calculated using several prominent gamma lines of  $^{214}\text{Bi}$  and  $^{214}\text{Pb}$  appearing in all spectra for moss samples from Serbia. In several moss samples taken from locations in Thailand, no  $^{214}\text{Bi}$  and  $^{214}\text{Pb}$  lines were observed. For those samples  $^{226}\text{Ra}$  activity was at the detection limit. The results obtained are outlined in Table 2. Uranium (as well as Th) originates usually from the soil by dry deposition of the dust particles. Sampling sites in Thailand are located in mountainous area and usually sit onto the bedrock which is sedimentary rock (mostly shale) and metamorphic rock. Serbian mosses were taken in the area when the cultivated soil is dominant. It means that dry deposition of the dust can be most significant source of natural radionuclides from

**Table 2**

Activity concentrations of  $^{226}\text{Ra}$  and  $^{232}\text{Th}$  detected in dried moss samples ( $1\sigma$  statistic uncertainty in parenthesis).

Sample No	Thailand		Serbia	
	Ra-226 [Bq/kg]	Th-232 [Bq/kg]	Ra-226 [Bq/kg]	Th-232 [Bq/kg]
1	<9	2.5(14)	34(5)	<11
2	<9	9.8 (17)	36(5)	<9
3	<14	18.3(26)	2.2(1.7)	8(3)
4	<10	19.3(21)	27(3)	14(3)
5	16(2)	30.3(27)	29(2)	5(2)
6	32(6)	10.4(12)	26(7)	<10
7	300(19)	327(16)	12(4)	<20
8	150(14)	175(12)	24(9)	17(3)
9	30(5)	10.9(19)	23(4)	<10
Mean		67(111)	24(11)	

uranium and thorium chains in Serbian moss samples. Lower concentrations of  $^{226}\text{Ra}$  measured at some Thailand moss samples could be a result of the lower uptake of dust by mosses. It is very difficult to find the mosses far from the water in Thailand. The mosses measured in this pilot study were collected in mountain area reach in surface water flows. Moreover, raining is very often in south Thailand. It is possible that frequent rains can wash new coming dust from the mosses. Measured values of  $^{226}\text{Ra}$  in Serbian moss samples had a mean value of 24(11) Bq/kg. It is evident that the activity of  $^{226}\text{Ra}$  is significantly lower than the measured activity of  $^{210}\text{Pb}$  in the Serbian as well as in the Thailand moss samples. Lead-210 is not in equilibrium with  $^{214}\text{Bi}$  and other short-lived daughter nuclei of  $^{222}\text{Rn}$ . It implies that  $^{210}\text{Pb}$  does not originate from the soil and probably was accumulated through deposition of aerosols.

Several gamma lines originating from radionuclide members of the  $^{232}\text{Th}$  chain ( $^{232}\text{Th}$ ,  $^{228}\text{Ac}$ ,  $^{228}\text{Ra}$ ,  $^{212}\text{Bi}$ ,  $^{212}\text{Pb}$ ) were used to calculate activity concentrations of this radionuclide in all moss samples. The results are presented in Table 2. It can be seen that concentrations of  $^{232}\text{Th}$  in moss samples from Serbia were lower than concentrations of  $^{226}\text{Ra}$ , moreover concentrations in several moss samples were under detection limit. The activity concentrations of  $^{238}\text{U}$  were generally slightly higher than  $^{232}\text{Th}$  in soil all over Serbia (Bikit et al., 2005). A similar trend was also observed in samples of mosses. Such a trend can be observed in Thailand mosses, too. It was established that in Southern Thailand activity of  $^{232}\text{Th}$  was higher than activity of  $^{238}\text{U}$  in the area where sedimentary rock (mostly shale) was exposed. The characteristic measured values for  $^{226}\text{Ra}$  and  $^{232}\text{Th}$  are 260 Bq/kg and 116 Bq/kg for granite; 16 Bq/kg and 40 Bq/kg for sedimentary (shale) and 26 Bq/kg and 31 Bq/kg for metamorphic rock, respectively (Bhongsuwan, 2010). It can be a reason why activity concentrations of  $^{232}\text{Th}$  in Thailand moss samples were slightly higher than concentrations of  $^{226}\text{Ra}$ .

In two of Thailand samples (sample 7 and 8), relatively high activity concentrations of  $^{226}\text{Ra}$  and  $^{232}\text{Th}$  were determined. Measured values of  $^{226}\text{Ra}$  and  $^{232}\text{Th}$  were significantly higher than the average values of same radionuclides detected in Serbian moss samples. Moreover, at Thai sampling sites 7 and 8, measured activities of  $^{210}\text{Pb}$  in mosses were higher than the mean value. The Thai samples 7 and 8 containing significantly elevated level of  $^{232}\text{Th}$  and  $^{226}\text{Ra}$  activity were collected near a big water fall. Mosses are most probably exposed to moist air for the whole year. It seems that water in waterfall may contain  $^{226}\text{Ra}$ ,  $^{232}\text{Th}$  and even dissolved  $^{222}\text{Rn}$  and daughter nuclei. Water droplets in water fall region can deposit dissolved  $^{226}\text{Ra}$  and  $^{232}\text{Th}$  to the mosses growing in near vicinity. If it is true, mobility of  $^{226}\text{Ra}$  and  $^{232}\text{Th}$  in water can be a significant parameter in future research. However dissolved  $^{222}\text{Rn}$  can emanate from water and diffuse far from the fall becoming a source of  $^{210}\text{Pb}$  in mosses. The highest concentration of  $^{210}\text{Pb}$  recorded at Thai sampling site 6 is not followed by the highest

values of  $^{226}\text{Ra}$  and  $^{232}\text{Th}$ . Sampling site 6 is located downstream and it is highly probable that radon gas (heavier than air) after emanation in water fall region concentrates in this area.

In almost all moss samples taken from the Northern hemisphere, measurable amounts of  $^{137}\text{Cs}$  can be detected. The lowest  $^{137}\text{Cs}$  activity measured in this study in Serbia was 7.4(2.1) Bq/kg and the highest one was 82(4) Bq/kg. Higher concentrations of  $^{137}\text{Cs}$  measured in the Serbian samples were probably a result of a random re-suspension and re-deposition of  $^{137}\text{Cs}$  emitted from the Chernobyl accident or a prior above-ground weapons testing deposited on the soil. In all samples taken from Thailand locations,  $^{137}\text{Cs}$  activity was lower than the detection threshold of detection system used.

#### 4. Conclusions

Mosses could be a sampling medium for the detection of  $^7\text{Be}$  and other airborne radionuclides accumulated through some period. A detailed spatial distribution of the integral amount of  $^7\text{Be}$  and other airborne radionuclides deposited over the chosen area during some period can be measured by the use of the mosses. The seasonal  $^7\text{Be}$  and other isotope deposition can be achieved by repeating the described measurements. Mapping of  $^7\text{Be}$  activity distribution in moss samples finally can provide information about some regularity of atmospheric deposition over some large area. Preliminary results showed noticeable non uniformity in  $^7\text{Be}$  content in moss samples taken in two countries. In both cases, the highest measured concentration of  $^7\text{Be}$  is about 2.5 times higher than the lowest one. The difference between particular sampling sites can originate from some local condition determining air transport and consequently atmospheric deposition of  $^7\text{Be}$ .

It is difficult to compare absolute values of measured activity concentrations of  $^7\text{Be}$  measured in Thailand and Serbia because different moss species were used in measurements. However some initial conclusions can be done. Measured values of  $^7\text{Be}$  do not differ significantly, and in the frame of experimental uncertainty agree with previous measured values of  $^7\text{Be}$  activity in mosses collected in England.

Concentrations of  $^{210}\text{Pb}$  measured in Serbia are about two times higher than concentrations of  $^{210}\text{Pb}$  in Thailand. Previous measured results implied that concentration of  $^{210}\text{Pb}$  in mosses can be even an order of magnitude lower than concentrations measured in Serbia and Thailand. It can be expected that activity concentrations of  $^{210}\text{Pb}$  in mosses all around the world can differ significantly, depending on soil structure. The part of the  $^{210}\text{Pb}$  activity in mosses can originate from dust particles containing  $^{238}\text{U}$  daughters. Mean value of the measured concentrations of  $^{226}\text{Ra}$  are at least an order of magnitude lower than concentrations of  $^{210}\text{Pb}$  measured in moss samples. This means that most of  $^{210}\text{Pb}$  in the moss like  $^7\text{Be}$  arrived via aerosol deposition.

It is interesting to note the absence of  $^{226}\text{Ra}$  (and  $^{238}\text{U}$ ) in most of Thailand samples. Just two moss samples have relatively high concentrations of  $^{226}\text{Ra}$ . Considering that two samples having unusually high concentrations of  $^{226}\text{Ra}$  originate from areas near the water falls and an area of surface turbulent water, it is highly probable that  $^{238}\text{U}$  and  $^{232}\text{Th}$  chain members, dissolved in water can be transported by small water droplets and aerosols. It is probable that in area of water falls radon gas emanates making concentration of  $^{210}\text{Pb}$  in mosses collected in vicinity higher than usual.

In Thailand mosses the concentration of man-made  $^{137}\text{Cs}$  was observed to be lower than detectable limit. High values of  $^{137}\text{Cs}$  concentrations in Serbian mosses probably originate from re-deposition from soil.

#### Acknowledgement

This paper was realized as a part of the project "Studying climate change and its influence on the environment: impacts, adaptation and mitigation" (43007) financed by the Ministry of Education and Science of the Republic of Serbia within the framework of integrated and interdisciplinary research for the period 2011–2014.

The second author (K. Wattanavatee) would like to express his gratitude to the graduate school, Prince of Songkla University for funding of this work on the Thailand side.

#### References

- Bhongsuwan, T., 2010. Is tin tailing sand the source of a high natural gamma background in Na Mom districts, Songkhla Province, Southern Thailand? NORM VI March 22–26, 2010, Marrakech, Morocco).
- Bikit, I., Slivka, J., Conkić, Lj., Krmar, M., Vesković, M., Žikić-Todorović, N., Varga, E., Curčić, S., Mrdja, D., 2005. Radioactivity of the soil in Vojvodina (northern province of Serbia and Montenegro). *Journal of Environmental Radioactivity* 78, 11–19.
- Buse, A., Norris, D., Harmens, H., Bükler, P., Ashenden Mills, G., 2003. Heavy metals in European mosses: 2000/2001 survey. UNECE ICP Vegetation.
- Delfanti, R., Papucci, C., Benco, C., 1999. Mosses as indicators of radioactivity deposition around a coal-fired power station. *The Science of the Total Environment* 227, 49–56.
- Dib, J.E., Meeker, L.A., Finkel, R.C., Southon, J.R., Caffee, M.W., Barrie, L.A., 1994. Estimation of stratospheric input to the Arctic troposphere:  $^7\text{Be}$  and  $^{10}\text{Be}$  in aerosols at Alert, Canada. *Journal of Geophysical Research* 99, 12855–12864.
- Florek, B., Mankovska, M.V., Frontasyeva, S.S., Pavlov, I., Sykora, E., Steinnes, 2001. Air Pollution with Heavy metals and radionuclides in Slovakia Studied by the moss Biomonitoring technique. (ISINN-9) JINR, Dubna, Russia, ISBN 5-85165-680-8 442–449.
- Godoy, J.M., Schuch, L.A., Nordemann, D.J.R., Reis, V.R.G., Ramalho, M., Reico, J.C., Brito, R.R.A., Olech, M.A., 1998.  $^{137}\text{Cs}$ ,  $^{226,228}\text{Ra}$ ,  $^{210}\text{Pb}$  and  $^{40}\text{K}$  concentrations in Antarctic soil, sediment and selected moss and Lichen samples. *Journal of Environmental Radioactivity* 41, 33–45.
- Koch, D.M., Jacob, D.J., Graustein, W.C., 1996. Vertical transport of tropospheric aerosols as indicated by  $^7\text{Be}$  and  $^{210}\text{Pb}$  in a chemical tracer model. *Journal of Geophysical Research* 101, 18651–18666.
- Krmar, M., Radnović, D., Rakić, S., Matavuly, M., 2007. Possible use of terrestrial mosses in detection of atmospheric deposition of  $^7\text{Be}$  over large areas. *Journal of Environmental Radioactivity* 95, 53–61.
- Krmar, M., Radnović, D., Mihailović, D.T., Lalić, B., Slivka, J., Bikit, I., 2009. Temporal variations of  $^7\text{Be}$ ,  $^{210}\text{Pb}$  and  $^{137}\text{Cs}$  in moss samples over 14 month period. *Applied Radiation and Isotopes* 67, 1139–1147.
- Kulan, A., Aldahan, A., Possnert, G., Vintersved, I., 2006. Distribution of  $^7\text{Be}$  in surface air of Europe. *Atmospheric Environment* 40, 3855–3868.
- Masarik, J., Beer, J., 1999. Simulation of particle fluxes and cosmogenic nuclide production in the earth's atmosphere. *Journal of Geophysical Research* 104, 12099–12111.
- Moen, L., De Donder, J., De Corte, F., De Wispelaere, A., Simonits, A., Hoste, J., 1981. Calculation of the absolute peak efficiency of gamma-ray detectors for different counting geometries. *Nuclear Instruments and Methods* 187, 451.
- Nifontova, M.G., 1997. Dynamic of concentration of long-lived artificial radionuclides in moss-lichens cover. *Ecology* (4), 273–277 (in Russian).
- Papastefanou, C., Ioannidou, A., 1995. Aerodynamic size association of  $^7\text{Be}$  in ambient aerosols. *Journal of Environmental Radioactivity* 26, 273–282.
- Rehfield, S., Heimann, M., 1995. Three dimensional atmospheric transport simulation of the radioactive tracers  $^{210}\text{Pb}$ ,  $^7\text{Be}$ ,  $^{10}\text{Be}$ , and  $^{90}\text{Sr}$ . *Journal of Geophysical Research* 100 (12), 26141–26161.
- Rühling, A., Tyler, G., 1973. Heavy metal deposition in Skandinavia. *Water, Air and Soil Pollution* 2, 445–455.
- Steinnes, E., Njåstad, O., 1993. Use of mosses and lichens for regional mapping of  $^{137}\text{Cs}$  fallout from the Chernobyl accident. *Journal of Environmental Radioactivity* 21, 65–73.
- Sumerling, T.J., 1984. The use of mosses as indicators of airborne radionuclides near a major nuclear installations. *The Science of the Total Environment* 35, 251–265.
- Todorović, D., Popović, D., Djurić, G., 1999. Concentration measurements of  $^7\text{Be}$  and  $^{137}\text{Cs}$  in ground level air in the belgrade city area. *Environmental International* 25, 59–66.
- Uğur, A., Özden, B., Saç, M.M., Yener, G., 2003. Biomonitoring of  $^{210}\text{Po}$  and  $^{210}\text{Pb}$  using lichens and mosses around uraniumiferous coal-fired power plant in western Turkey. *Atmospheric Environment* 37, 2237–2245.

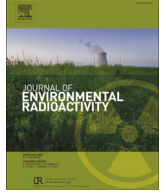


**Appendix A4** Second publication “A Survey of Natural Terrestrial and Airborne Radionuclides  
in Moss Samples from the Peninsular Thailand”



Contents lists available at ScienceDirect

## Journal of Environmental Radioactivity

journal homepage: [www.elsevier.com/locate/jenvrad](http://www.elsevier.com/locate/jenvrad)

# A survey of natural terrestrial and airborne radionuclides in moss samples from the peninsular Thailand



Komrit Wattanavatee<sup>a</sup>, Miodrag Krmar<sup>b</sup>, Tripob Bhongsuwan<sup>a,\*</sup>

<sup>a</sup> Department of Physics, Prince of Songkla University, Hatyai 90112, Thailand

<sup>b</sup> Department of Physics, University of Novi Sad, Trg Dostiteja Obradovica 4, 21000, Novi Sad, Republic of Serbia

## ARTICLE INFO

### Article history:

Received 25 August 2016

Received in revised form

30 May 2017

Accepted 8 June 2017

Available online 20 June 2017

### Keywords:

Moss

Airborne and terrestrial radionuclides

Atmospheric depositions

## ABSTRACT

The aim of this study was to determine the activity concentrations of natural terrestrial radionuclides ( $^{238}\text{U}$ ,  $^{226}\text{Ra}$ ,  $^{232}\text{Th}$  and  $^{40}\text{K}$ ) and airborne radionuclides ( $^{210}\text{Pb}$ ,  $^{210}\text{Pb}_{\text{ex}}$  and  $^7\text{Be}$ ) in natural terrestrial mosses. The collected moss samples (46) representing 17 species were collected from 17 sampling localities in the National Parks and Wildlife Sanctuaries of Thailand, situated in the mountainous areas between the northern and the southern ends of peninsular Thailand ( $\sim 7\text{--}12^\circ\text{N}$ ,  $99\text{--}102^\circ\text{E}$ ). Activity concentrations of radionuclides in the samples were measured using a low background gamma spectrometer. The results revealed non-uniform spatial distributions of all the radionuclides in the study area. Principal component analysis and cluster analysis revealed two distinct origins for the studied radionuclides, and furthermore, the Pearson correlations were strong within  $^{226}\text{Ra}$ ,  $^{232}\text{Th}$ ,  $^{238}\text{U}$  and  $^{40}\text{K}$  as well as within  $^{210}\text{Pb}$  and  $^{210}\text{Pb}_{\text{ex}}$ , but there was no significant correlation between these two groups. Also  $^7\text{Be}$  was uncorrelated to the others, as expected due to different origins of the airborne and terrestrial radionuclides. The radionuclide activities of moss samples varied by moss species, topography, geology, and meteorology of each sampling area. The observed abnormally high concentrations of some radionuclides probably indicate that the concentrations of airborne and terrestrial radionuclides in moss samples were directly related to local geological features of the sampling site, or that high levels of  $^7\text{Be}$  were most probably linked with topography and regional NE monsoonal winds from mainland China.

© 2017 Elsevier Ltd. All rights reserved.

## 1. Introduction

The terrestrial radionuclides,  $^{40}\text{K}$ ,  $^{232}\text{Th}$ , and  $^{238}\text{U}$ , originate from crustal materials in the soil dust and can be detected in mosses. Global average activities of  $^{40}\text{K}$ ,  $^{232}\text{Th}$  and  $^{238}\text{U}$  in soil are around 400, 35 and 30 Bq/kg, respectively (UNSCEAR, 2000). The contents of these radionuclides in the environment depend on the geological setting (McCartney et al., 2000). These radionuclides can be transported and removed from the atmosphere by dry or wet deposition of dust particles (Karunakara et al., 2003; Dragović and Mandić, 2010; Krmar et al., 2007). The presence of terrestrial radionuclides in atmosphere (as well as in biota) is affected by a number of factors, mainly related to the emission of dust particles, such as ash from coal-fired power plants, fossil fuel combustion, phosphate fertilizers, and phosphate manufacturing plants (Belivermiş and Çotuk, 2010). On the other hand, artificial

radionuclides such as  $^{137}\text{Cs}$  are associated with nuclear fission and released into the environment by atmospheric deposition, which varies by geographical location and precipitation (Ritchie et al., 1990).

The airborne radionuclides  $^7\text{Be}$  and  $^{210}\text{Pb}$  originate in various ways. Beryllium-7 is produced by spallation reactions of galactic cosmic rays with nitrogen-14, oxygen-16 and carbon-12 in the lower stratosphere and the upper troposphere. The amount of  $^7\text{Be}$  in the atmosphere depends on the galactic cosmic ray flux, proton flux from the sun during solar events, stratosphere-troposphere exchange, and meteorological parameters affecting transportation of aerosols in ground level air (Petrova et al., 2009). Lead-210 is a progeny from the decay of  $^{222}\text{Rn}$  in the  $^{238}\text{U}$  decay chains. Its concentration in surface air depends mainly on the rate of emanation of  $^{222}\text{Rn}$  and on local meteorological parameters. After release to atmosphere with aerosol particles,  $^{210}\text{Pb}$  returns to the earth surface by washout and by sedimentation (Uğur et al., 2003).

The interest in mosses as bio-monitors has rapidly increased since the work of Jenkins and coworkers (1972), who reported the activity concentrations of some radionuclides in mosses collected

\* Corresponding author.

E-mail address: [tripob.b@psu.ac.th](mailto:tripob.b@psu.ac.th) (T. Bhongsuwan).

from the Olympic National Park, Washington, U.S.A. (Jenkins et al., 1972), and after the use of mosses in biomonitoring of heavy metals in European countries (Rühling and Tyler, 1973). The use of terrestrial mosses in detection of radionuclides over large areas has been reported, for example for around 100 km along the coast in Syrian mountains (Al-Masri et al., 2005), for over 400 km along an international freeway in Serbia (Krmr et al., 2007), and for over 67,000 km<sup>2</sup> in the Marmara region, Turkey (Belivermiş and Çotuk, 2010). These publications demonstrated the high potential of moss sampling, suggesting that biomonitors can be used in monitoring radionuclide deposition over large areas, provided adequate number and density of sampling locations.

It is well-known that terrestrial mosses grow in various climate zones in the forests. Mosses have no well-developed root system, and the nutrients for growth are directly taken from the air via precipitation or by dry deposition. Their accumulation capacity of airborne elements is higher than that of other vascular plants growing in the same habitats (Aleksiayenak et al., 2013). Furthermore, their morphologies do not vary with the seasons, so they can retain and accumulate pollutants throughout the whole year (Szczepaniak and Biziuk, 2003). Mosses have been widely used in the field of radiology as monitors of radionuclides in the environment, for example in (i) a uranium mine (Pettersson et al., 1988), (ii) a lignite center (Tsikritzis, 2005), (iii) areas near nuclear and coal-fired power plants (Sumerling, 1984; Delfanti et al., 1999; Karunakara et al., 2003; Uğur et al., 2003; Sert et al., 2011), and (iv) the monitoring of <sup>137</sup>Cs in many European countries after the Chernobyl nuclear accident (Kirchner and Dailant, 2002; Dragović and Mihailović, 2009; Krmr et al., 2007).

Although the moss sampling technique is widely used, there are no prior reports of using mosses for natural radioactivity measurements in Thailand, with the exception of a pilot study in 2011, which focused on Hatyai City, a regional center of Southern Thailand in Songkhla province (Krmr et al., 2013). The current study is the first to attempt at utilizing Thai mosses as bio-monitors of radionuclides over a large area of peninsular Thailand.

The objectives of this work were to measure the activity concentrations of radionuclides in moss samples collected from peninsular Thailand, to assess/explain the spatial distributions and correlations of the activity concentrations of radionuclides, and to analyze probable factors affecting those distributions.

## 2. Materials and methods

### 2.1. Geography, meteorology, and geology of the sampling area

Peninsular Thailand is located between latitude 7–12 °N and longitude 99–102 °E) and covers around 70,715 km<sup>2</sup> area. The longest distance from the northern end to the southern end is about 750 km. It is located north of the Malay Peninsula and is geographically separated into two parts by a number of high mountain ridges laid in the center along the north to south direction that affect the climate of these parts (Fig. 1 (a)). The eastern side of the Thai peninsula is wet, with highest precipitation during November to February because of the NE monsoon, with cold air mass transported from the Chinese mainland and marine air masses from the Gulf of Thailand. This area is warm and dry in the summer season from March to June, but it often rains even in this relatively dry period due to depressions or typhoons. In contrast, the west side of the peninsula is affected by the SW monsoon from the Indian Ocean to the Andaman Sea carrying mainly marine air masses. High precipitation from June to October makes the climate on the west side considerably different from that on the east side (Wangwongchai et al., 2005; Tipayamongkholgul et al., 2009).

In the geologic setting, peninsular Thailand has two parts called

the middle and the southern peninsula (Bunopas, 1981; Bhongsuwan, 1993), as shown in Fig. 1(b). The geology of the west side of middle peninsula is dominated by Permo – Carboniferous rock (Paleozoic sedimentary rock), which consists of mudstones and sandstones. Samples W04, W06 and W08 were collected from this part. Along the mountain areas from north to south, Mesozoic granite intrudes into Paleozoic sedimentary rock and is surrounded by narrow metamorphic aureoles. Samples W05 and W07 were collected from this area. On the east side of the peninsula, Quaternary sediments have deposited on the valley floor and the coastal area, from which samples E09 were collected. This area is surrounded by cultivated areas. There are two major active faults called Khlong Marui Fault (KMF) and Ranong Fault (RF). The KMF lies in NE direction from Changwat Phung Nga (sample W05) to Suratthani, and the RF extends from Changwat Phung Nga to Ranong. Samples W07 and W08 were collected from the RF fault zone.

The southern peninsula extends south – eastward from Changwat Krabi and Changwat Suratthani to south of Changwat Songkhla and Changwat Narathiwat (near the Malaysian border). It has a number of granite mountain lines from north to south in the middle part of the peninsula and continues into the Gulf of Thailand, where the Mesozoic granites are exposed and there are several basins of Cenozoic coal-bearing beds. Four of our sampling sites are located in the mountain forests in Changwat Suratthani (E10), Changwat Nakorn Sithammarat (E11, E12) and Changwat Phthalung (E13) near the Mesozoic granite exposure. In the mountain ranges extending from north to south between Changwat Nakorn Sithammarat and Changwat Satun, Mesozoic granite intrudes into Paleozoic sedimentary rocks (Ordovician limestone) at the places where sampling sites W01, W02, E13, W14 – W16 are located. Only site W03 is located in a cultivated area in Changwat Trang, where Mesozoic sedimentary rocks are exposed on the ground surface. At Changwat Songkhla, Paleozoic sedimentary rock (Carboniferous shale) is exposed at the northern part of Ko Yo, and extends southward into the north-western part of the Malay Peninsula; the sampling site E17 is located in this area.

### 2.2. Sample preparation and measurement

The 46 moss samples from 17 locations in peninsular Thailand were collected in March 2012. The sampling locations are presented in Fig. 1(a). The sampling sites W01 – W02, W04 – W06, W08, E12 – E13, and W14 – W18 are located in mountainous areas of the National Parks and Wildlife Sanctuaries. These sites are remote from human activities and industrial zones. Sampling sites W03, W08, E10 and E17 are located near cultivated areas and villages.

Sites W01 – W08 and W14 – W16 are geographically on the west side of the Peninsula, while E09 – E13 and E17 are on the east side. At the time of sampling moss the peninsula faced the NE monsoon coming from the Chinese continent and from the South China Sea.

It is noted that in this study a variety of moss species were collected at each site, because it is difficult to collect a specific moss species from all the different sampling sites. The list of moss species sampled is presented in Table 1. At most sites the moss samples were collected in areas near water (small streams) with the exceptions of sites E11 – 2, E11 – 3, E11 – 4, E12, and W16. In these study areas the air moisture is probably an important factor with large amounts of water droplets continuously absorbed onto the bryophytes. This factor probably affects the radionuclide contents in the moss samples as well. Samples E12 – 1 to E12 – 4 were collected from topsoil at the top of a mountain (Khao Ram Rome) about 1000 m above mean sea level.

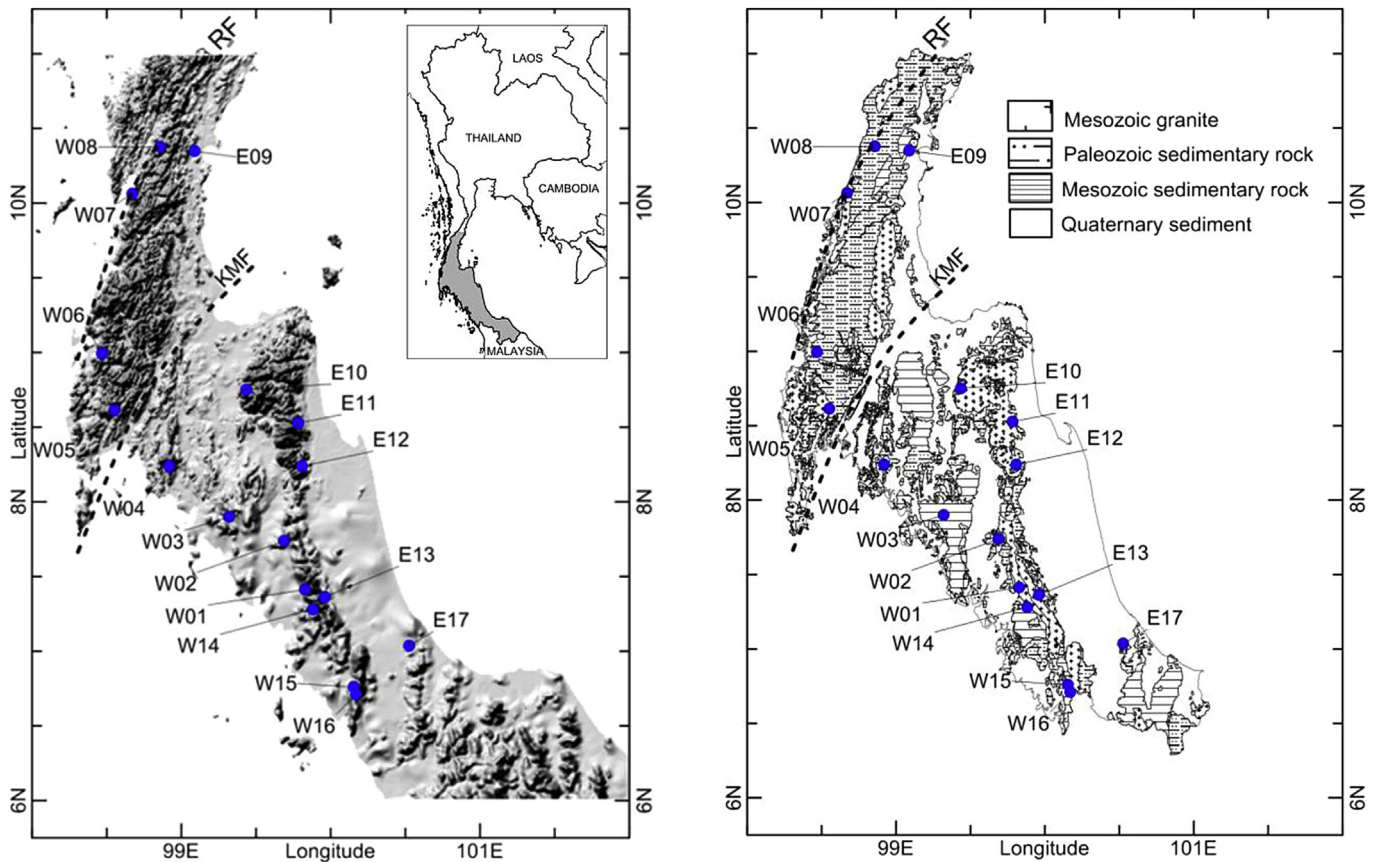


Fig. 1. Map of the study area, (a) SRTM digital elevation model of the Peninsular Thailand and sampling locations and (b) simplified geologic map of the study area.

The samples were packed into plastic bags, and carefully cleaned of soil, grasses, plants and other debris using tap water. The cleaned mosses were weighed and then dried for 24 h at 110 °C to constant weight. The difference of fresh and dry weight shows the water content in samples, varying from 65.2 to 98% (average ~ 84.2%). The dried samples were packed and sealed into 105 mm × 55 mm cylindrical plastic boxes of a similar geometry as the calibration standard. All the sealed samples were analyzed for  $^7\text{Be}$ ,  $^{40}\text{K}$ ,  $^{210}\text{Pb}$ ,  $^{226}\text{Ra}$ ,  $^{232}\text{Th}$  and  $^{238}\text{U}$  using an ultra-low background HPGe gamma spectrometer at the Department of Physics, University of Novi Sad, Republic of Serbia. The system includes a HPGe detector of 100% relative efficiency equipped with a multichannel analyzer. The gamma spectra were analyzed using Genie2000 acquisition system (Canberra, USA). The detector efficiency calibration was performed using the NIST standard reference material 4350B (Columbia River sediment) in the same geometry.

Measuring times for the moss samples varied from 58,000 to 258,000 s, to reduce the statistical count errors. After background subtraction and peak analysis, concentrations of radionuclides in the moss samples were determined as follows. Beryllium-7 was determined from the intensity of the 477.6 keV gamma line. For the concentration of  $^{238}\text{U}$ , the intensity of the 63.288 keV gamma line from decay of  $^{234}\text{Th}$  (a direct daughter of  $^{238}\text{U}$ ) was used. Under the assumption of radioactive equilibrium, the activity of  $^{226}\text{Ra}$  was determined using the weighted mean activity of its progenies ( $^{214}\text{Pb}$  and  $^{214}\text{Bi}$ ), while unsupported lead-210 ( $^{210}\text{Pb}_{\text{ex}}$ ) was also carefully calculated by subtraction of the intensity of 45 keV gamma line (from decay of  $^{210}\text{Pb}$ ) with intensity of the supported  $^{210}\text{Pb}$  (calculated from decay of  $^{214}\text{Bi}$  and  $^{214}\text{Pb}$ ) under assumed secular equilibrium. The intensity of gamma lines from the decay of  $^{228}\text{Ac}$ ,  $^{212}\text{Pb}$ , and  $^{212}\text{Bi}$  can also be utilized to determine the activity of

$^{232}\text{Th}$ . Finally, the activity of  $^{40}\text{K}$  was determined directly from the intensity of the 1460 keV gamma line.

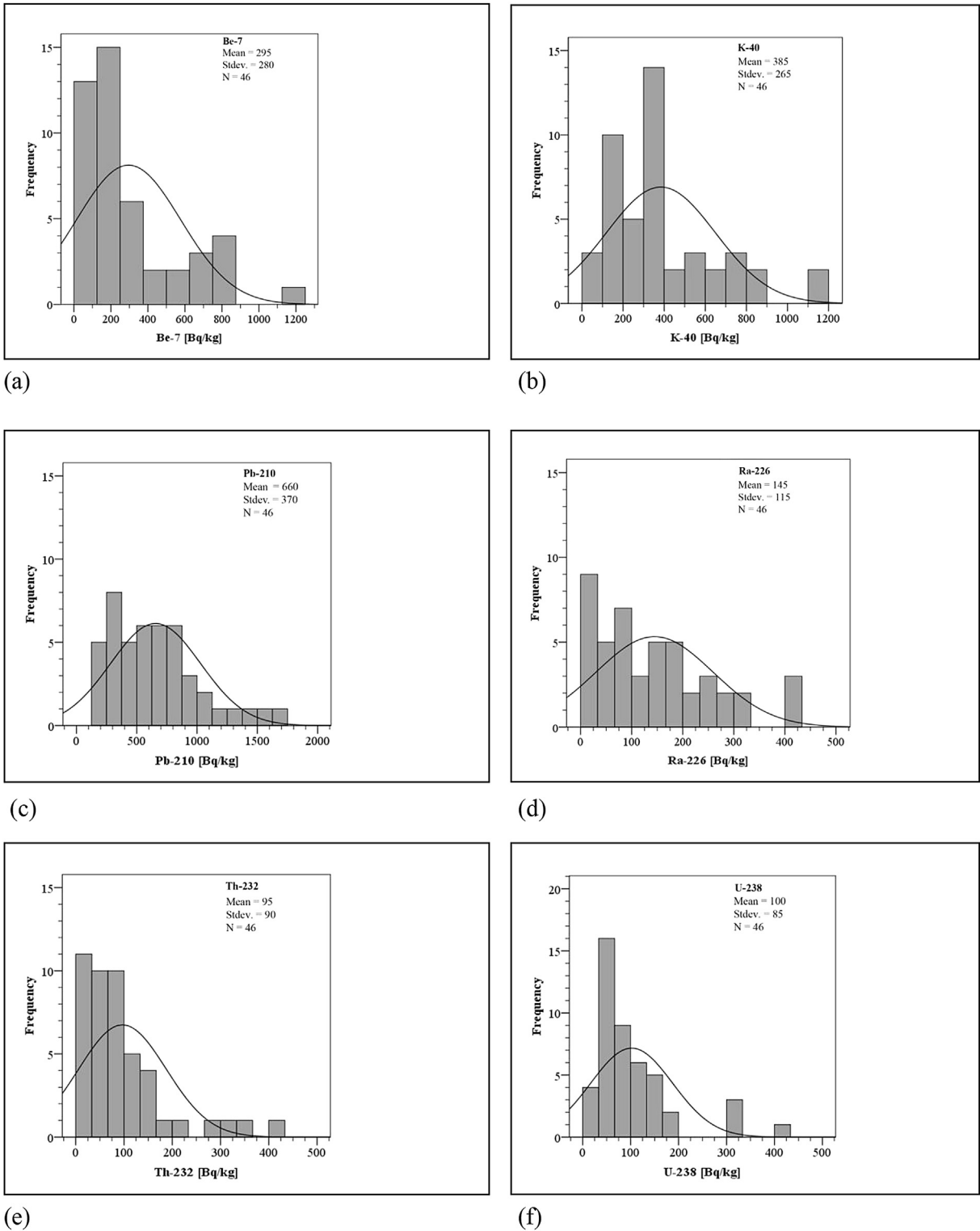
General and multivariate statistical procedures for data analysis were applied using the commercial statistics software package QI Macro 2015 for Windows. Pearson correlations were determined in order to clarify the relationships between the measured radionuclides. Principal component analysis (PCA) was used to analyze for elements that correlate and their similar behaviors might be associated with their origins in the studied area. Then, PCA with VARIMAX normalized rotation were applied and the principal factors with eigenvalue larger than unity were retained for the activity concentrations of radionuclides, as suggested by the Kaiser criteria (Kaiser, 1960). The PCA performs linear dimensional reduction with minimal loss of information (Krzanowski, 2000; Seddeek et al., 2009). Furthermore, it can be used to identify the sources of heavy metal pollution (Culicov et al., 2002; Frontasyeva et al., 2004; Viet et al., 2010) as well as of radionuclides (Tsikritzis, 2005; Popovic et al., 2008; Gordo et al., 2015). Cluster analysis (CA) with Ward's method was also applied to obtain a dendrogram illustrating similarities in activity between the radionuclides. The distance axis displays the degree of association between groups, i.e., a lesser distance indicates the more significant similarity (Dragović and Mihailović, 2009; Elena et al., 2013). The PCA and CA results will be presented and discussed below.

### 3. Results and discussion

#### 3.1. Statistical analysis of measured radionuclides

The measured activity concentrations (as well as  $1\sigma$  uncertainty of counts) for both atmospheric radionuclides ( $^7\text{Be}$  and  $^{210}\text{Pb}$ ) and





**Fig. 2.** Frequency distribution of measured radionuclides in moss samples, (a) <sup>7</sup>Be, (b) <sup>40</sup>K, (c) <sup>210</sup>Pb, (d) <sup>226</sup>Ra, (e) <sup>232</sup>Th and (f).

within 135–1630 Bq/kg (660 Bq/kg). The highest activity concentrations of <sup>40</sup>K, <sup>232</sup>Th and <sup>238</sup>U in the moss samples are found in sample W16 – 1 (Thalae Bun National Park), while the highest values of <sup>7</sup>Be, <sup>226</sup>Ra and <sup>210</sup>Pb are found in samples W04– 1 (Hoi Tho Waterfall), W15 – 5 (Ya Roi Waterfall) and W06 – 1 (Sri – Phung – Nga National Park). In addition, activity concentrations of

the studied radionuclides were detectable in all the moss samples, except for the activity concentration of <sup>7</sup>Be in moss samples W08 – 1, W08 – 2, E09 – 1, W14 – 3, W14 – 4, and W16 – 2 (below MDA: < 70 Bq/kg, < 170 Bq/kg, < 80 Bq/kg, < 80 Bq/kg, < 100 Bq/kg and < 100 Bq/kg, respectively). The half – life of <sup>7</sup>Be is rather short (about 53 days) and there was a long delay from field sampling to

**Table 2**  
Pearson's correlation analysis of various radionuclides; correlation coefficient (top right of diagonal) and the p-value (italics in bracket; bottom left of diagonal). The p-value < 0.05 indicates that there is a significant relationship between the two variables at 95% confidence level.

	Altitude	<sup>7</sup> Be	<sup>40</sup> K	<sup>226</sup> Ra	<sup>232</sup> Th	<sup>238</sup> U	<sup>210</sup> Pb	<sup>210</sup> Pb <sub>ex</sub>
Altitude	1.000	0.365	−0.200	−0.225	−0.279	−0.247	0.100	0.156
<sup>7</sup> Be	(0.013)	1.000	−0.149	0.073	−0.015	0.004	−0.238	−0.237
<sup>40</sup> K	(0.183)	(0.324)	1.000	0.750	0.821	0.830	−0.101	−0.306
<sup>226</sup> Ra	(0.133)	(0.628)	(0.000)	1.000	0.848	0.885	−0.102	−0.372
<sup>232</sup> Th	(0.060)	(0.922)	(0.000)	(0.000)	1.000	0.978	−0.146	−0.371
<sup>238</sup> U	(0.098)	(0.982)	(0.000)	(0.000)	(0.000)	1.000	−0.191	−0.423
<sup>210</sup> Pb	(0.509)	(0.112)	(0.503)	(0.501)	(0.333)	(0.204)	1.000	0.961
<sup>210</sup> Pb <sub>ex</sub>	(0.299)	(0.119)	(0.035)	(0.009)	(0.009)	(0.003)	(0.000)	1.000

analysis (over 4 months). After field sampling in early March 2012, it took two weeks with sample preparation in the laboratory (Thailand), about a month later the samples were transported to Novi Sad (Rep. of Serbia), and finally about 2 months later the spectra were measured for the 46 moss samples (June – July 2012). If <sup>7</sup>Be had accumulated in the moss that was sampled, on measurement about 4 months later its activity had decayed to below MDA.

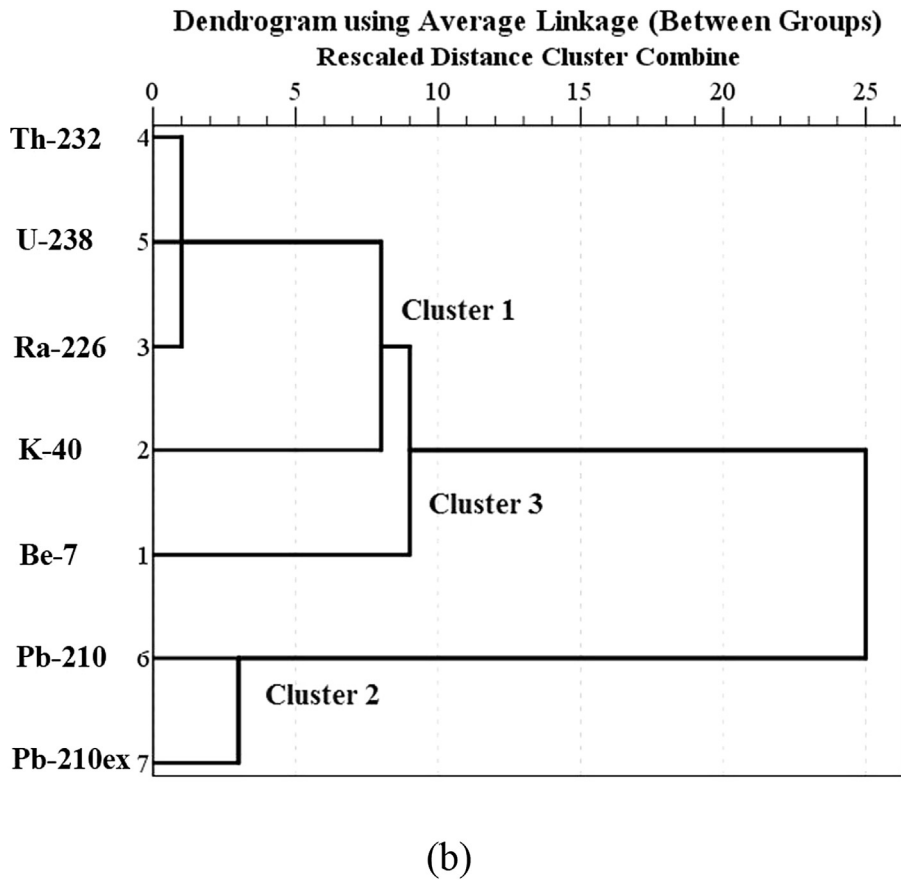
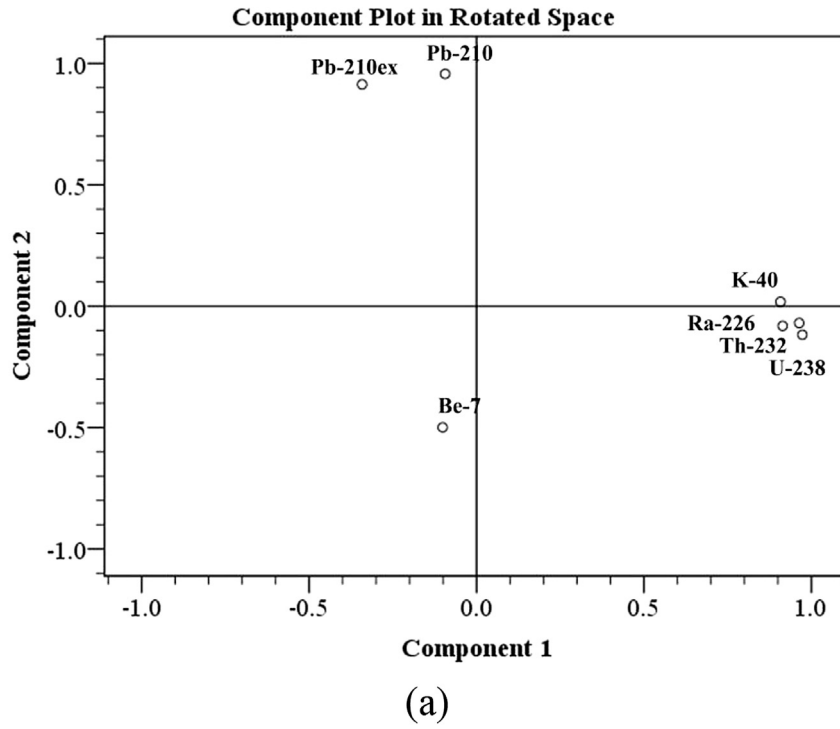
The radionuclide contents in moss samples from the same location are observed to vary by species (Table 1). For example, in samples W08 – 1 and W08 – 2 (*Arthrocnemum schimperi* Dozy & Molk.), and W14 – 2 and W14 – 5 (*Himantocladium* sp.), the activity concentrations of most radionuclides differ significantly. On the other hand, the atmospheric radionuclides <sup>7</sup>Be and <sup>210</sup>Pb in samples W05 – 1 and W05 – 2 (*Leucobryum aduncum* Dozy & Molk.) differ while the terrestrial radionuclides <sup>40</sup>K, <sup>226</sup>Ra, <sup>232</sup>Th and <sup>238</sup>U are almost the same. Similar observations have been reported in previous studies (Dragović et al., 2010; Mietelski et al., 2000; Al-Masri et al., 2005), which confirms that the activity concentrations of radionuclides can significantly differ between species of moss, possibly due to their different morphological structures. The different species could also have diverse uptake mechanisms. The interception and retention of airborne radionuclides in mosses are mainly influenced by the surface morphology and the degree of local shelter, level of saturation, adsorption at different concentration intervals, and competition between the mosses and the cover-plants (Boileau et al., 1982; Zechmeister, 1995; Denayer et al., 1999). Moreover, differences in activity concentrations of <sup>7</sup>Be and <sup>210</sup>Pb between identical moss samples from a particular sampling site may be explained by different growth strategies of the bryophytes. A good example is the moss sample W05 – 1 growing on a rock outcrop, under a tree trunk, and directly exposed to sunlight in the daytimes; and sample W05 – 2 which grew on top soil, covered by grasses and taller plants, and exposed to sun only for some part of each day (similar to moss samples W08 – 1 and W08 – 3). In general, in most sampling sites, the moss was covered by a number of vascular plants, which have the ability to retain aerosols from atmospheric deposition (Sugihara et al., 2008). The aerosols may be attached onto the leaves by several mechanisms, i.e., wax or resin, or the ability to retain rainwater in 'wet deposition'. In addition, during a specific sampling period, if identical mosses are exposed to similar atmospheric deposition rates and re-suspension of soil dust particles in the same habitat, their activity concentrations will still generally differ due to the growth strategy of bryophytes. It can also be hypothesized that different coverings of mosses will significantly affect the concentrations of airborne radionuclides in the moss samples. The moss grown in an open field was exposed directly to the atmospheric deposition of airborne radionuclides, while in contrast trees or other covering plants will significantly affect the uptake of airborne radionuclides by the underlying moss.

Fig. 2 presents the distributions of <sup>7</sup>Be, <sup>40</sup>K, <sup>226</sup>Ra, <sup>232</sup>Th, <sup>238</sup>U

and <sup>210</sup>Pb in moss samples, and skewness and kurtosis for each distribution is included in Table 1. Although all the distributions have small positive kurtosis, it can be seen that only <sup>226</sup>Ra and <sup>210</sup>Pb were approximately Gaussian normal, while <sup>7</sup>Be, <sup>40</sup>K, <sup>232</sup>Th and <sup>238</sup>U show clearly non-normal distributions with positive skewness (see Fig. 2). In addition, it should be noted that highest measured values of <sup>40</sup>K and <sup>226</sup>Ra are within 3σ of the mean, while the largest measured values of <sup>232</sup>Th and <sup>238</sup>U are within 4σ. The Pearson correlations in Table 2 are strong among the terrestrial radionuclides <sup>238</sup>U, <sup>232</sup>Th, <sup>226</sup>Ra and <sup>40</sup>K: <sup>238</sup>U–<sup>232</sup>Th ( $r = 0.978$ ,  $p < 0.01$ ), <sup>226</sup>Ra – <sup>238</sup>U ( $r = 0.885$ ,  $p < 0.01$ ), <sup>210</sup>Pb – <sup>210</sup>Pb<sub>ex</sub> ( $r = 0.961$ ,  $p < 0.01$ ). An intermediate correlation was observed for <sup>226</sup>Ra – <sup>40</sup>K ( $r = 0.750$ ,  $p < 0.01$ ), while there was no correlation between <sup>226</sup>Ra and <sup>210</sup>Pb (as well as the atmospheric radionuclides <sup>210</sup>Pb<sub>ex</sub> and <sup>7</sup>Be).

In the present study, PCA was applied to assess relationships between radionuclide concentrations, and the processes affecting their concentration in moss samples. The PCA was performed with Varimax rotation scheme by Kaiser Normalization. Table 3 presents the total variances of eight components, as Kaiser's criteria accept only eigenvalues exceeding unity, and the first two principal components (PC) explained about 81.34% of the total variance. The factor loadings of radionuclides were calculated and are shown in Table 4. The high positive loadings indicate that PC1 (52.42% of variance) represented the terrestrial radionuclides <sup>238</sup>U, <sup>232</sup>Th, <sup>226</sup>Ra and <sup>40</sup>K (high positive loadings 0.973, 0.964, 0.914 and 0.908, respectively), while PC2 (28.92%) represented the supported/unsupported lead-210 (loadings 0.957 and 0.913, respectively) and <sup>7</sup>Be (intermediate negative loading −0.499). Fig. 3(a) shows the factor score plot (component 1 vs. component 2) that reveals two clear clusters. The x-axis represents PC1 while the y-axis is PC2, so points close to each axis are associated with PC1 or PC2. The dendrogram from the cluster analysis (CA) is shown in Fig. 3(b). The 7 radionuclides fell into 3 statistically significantly separated clusters, with <sup>238</sup>U, <sup>232</sup>Th, <sup>226</sup>Ra and <sup>40</sup>K in the first branch (cluster 1), <sup>210</sup>Pb and <sup>210</sup>Pb<sub>ex</sub> in the second one (cluster 2) and <sup>7</sup>Be having its own cluster (cluster 3). The natural terrestrial radionuclides represented by PC1 (in CA as well) are associated with soil dust and may have accumulated into the mosses by deposition. This first factor can be called "Factor of soil dust origin". On the other hand, <sup>210</sup>Pb, <sup>210</sup>Pb<sub>ex</sub> and <sup>7</sup>Be are aligned with PC2, which can be called "Factor of atmospheric aerosol origin". However, these atmospheric radionuclides formed two clusters due to the fact that <sup>7</sup>Be and <sup>210</sup>Pb possess different atmospheric origins, even though they entered the moss samples by similar processes (i.e., atmospheric wet/dry deposition). This concept is supported by the lack of correlation between <sup>7</sup>Be and <sup>210</sup>Pb ( $r = -0.238$ ) and their factor loadings being of opposite signs. This indicates that there are various atmospheric processes and geographic conditions affecting radionuclide concentrations in moss samples. A detailed discussion will be given below.

In addition, if <sup>210</sup>Pb originated from the soil dust or bed rock



**Fig. 3.** (a) Component plot in a rotated space for 7 radionuclides and (b) A dendrogram obtained by CA of activity concentrations in moss samples (the degree of correlation between variables relates to the distances).



**Table 3**  
Total variance explained for the analyzing of moss samples.

Component	Initial Eigenvalues			Extraction Sums of Squared Loadings			Rotation Sums of Squared Loadings		
	Total	% of Variance	Cumulative %	Total	% of Variance	Cumulative %	Total	% of Variance	Cumulative %
1	3.860	55.136	55.136	3.860	55.136	55.136	3.670	52.423	52.423
2	1.835	26.207	81.343	1.835	26.207	81.343	2.024	28.920	81.343
3	0.898	12.823	94.167						
4	0.227	3.245	97.412						
5	0.164	2.336	99.748						
6	0.017	0.246	99.994						
7	0.000	0.006	100.000						

Extraction Method: Principal Component Analysis.

**Table 4**  
Factor loadings for the analysis of moss samples.

	Component	
	PC1	PC2
<sup>7</sup> Be	-0.101	-0.499
<sup>40</sup> K	0.908	0.018
<sup>226</sup> Ra	0.914	-0.081
<sup>232</sup> Th	0.964	-0.069
<sup>238</sup> U	0.973	-0.118
<sup>210</sup> Pb	-0.094	0.957
<sup>210</sup> Pb <sub>ex</sub>	-0.342	0.913

Extraction Method: Principal Component Analysis.

Rotation Method: Varimax with Kaiser Normalization.

where the mosses are seated, it should deposit into the moss by the same processes as <sup>226</sup>Ra. However, there is no correlation between <sup>226</sup>Ra and <sup>210</sup>Pb (as well as <sup>210</sup>Pb<sub>ex</sub>). This is probably because the unsupported lead-210 is calculated under the assumption of secular equilibrium between <sup>226</sup>Ra, <sup>214</sup>Pb and <sup>214</sup>Bi, while a strong correlation between <sup>210</sup>Pb and <sup>210</sup>Pb<sub>ex</sub> ( $r = 0.961$ ,  $p < 0.01$ ) is observed. Possibly most of the total <sup>210</sup>Pb in moss samples was unsupported from the decay of radon in air.

### 3.2. Activity concentrations of terrestrial radionuclides <sup>40</sup>K, <sup>226</sup>Ra, <sup>232</sup>Th and <sup>238</sup>U in moss samples

The correlation of <sup>238</sup>U and <sup>232</sup>Th ( $r = 0.978$ ,  $p < 0.01$ ) was strong in selected moss samples. The ratio of <sup>238</sup>U and <sup>232</sup>Th activity concentrations (<sup>232</sup>Th/<sup>238</sup>U) is approximately unity (Fig. 4(a)) ranging from 0.2 to 2.1. The correlation between <sup>226</sup>Ra and <sup>238</sup>U concentrations is also strong with the former concentration generally slightly higher (Fig. 4(b)). The <sup>226</sup>Ra/<sup>238</sup>U ratio ranged from 0.3 to 3.1, which mean a low degree of secular equilibrium within the uranium-238 series in the moss samples. In general, disequilibrium may be caused by a number of factors such as the degree of rock weathering and the oxidation/reduction processes that relate to the occurrence and the physical and chemical behavior of uranium and radium (Psichoudaki and Papaefthymiou, 2008).

A possible explanation for the disequilibrium of radium and uranium in the moss samples is their respective solubility in natural water. It is generally known that in a similar fashion to the alkaline earth elements, radium presents only one valence state (+H), and the Ra<sup>2+</sup> ion is moderately soluble in natural water while its isotopes are strongly absorbed onto riverine particles and tend to bind with sediment in a river (Silva et al., 2006). Radium solubility increases with salinity due to desorption and diffusion from estuarine and coastal sediments and river-borne suspended particulates (Moore, 1969, 1981). The solubility of uranium depends on its valence state, and it forms various soluble complexes with carbonate, phosphate, sulfate, fluoride and silicate ions, and adsorbs

onto organic compounds (Ivanovich and Harmon, 1992). The most often encountered complex in natural waters is the soluble uranyl carbonate complex (U<sup>6+</sup>, oxidizing condition) linked with organic matter in riverine, estuarine and coastal sediments (Langmuir, 1978). As with radium, uranium is also more soluble in saline water than in fresh water (Mlakar and Branica, 1994; Djogić et al., 2001), but Landais suggested that dissolved uranium in fresh water is low due to its sorption onto particulate organic matter and carbonate particles (Landais, 1996). In this study, the sampling sites are located in mountain areas far from human communities, so the main sources of dissolved uranium and radium are probably bed rocks and soil dust. Almost all the moss samples were collected close to a stream or waterfall, for example W01 PSW, W02 PJ, W04 HT on the west side and E10 MT, E13 PW on the east side, and the measured activity concentration of <sup>226</sup>Ra was higher than of <sup>238</sup>U (or <sup>226</sup>Ra/<sup>238</sup>U larger than unity), reflecting the slightly greater solubility of radium compared to uranium in fresh water. The additional <sup>226</sup>Ra (<sup>226</sup>Ra<sub>excess</sub>) could be dissolved into water and transported to the mosses. Moreover, this can also explain the significantly elevated level (over 4 fold the mean values) of activity concentration of <sup>226</sup>Ra and <sup>232</sup>Th in sample sites W15 – 5 (B, *Himantocladium* sp.) and W16 – 1 (H, *Leucoloma* sp.).

As well as <sup>238</sup>U, <sup>226</sup>Ra was strongly correlated with <sup>232</sup>Th (Fig. 4(c)) but radium content was generally higher than thorium. This conflicts with the previous study of Krmar (Krmar et al., 2013), which suggested that the differences in bedrock (mostly shale and granite) at sampling sites might explain why thorium was slightly higher than radium (similar to uranium). The sampling site E17 (Ton Yha Plong Waterfall) of the present study will therefore be assessed in more detail.

Considering that sampling site E17 of this study is at a place sampled and analyzed in Krmar et al. (2013), it is interesting to compare the obtained results. Clearly the activity concentrations of <sup>226</sup>Ra and <sup>232</sup>Th in moss samples from this site are comparable with the previous study. However, the previous results were obtained from a small number of sampling sites (3 sampling sites) and with short distances between the sites (not more than 50 km from site-to-site), while in this current study there were 17 sampling sites covering about 800 km distance of peninsular Thailand. The measured activities of <sup>226</sup>Ra and <sup>232</sup>Th in various rocks from peninsular Thailand were reported as 260 and 116 Bq/kg for granite rock, 16 and 40 Bq/kg for sedimentary rock, and 26 and 31 Bq/kg for metamorphic rock (Bhongsuwan, 2010). Analogous to the discussion by Krmar (Krmar et al., 2013), radium will be generally higher than thorium when the bedrock in the sampling site is granite, and less than thorium for sites where the bedrock is sedimentary or metamorphic.

The mean value of <sup>40</sup>K in moss samples is higher than the means of <sup>232</sup>Th and <sup>238</sup>U. It is known that the average activity concentrations of <sup>40</sup>K: <sup>232</sup>Th: <sup>238</sup>U in soil are about 400: 35: 30 Bq/kg (UNSCEAR, 2000). Both activity concentrations of thorium and

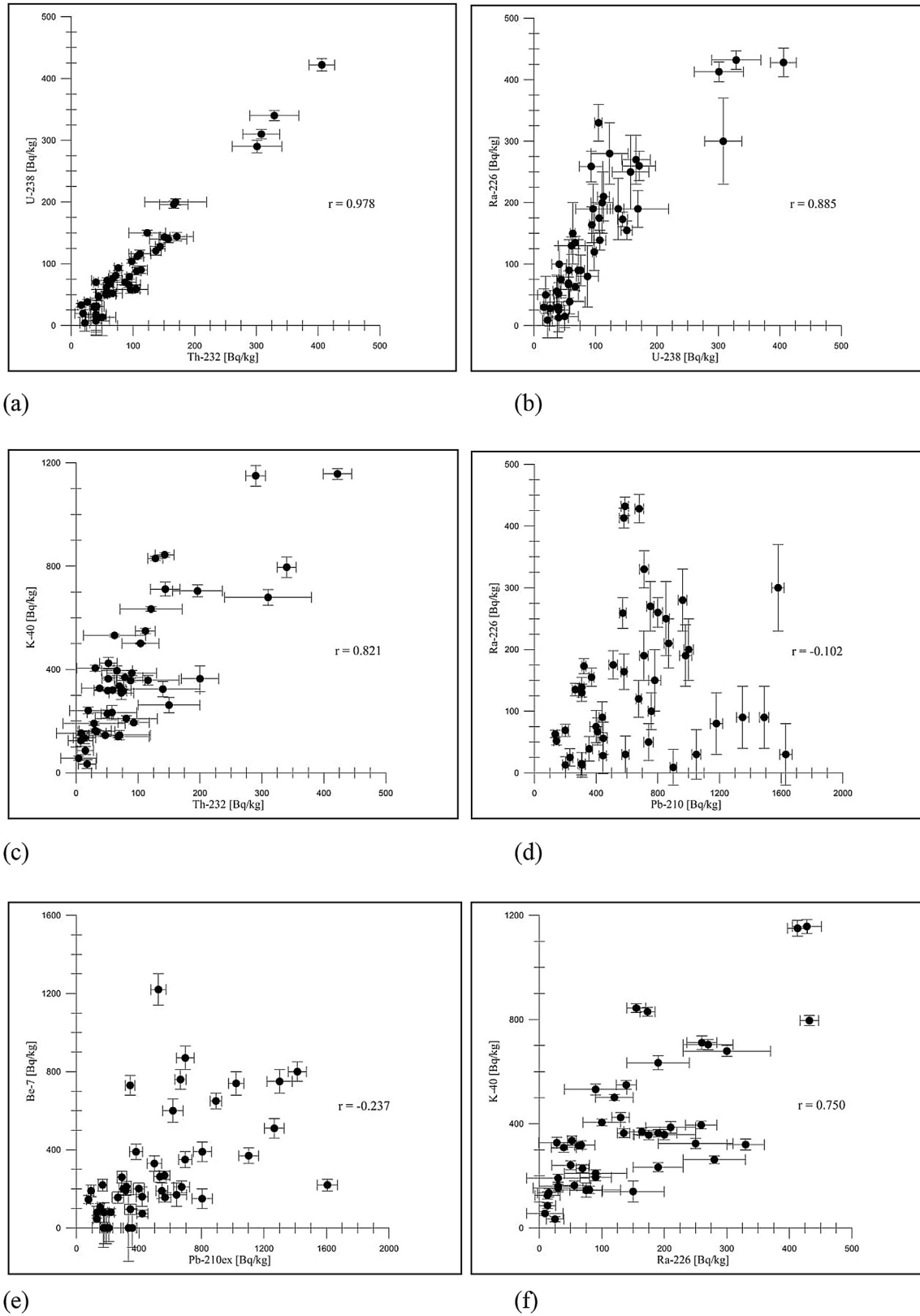


Fig. 4. The scatter plots of activity concentrations measured in moss samples (a)  $^{238}\text{U}$ – $^{232}\text{Th}$ , (b)  $^{226}\text{Ra}$  –  $^{238}\text{U}$ , (c)  $^{40}\text{K}$ – $^{232}\text{Th}$ , (d)  $^{226}\text{Ra}$  –  $^{210}\text{Pb}$ , (e)  $^7\text{Be}$  –  $^{210}\text{Pb}_{\text{ex}}$ , and (f)  $^{40}\text{K}$ – $^{226}\text{Ra}$ .

uranium correlate well with the measured  $^{40}\text{K}$  values ( $r = 0.821$  for  $^{40}\text{K}$ – $^{232}\text{Th}$  ( $p < 0.01$ ) and  $0.830$  for  $^{40}\text{K}$ – $^{238}\text{U}$  ( $p < 0.01$ )). Thus, geological information was considered. Activity concentrations of

$^{238}\text{U}$  in moss samples and a simplified geological map are shown in Fig. 5(a) – 5(d). The mean activity concentrations of radionuclides by sampling site and by classification of bedrock are presented in

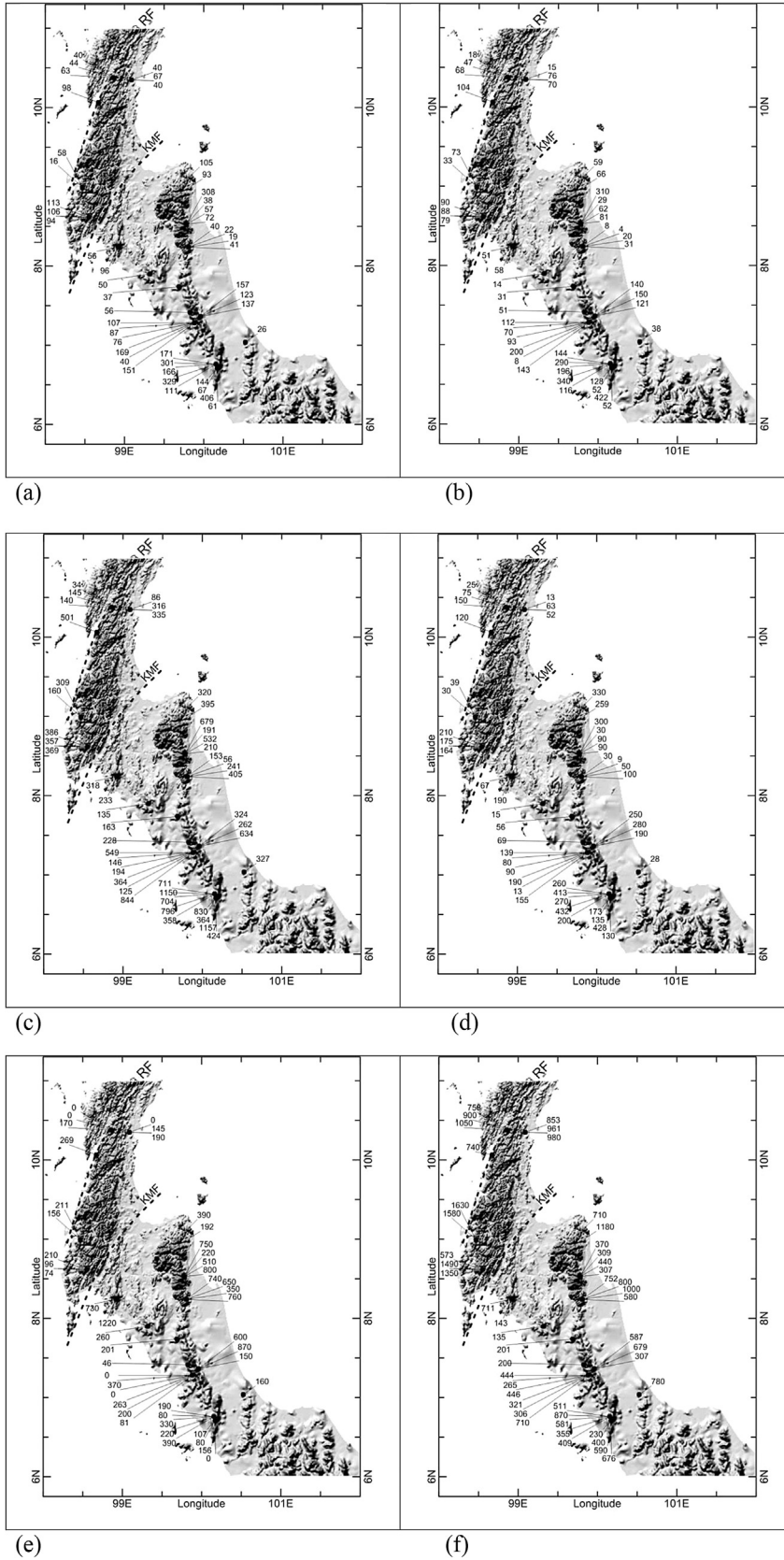


Fig. 5. Activity concentrations of radionuclides at the sampling locations on the SRTM elevation map of the study area; (a)  $^{238}\text{U}$ , (b)  $^{232}\text{Th}$ , (c)  $^{40}\text{K}$ , (d)  $^{226}\text{Ra}$ , (e)  $^7\text{Be}$  and (f)  $^{210}\text{Pb}$ .

**Table 6.** Although there are large uncertainties due to the variety of moss species, it can be seen that the sampling areas located on the Triassic granitic zones correspond with higher activity concentrations of  $^{40}\text{K}$ ,  $^{232}\text{Th}$  and  $^{238}\text{U}$  (as well as  $^{226}\text{Ra}$ ) (i.e. sampling sites, E13, W14, W15) when comparing with Mesozoic sedimentary zone (as well as the older Paleozoic sedimentary zone) (W01, W03, W04). This could be due to the degree of decomposition and porosity of the rock, which probably depends on age. Some older granite in peninsular Thailand was intruded by aplite dike and quartz veins under the influences of pneumatolytic and hydrothermal activities. It decomposed to soil, leaving the elements dissolved. Torbernite and monazite, highly radioactive minerals, were discovered in some areas, for example in dikes and joints of granite and in quartz, quartzite and decomposed granite

(Punggrassami, 1984). Faults in the rock cause dissolution of heavy metals in underground water, including radium, an important daughter element of uranium. Over a longer period, the decomposed (highly porous) granites are exposed on the earth surface and start to weather and erode (transport) forming soil-dust carried by winds, and accumulate in moss samples by dry deposition.

It can be seen that  $^{226}\text{Ra}$  also has an intermediate correlation with  $^{40}\text{K}$  (Fig. 4(f)). It is probably due to the fact that both  $^{40}\text{K}$  and  $^{226}\text{Ra}$  are transported to mosses and eventually captured by the same mechanism. However, there is another aspect that should be mentioned. Potassium (and also calcium) is a necessary element for the metabolic processes of plants. Good  $^{40}\text{K}$ – $^{226}\text{Ra}$  correlation could be partly due to the similar chemical behavior of calcium and radium. Necessary elements (potassium) and calcium (as well as

**Table 5**

Range and mean values of activity concentrations of various radionuclides in this study comparing to those reported in previous studies.

Area (reference)	Location	Activity concentrations (Bq/kg)					
		$^7\text{Be}$	$^{40}\text{K}$	$^{226}\text{Ra}$	$^{210}\text{Pb}$	$^{232}\text{Th}$	$^{238}\text{U}$
Kaiga, India [Tree mosses] (Karunakara et al., 2003)	14°51'08"N, 74°26'40"E	234.5–1061 [680.1]	12.01–40.1 [22.1]	BDL–2.2 [1.5]	NR	NR	NR
Coastal Syrian mountain (Along sea coast) (Al-Masri et al., 2005)	–	NR	NR	NR	165–2392 [ - ]	NR	NR
Belarus and Slovakia (Aleksiayenak et al., 2013)	48°12'–49°20'N 17°05'–22°05'E	NR	NR	NR	163–572 [312]	NR	NR
-Belarus					330–1521		
-Slovakia					[771]		
Marmara region, Turkey (Belivermiş and Çotuk, 2010)	–	NR	17.1–181.1	NR	NR	1.51 –6.17	0.87 –6.70
Nine semi-natural highland in Rep. of Serbia (Dragović et al., 2010)	–	NR	60–537 [207]	7.3–29 [16]	NR	NR	NR
Zlatibor Mountain, Western Serbia (Dragović et al., 2010)	43°31'–43°51'N 19°28'–19°56'E	NR	44–692 [-]	0.9–25.8 [-]	NR	0.8–13.7 [-]	1.7–25.1 [-]
Northern Province of Vojvodina to Southern border of Rep. Serbia (Krmr et al., 2013)	42°43'–45°38'N 19°35'–22°8'E	200–494 [314]	ND	2.2–36 [24]	526–881 [695]	BDL–17	NR
King George Island, West Antarctica, South Shetland (Mietelski et al., 2000)	–	NR	125–300 [221]	NR	BDL–125 [27.6]	0.15 –2.18 [1.1]	NR
Over 400 km along the high way of Rep. of Serbia (Krmr et al., 2007)	42°26'–45°23'N 19°58'–22°13'E	195–560 [363]	30–800 [281]	NR	NR	NR	NR
Eastern Anatolia (Topcuoğlu et al., 2003)	–	NR	BDL–437 [ - ]	NR	NR	BDL–20 [ - ]	22–51 [ - ]
Location	Location	Specific activities (Bq/kg)					
		$^7\text{Be}$	$^{40}\text{K}$	$^{226}\text{Ra}$	$^{210}\text{Pb}$	$^{232}\text{Th}$	$^{238}\text{U}$
Novi Sad, Rep. of Serbia (Krmr et al., 2009)	42°14'45"N, 19°51'35"E	100–900 [248] [340]	NR	NR	347–885 [-]	NR	NR
-Jan-Feb 2007							
-Jan-Feb 2008							
Eastern of Serbia (Ćuculović et al., 2014)	–	41–122 [-]	100–500 [-]	5–50 [-]	NR	5–50 [-]	NR
This study	6°71'–10°37'N 98°46'–100°53'E	0–1220 [295]	34–1157 [385]	9–432 [145]	135–1630 [660]	4–422 [95]	16–406 [100]

NR = Not Report.

[ ] = Mean value.

**Table 6**

Average activity concentrations of  $^{40}\text{K}$ ,  $^{210}\text{Pb}_{\text{ex}}$ ,  $^{232}\text{Th}$  and  $^{238}\text{U}$  and types of bedrock in the vicinity of sampling sites.

Rock	Average activity concentrations (Bq/kg)				Sampling sites
	$^{40}\text{K}$	$^{210}\text{Pb}_{\text{ex}}$	$^{232}\text{Th}$	$^{238}\text{U}$	
C	106 ± 63	393 ± 223	44 ± 25	49 ± 12	W08
C,CP	206 ± 120	195 ± 158	50 ± 29	43 ± 17	E09 and E17
C,P,Gr	336 ± 250	447 ± 298	91 ± 61	88 ± 53	W06 and W14
K-J Gr	293 ± 166	775 ± 478	60 ± 76	75 ± 72	W01, W03, W04, E10, E11 and E12
P	371 ± 15	480 ± 172	86 ± 6	104 ± 10	W05
TrGr	598 ± 312	428 ± 251	163 ± 113	165 ± 108	W02, W07, E13, W15 and W16

**Remark:** C, CP = Pebbly mudstone, P = Permian limestone, O = Ordovician limestone, KGr = Cretaceous granite, JGr = Jurassic granite and TrGr = Triassic granite.

$^{226}\text{Ra}$ ) deposited are taken up by the mosses that were sampled in this study (Karunakara et al., 2003; Belivermiş and Çotuk, 2010). Table 5 compares the mean activity concentrations of terrestrial radionuclides in this study with those from previous ones. Due to the relatively small differences between the median values and the mean values, and the small skewness in our measurements, it was appropriate to use the mean values in a comparison. This can only be a rough comparison because there are large differences in the moss species and the numbers of moss samples analyzed, period of the studies, etc. However, it can be seen that our measurements generally gave slightly higher values than those reported from other regions of the world.

### 3.3. Airborne radionuclides; $^7\text{Be}$ and $^{210}\text{Pb}$

The mean value of  $^7\text{Be}$  in this study (295 Bq/kg) is slightly lower than that observed in England (360 Bq/kg) (Sumerling, 1984), Rep. of Serbia (363 Bq/kg, Krmar et al., 2007, 2013; 314 Bq/kg). This result supports the fact that a higher activity concentration of  $^7\text{Be}$  in mosses is generally found in regions of mid-latitude of the northern hemisphere due to higher deposition rate of  $^7\text{Be}$  in surface air with increasing latitude (Kulan et al., 2006). One exception is the activity concentration of  $^7\text{Be}$  measured in mosses collected in Kaika, India where the mean value (680 Bq/kg) is very high compared to those from the other regions suggesting high deposition rates of  $^{210}\text{Pb}$ ,  $^{210}\text{Po}$  and  $^{137}\text{Cs}$  (Karunakara et al., 2003). However, it can be concluded that the activity concentrations of  $^7\text{Be}$  in moss samples in this study do not significantly differ from the values measured worldwide (Table 5).

Unfortunately, previous systematic studies of  $^7\text{Be}$  concentration in surface air, top soils or terrestrial plants (including mosses) in Thailand are not available. However, the measurement of  $^7\text{Be}$  in moss samples in the study area confirms an abundant atmospheric deposition flux of  $^7\text{Be}$ . The maximum  $^7\text{Be}$  deposition flux in China was reported to occur from January to April, which was caused probably due to seasonal stratosphere – troposphere air exchange in mid-latitude of the northern hemisphere (Momoshima et al., 2006; Cho et al., 2007; Yi et al., 2007; Du et al., 2008; Petrova et al., 2009).

In addition, both the vertical convection of air mass from lower stratosphere and upper troposphere and the transportation of air mass from the Chinese mainland have also affected the variation of  $^7\text{Be}$  concentration in air in Japan (Sato et al., 2003; Ueno et al., 2003). Beryllium-7 deposition flux increases with both altitude and latitude; the highest production rate of  $^7\text{Be}$  was found at around  $50^\circ\text{N}$  and decreases toward the equator (Nagai et al., 2000). The activity concentration of  $^7\text{Be}$  in this study shows a large variation, depending on geography differences of the study areas. Pearson correlation of the activity concentration of  $^7\text{Be}$  with the altitude of sampling site is weak (0.365,  $p < 0.05$ ). This indicates that the activity concentration of  $^7\text{Be}$  in moss samples slightly increased with altitude of the sampling site.

The  $^7\text{Be}$  concentration in ground level air is influenced by meteorological factors such as changes in production rate due to solar heating, stratosphere-troposphere exchange, and advection of air mass containing  $^7\text{Be}$  at different latitudes (Aldahan et al., 2001; Pham et al., 2011). Not only these meteorological factors, but also morphology of the study area affects the concentration of  $^7\text{Be}$  (as shown in Fig. 5(e)). In mid-latitude countries such as China,  $^7\text{Be}$  is accumulated in the air over the continental area. During the period of sampling in this study (March 2012), the North-East monsoon was entering from the continental China, so high  $^7\text{Be}$  content in cold and dry air mass was transported to Thailand, this may increase deposition of  $^7\text{Be}$  over large areas in peninsular Thailand by both (1) dry deposition by wind and (2) wet deposition by rain.

There were rains during the sampling period. It is possible that new precipitation of airborne radionuclides entered with rain into these samples.

However, our measurements failed to confirm this hypothesis due to high variation of the measured activity concentrations of  $^7\text{Be}$  in the mosses collected from peninsular Thailand. The mean value of  $^7\text{Be}$  activity in sampling sites located along the east side is higher than in those on the west side of the peninsula,  $440 \pm 285$  and  $211 \pm 248$  Bq/kg, respectively. This difference is statistically significant (independent Student's t-test,  $F = 4.098$ , sig. level = 0.049,  $t = -2.756$ , sig. level = 0.01). A possible explanation of this result is an effect of regional topography, as the north – south mountain range separates peninsular Thailand into the western and eastern low lands. During the sampling period the east side of peninsular Thailand faced cold and dry air masses coming from higher latitudes over continental China, enriching  $^7\text{Be}$  in the atmosphere. For example, 0.11 (January 2005) – 2.93 (February 2005) Bq/m<sup>2</sup>/day (Yi et al., 2007) and 0.02 (December 2006) – 15.0 (April 2006) Bq/m<sup>2</sup>/day (Du et al., 2008), respectively. The west side of peninsular Thailand was under the influence of air masses from the Andaman Sea and Indonesia, with comparatively lower  $^7\text{Be}$  concentrations in air from lower latitudes. While there is no systematic report on  $^7\text{Be}$  in ground surface air over Indonesia and Andaman Sea, the measured  $^7\text{Be}$  concentrations in surface air in Oceania ( $0.5\text{--}46.4^\circ\text{S}$ ) range from  $1.4 \pm 0.3$  ( $0.5^\circ\text{S}$ ) to  $4.9 \pm 1.2$  ( $27.5^\circ\text{S}$ ) as reported by Doering and Akber (2008). The  $^7\text{Be}$  production rates in the atmosphere, as well as the increment in its measured concentrations, depend on latitude (Lavrenchuk et al., 1962; Larin et al., 2014). This may imply that the  $^7\text{Be}$  concentration in surface air over areas located in lower latitudes (Northern – Southern Hemisphere) such as Indonesia and Andaman Sea should be low. These provide plausible reasons for the differences in  $^7\text{Be}$  concentration in mosses collected from the east and the west side of peninsular Thailand, and future studies could further address these phenomena.

The high  $^7\text{Be}$  content in cold air masses coming from China elevated the  $^7\text{Be}$  concentration in moss samples W04 ( $1220 \pm 80$  Bq/kg) from the west side of the peninsula, contrary to what we found at other sampling sites located on the west side. This site W04 may have been affected by the north-east monsoon in the sampling period, similar to the sampling sites located on the east side (E09 – E13 and E17; Fig. 1). Consider that site W04 is located near a hill summit surrounded by a channel of lowland connecting eastern and western coastlines and is not sheltered by any high mountain ridge, while the sampling sites W01, W02, W14 – W16 and W06 – W08, located in Ban-Thud and Ta-Now-Wa-Sri Mountain Range, are sheltered by a long N – S mountain ridge. This could be a reason why the activity concentrations of  $^7\text{Be}$  in moss samples collected in the west side were slightly lower than in the samples from the east side of peninsular Thailand.

Lead-210 was detectable in all moss samples, but the activity concentrations varied significantly from 135 to 1630 Bq/kg, with mean value ( $660 \pm 370$  Bq/kg). These are slightly higher than those of mosses collected in Belarus (Aleksiayenak et al., 2013), Novi Sad (Krmar et al., 2009), and West Antarctica (Mietelski et al., 2000). In cases with low content of  $^{226}\text{Ra}$  in soil and dust, low concentration of  $^{210}\text{Pb}$  should be expected, if there is no abundant atmospheric deposition of  $^{210}\text{Pb}$ . High  $^{210}\text{Pb}$  concentrations in mosses have been associated with human activities, namely nuclear power stations (900 Bq/kg; Sumerling, 1984), coal-fired power stations (1898 Bq/kg; Delfanti et al., 1999), and areas with high level of  $^{222}\text{Rn}$  emanations from soil air to surface air, for example, in fault zones (Al-Masri et al., 2005). However, almost all the moss samples in this study were collected under tree leaves, topsoil and rock exposures close to flowing water or by stream side in mountain areas, relatively far from any human industrial communities and coal-fired

power stations. The exceptions are site W07 located (close to a local road), and sites E09 and E17 (surrounded by cultivated areas). Furthermore, the activity concentrations of  $^{210}\text{Pb}$  in moss samples are significantly higher than  $^{226}\text{Ra}$ , with no correlation between these as shown in Fig. 4(d). This means that the secular equilibrium of  $^{226}\text{Ra}$  and its decay products is broken;  $^{210}\text{Pb}$  is not in equilibrium with  $^{214}\text{Bi}$  (or  $^{226}\text{Ra}$ ) and other short-lived daughters of  $^{222}\text{Rn}$ . Therefore, the contribution of unsupported lead-210 ( $^{210}\text{Pb}_{\text{ex}}$ ) in samples is significant. The levels of  $^{210}\text{Pb}_{\text{ex}}$  were carefully calculated from  $^{214}\text{Bi}$ ,  $^{214}\text{Pb}$  and  $^{210}\text{Pb}$  gamma lines, and are presented in Fig. 4(e).

Relatively low activity concentrations of  $^{226}\text{Ra}$  in mosses collected in Thailand were observed in a previous study (Krmár et al., 2013), but these represented only a few sampling sites. This indicates that most  $^{210}\text{Pb}$  in the moss samples does not relate to  $^{226}\text{Ra}$  content in the ground soil, instead a significant portion of  $^{210}\text{Pb}$  is deposited from aerosols. In contrast to that previous study, the higher  $^{210}\text{Pb}$  concentrations observed in this study may be associated, not only to deposition of aerosols, with reference to dissimilar  $^7\text{Be}$  ( $r = -0.238$ ;  $p = 0.112$ ) (Fig. 4(e) and Table 6), but also to the high  $^{222}\text{Rn}$  emanation from the ground in the sampling areas. The sampling sites W05 and W06 – W08 are located near active faults of peninsular Thailand, the Khlong Marui fault (KMF) and the Ranong fault (RF), respectively (Figs. 1 and 5(f)). The levels of  $^{222}\text{Rn}$  and  $^{210}\text{Pb}$  in air near those sites are expected to be higher than in the other sites (Al-Masri et al., 2005). Moss samples from sites E09, E12, W15, W16 and E17 are located far from any fault zones, but the activity concentration of  $^{210}\text{Pb}$  is still slightly elevated, especially in sites E09 and E12. The higher values of  $^{210}\text{Pb}$  are not correlated with the relatively low values of both  $^{226}\text{Ra}$  and  $^{238}\text{U}$  in these samples. Sampling sites E09 and E17 are located in areas with limestone dominant (lower concentration of  $^{238}\text{U}$ ,  $^{232}\text{Th}$  and  $^{40}\text{K}$ ). In addition, they are surrounded by cultivated areas (oil palm plantations at E09, and para-rubber plantations at E17). If phosphate fertilizers were used they could elevate  $^{238}\text{U}$  without significant presence of the other radionuclides in the decay chain. Furthermore, all the moss samples were collected from topsoil by stream sides, so the samples were exposed to moist air. However, the high activity concentrations of  $^{210}\text{Pb}$  in moss did not incur high values of  $^{238}\text{U}$  or  $^{226}\text{Ra}$ . This could be because water droplets in the moist air contained more dissolved  $^{222}\text{Rn}$  than  $^{226}\text{Ra}$ , and after uptake and decay of radon, its progenies accumulated in the moss. This could explain the high activity concentrations of  $^{210}\text{Pb}$  observed in these areas.

It is interesting that there was no correlation between  $^{210}\text{Pb}_{\text{ex}}$  and  $^7\text{Be}$ , and that these radionuclides have distinct sources;  $^{210}\text{Pb}$  is produced by the decay of  $^{222}\text{Rn}$  from the land surface, while  $^7\text{Be}$  is produced in the upper atmosphere and transported by stratosphere – troposphere exchange processes. The vertical transport of air mass mixes them in the troposphere (Kuroda et al., 1962; Hirose et al., 2004), so they are mainly transported from remote areas through the upper troposphere (Church et al., 1992), and finally, they are deposited on the Earth surface by similar processes. Consequently, in the atmosphere they are significantly correlated as reported by several authors (Baskaran et al., 1993; Baskaran, 1995; Kim et al., 2000; Hirose et al., 2004; Du et al., 2008). In this study the moss samples were collected at the end of winter and in early summer, when solar heating warms the surface air – not only at the ground surface air of peninsular Thailand that may contain aerosols enriched in  $^{210}\text{Pb}$ , but also within the marine air in the Gulf of Thailand that may contain aerosols depleted in  $^{210}\text{Pb}$  (Hirose et al., 2004; Du et al., 2008). Both the heated air masses move upward and mix with cold air from China, and then get transported to the peninsula by the North – East Monsoon. However, unlike the activity concentration of  $^7\text{Be}$  in surface air, the activity concentration

of  $^{210}\text{Pb}$  is controlled by “local meteorological conditions”, such as temperature, rainfall amount, and relative humidity (Kim et al., 2000; Pham et al., 2011; Bourcier et al., 2011; Gordo et al., 2015). Since it rains often in peninsular Thailand, the washout may influence some control over the activity concentration of  $^{210}\text{Pb}$  in the aerosols. In this way, both the mixing processes and the local meteorological conditions are important factors controlling the activity concentration of  $^{210}\text{Pb}$  in the surface air of peninsular Thailand, which provides a possible explanation for the lack of correlation between  $^7\text{Be}$  and  $^{210}\text{Pb}$ .

At sampling location E12, the activities of airborne radionuclides in all moss samples were generally high; however, there is no correlation between  $^{210}\text{Pb}$  and  $^7\text{Be}$ . This site is located at the top of a granitic mountain (Fig. 1) around 1000 m above the mean sea level. All bryophytes growing on the top soil are covered by grasses and small trees, which are directly exposed to the atmospheric influences continuously. It is well known that the local meteorological conditions can affect the ground surface air and concentrations of radionuclides in the air (Pham et al., 2011). The sampling period was at the end of rainy season and in early summer time. With lack of rain or any precipitation the airborne radionuclides can be enriched by solar heating:  $^7\text{Be}$  can be accumulated in hot air while the presence of elevated  $^{210}\text{Pb}$  coincides with hot ground (earth) surface, which can increase the rate of  $^{222}\text{Rn}$  emanations.

In addition, if we expect that both radionuclides were directly deposited into the moss samples by similar atmospheric processes, then the atmospheric temperature inversion of surface air layer could be a possible explanation for the disagreement between their concentrations in moss samples. From evening to early morning the ground cools along with the surface air, and an inversion develops when the air temperature increases with altitude. This situation occurs frequently and is generally confined to a relatively shallow layer near the ground surface, blocking the atmospheric flow of air over the area. During daytime, the ground rapidly absorbs solar heat and transfers some of that heat to the surface air. This can create a buoyant air mass if the thermal properties of the surface are uniform, or there may be numerous parcels if the thermal properties vary. As the air warms and becomes less dense than the surrounding air, it rises from near the surface upwards and increases the concentrations of radon and its progenies there. Then the cool air mass with high concentration of  $^7\text{Be}$  in the higher altitudes cannot reach the moss due to the inversion layer, and  $^7\text{Be}$  is accumulated in this upper layer. However, from late evening till early morning the ground surface temperature decreases faster than the air temperature, and inversion builds up again as the cold air masses from the higher altitudes sink downward to the earth surface and increase the aerosol concentrations there, reaching the moss and causing  $^7\text{Be}$  accumulation in the bryophytes.

#### 4. Conclusion

This study uses moss samples to monitor the activity concentrations of terrestrial radionuclides  $^{40}\text{K}$ ,  $^{226}\text{Ra}$ ,  $^{232}\text{Th}$  and  $^{238}\text{U}$ , and of airborne radionuclides  $^7\text{Be}$  and  $^{210}\text{Pb}$  in peninsular Thailand. Most of the moss samples were collected from mountain areas in National Parks and Wildlife Sanctuaries. The activity concentrations of all radionuclides exhibited large variations, which may be explained by the biological variety of bryophytes and moss species by sampling sites and the degrees of local shelter to the moss by other plants that prevent direct atmospheric deposition to the moss.

Both principal components and cluster analysis with dendrogram representation were used, showing two PC dimensions and dividing the studied radionuclides into three well separated clusters. The PC axes can reasonably be named *factor of soil dust origin*







## VITAE

**Name** Mr. Komrit Wattanavatee

**Student ID** 6010230041

### **Educational Attainment**

<b>Degree</b>	<b>Name of Institution</b>	<b>Year of Graduation</b>
Primary School Grade 1 – 6	Anubal Narathiwat School	1986
Secondary School Grade 7 – 12	Narasikkhalai School	1992
Bachelor of Science (Physics)	Prince of Songkla University	1996
Master of Science (Physics)	Chiang Mai University	2002

### **Scholarship Awards during Enrolment**

Graduate School Dissertation Funding for Thesis

### **List of Publication**

Krmar, M., Wattanavatee, K., Radnović, D., Slivka, J., Bhongsuwan, T., Frontasyeva, M.V., Pavlov, S. S., 2013. Airborne radionuclides in mosses collected at different latitudes. *Journal of Environmental Radioactivity* 117, 45-48.

Wattanavatee K., Krmar, M., Bhongsuwan, T., 2017. A survey of natural terrestrial and airborne radionuclides in moss samples from the peninsular Thailand. *Journal of Environmental Radioactivity* 177, 113-127.